

**Characterization of DLIM1, a novel cytoskeleton-
associated LIM domain containing protein of
*Dictyostelium discoideum***

INAUGURAL-DISSERTATION

zur

Erlangung des Doktorgrades

der Mathematisch-Naturwissenschaftlichen Fakultät

der Universität zu Köln

vorgelegt von

Bharat Khurana
aus Neu Delhi, Indien
2000

Referees/Berichterstatter

Prof. Dr. Maria Leptin

Prof. Dr. Angelika A. Noegel

Date of oral examination/
Tag der mündlichen Prüfung

18.01.2001

The present research work was carried out under the supervision of Prof. Dr. Angelika A. Noegel in the Institute of Biochemistry I, Medical Faculty, University of Cologne, Cologne, Germany from June 1997 to October 2000.

Die vorliegende Arbeit wurde von Juni 1997 bis Oktober 2000 am Biochemischen Institut I der Medizinischen Fakultät der Universität zu Köln angefertigt. Die Betreuung der Arbeit erfolgte unter Anleitung von Frau Prof. Dr. Angelika A. Noegel.

*To my parents
& parent-in-laws...*

ACKNOWLEDGEMENTS

Today I meet the finale of my endeavour but the search for a suitable thanks is still not over as it is beyond the power of my expression for my esteemed advisor, Prof. Dr. Angelika A. Noegel, Institute of Biochemistry I, Medical Faculty, University of Cologne, Cologne, Germany. Her valuable guidance, creative suggestions, constructive criticism and constant encouragement during the course of present investigation are not only praiseworthy but also unforgettable. Her analytical perusal of the manuscript is highly acknowledged. It was indeed a pleasure for me to work under her superb guidance.

I feel it my profound privilege to express my deep sense of sincere thanks and gratitude to Prof. Dr. Maria Leptin, Director, Graduate College 'Genetics of Cellular Systems', Institute of Genetics, University of Cologne, Cologne, Germany for her inspiring suggestions and necessary help at every critical juncture. Thanks are also due to all the faculty members of the Graduate College for their constructive criticism and suggestions during the sessions of regular progress reports.

I record my special thanks to Dr. Andreas Hofmann for helping me in learning the molecular biological work and inculcating in me a spirit of independent research during the early period of the present investigation; Dr. Francisco Rivero for his instant, effectual cooperation and help as and when required.

I also owe thanks to Berthold and Maria for rendering efficient technical assistance and cooperation. Thanks are also due to Frau Michel and Frau Paulus, who helped a lot in all the necessary official works during the period of my stay in Germany. The constant cooperation, motivation and nice company provided by Stephan, Michael, Thorsten, Yen and all other lab colleagues is appreciated.

My indebtedness to my parents, who always bolstered my aspiration and enthusiasm for higher studies, is beyond expression. The incredible love and affection of my parents and parent-in-laws always stood by me as a long-lasting source of encouragement and without their blessings it would have been an uphill task to complete this work.

A word of praise will not be sufficient to express the deep understanding, whole hearted cooperation and sense of responsibility shown by my wife, Taruna, throughout the assiduous work.

Finally, the financial assistance received by me from the Graduate College 'Genetics of Cellular Systems', Institute of Genetics, University of Cologne, Cologne, Germany in the form of Stipend is highly acknowledged.

*Cologne, Germany
Nov. 02, 2000*

[Bharat Khurana]

Table of Contents

Chapter	Description	Page(s)
	ABBREVIATIONS	1-2
I.	INTRODUCTION	3-12
1.	The <i>Dictyostelium</i> actin cytoskeleton	3
2.	LIM domain: structure and function	4
3.	Classification of LIM proteins	6
4.	LIM proteins associated with the actin cytoskeleton	8
5.	LIM domain containing proteins of <i>Dictyostelium discoideum</i>	11
6.	Overview	12
II.	MATERIALS AND METHODS	13-71
1.	Materials	13
1.1.	Laboratory materials	13
1.2.	Instruments and equipments	14
1.3.	Kits	16
1.4.	Enzymes, antibodies, substrates, inhibitors and antibiotics	16
1.5.	Chemicals and reagents	17
1.6.	Media and buffers	18
1.6.1.	Media and buffers for <i>Dictyostelium</i> culture	18
1.6.2.	Media for <i>E. coli</i> culture	19
1.6.3.	Media for hybridoma cells	19
1.6.4.	Buffers and other solutions	20
1.7.	Biological materials	21
1.8.	Plasmids	22
1.9.	Oligonucleotide primers	22
2.	Cell biological methods	23
2.1.	Growth of <i>Dictyostelium</i>	23
2.1.1.	Growth in liquid nutrient medium	23
2.1.2.	Growth on SM agar plates	23
2.2.	Development of <i>Dictyostelium</i>	23
2.2.1.	Development in suspension culture	24
2.2.2.	Development on phosphate-buffered agar plates or water agar plates	24
2.2.3.	Development on plastic surface	24
2.3.	Preservation of <i>Dictyostelium</i>	24
2.3.1.	Preservation of <i>Dictyostelium</i> cells	24
2.3.2.	Preservation of <i>Dictyostelium</i> spores	25

Chapter	Description	Page(s)
2.4.	Transformation of <i>Dictyostelium</i> cells by electroporation	25
2.5.	Determination of cell size	26
2.6.	Viability assay of osmotically shocked cells	27
2.7.	Spore germination assay	27
2.8.	Qualitative phototaxis assay	27
2.9.	Analysis of agglutination	28
3.	Molecular biological methods	28
3.1.	Purification of plasmid DNA	28
3.2.	Digestion with restriction enzymes	29
3.3.	Generation of blunt ends in linearised plasmid DNA	30
3.4.	Dephosphorylation of DNA fragments	30
3.5.	Setting up of ligation reaction	31
3.6.	Isolation of <i>Dictyostelium</i> genomic DNA	31
3.7.	DNA agarose gel electrophoresis	32
3.8.	Recovery of DNA fragments from agarose gel	32
3.9.	Southern blotting	32
3.10.	Isolation of total RNA from <i>Dictyostelium</i> cells	33
3.11.	RNA formaldehyde-agarose gel electrophoresis	34
3.12.	Northern blotting	35
3.13.	Radiolabelling of DNA	35
3.13.1.	Chromatography through Sephadex G-50 spin column	36
3.13.2.	Hybridisation of Southern- or northern-blot with radiolabelled DNA probe	36
3.14.	PCR-mediated screening of <i>Dictyostelium</i> transformants	37
3.15.	Transformation of <i>E. coli</i>	38
3.15.1.	Transformation of <i>E. coli</i> cells by the CaCl ₂ method	38
3.15.2.	Transformation of <i>E. coli</i> cells by electroporation	38
3.16.	Glycerol stock of bacterial culture	39
3.17.	DNA colony blot for screening of <i>E. coli</i> transformants	39
3.18.	DNA sequencing	41
3.19.	Construction of vectors	41
3.19.1.	Amplification and cloning of the partial DLIM1 cDNA	41
3.19.2.	Cloning of full length DLIM1 cDNA	42
3.19.2.1.	Screening of λgt11 cDNA library	42
3.19.2.2.	Isolation and cloning of DLIM1 cDNA from bacteriophages	43
3.19.3.	Cloning of genomic DLIM1 DNA	44
3.19.4.	DLIM1 gene replacement vector	45
3.19.5.	Vector for expression of DLIM1 as a GFP-fusion protein	45
3.19.6.	N- and C-terminal DLIM1 deletion constructs	46
3.19.7.	Vector for expression of DLIM1 as a histidine-tagged protein	46
3.19.8.	Vector for expression of DLIM1 as a GST-fusion protein	47

Chapter	Description	Page(s)
4.	Biochemical methods	48
4.1.	Preparation of total protein from <i>Dictyostelium</i>	48
4.2.	SDS-polyacrylamide gel electrophoresis	48
4.2.1.	Coomassie blue staining of SDS-polyacrylamide gels	49
4.2.2.	Drying of SDS-polyacrylamide gels	50
4.3.	Western blotting using the semi-dry method	50
4.3.1.	Ponceau S staining of western blots	50
4.4.	Immunodetection of membrane-bound proteins	51
4.4.1.	Enzymatic chemi-luminescence (ECL) detection system	51
4.4.2.	BCIP/NBT colour development substrate reaction	52
4.5.	Expression and purification of histidine-tagged DLIM1	52
4.6.	Expression and purification of GST-DLIM1 fusion protein	53
4.6.1.	Small-scale protein expression	53
4.6.2.	Large-scale protein expression	54
4.6.3.	Preparation of cell homogenate	54
4.6.4.	Elution of GST-DLIM1 fusion protein by affinity chromatography	55
4.6.5.	Lyophilization of eluted GST-DLIM1 fusion protein	56
4.7.	Expression and purification of GST	56
4.8.	Quantification of protein	57
4.9.	Triton X-100 extraction of <i>Dictyostelium</i> cells	57
4.10.	Actin-sedimentation assays	57
5.	Immunological methods	58
5.1.	Generation of monoclonal antibodies	58
5.1.1.	Immunization of mice	58
5.1.2.	Preparation of mouse feeder cells for fusion and cloning	59
5.1.3.	Fusion	59
5.1.4.	Screening of hybridoma clones	61
5.1.4.1.	Indirect ELISA for screening of hybridoma clones	61
5.1.4.2.	Stripe test for screening of hybridoma clones	62
5.1.5.	Cloning of hybridoma cells	63
5.1.6.	Freezing and recovery of hybridoma cell lines	64
5.2.	Indirect immunofluorescence of <i>Dictyostelium</i> cells	65
5.2.1.	Preparation of <i>Dictyostelium</i> cells	65
5.2.2.	Fixation of <i>Dictyostelium</i> cells	65
5.2.2.1.	Methanol fixation	65
5.2.2.2.	Picric acid-paraformaldehyde fixation	65
5.2.3.	Immunolabelling of fixed cells	66
5.2.4.	Mounting of coverslips	67
5.3.	DAPI and phalloidin staining of fixed cells	67
5.4.	Immunolabelling of GFP-DLIM1 expressing <i>Dictyostelium</i> cells fixed during phagocytosis	68

Chapter	Description	Page(s)
6.	Microscopy	68
6.1.	Live cell imaging of GFP-DLIM1 expressing <i>Dictyostelium</i> cells	69
6.2.	Imaging distribution of GFP-DLIM1 during pinocytosis	70
6.3.	Imaging distribution of GFP-DLIM1 during phagocytosis	70
6.4.	Imaging distribution of GFP-DLIM1 in aggregation-competent cells	70
7.	Computer analyses	71
III.	RESULTS	72-123
1.	Analyses of the DLIM1 gene	72
1.1.	Cloning and sequence analysis of DLIM1 cDNA	72
1.2.	Amino acid sequence of DLIM1	74
1.3.	Southern blot analysis of DLIM1 gene	77
1.4.	Expression of DLIM1 specific RNA during development	77
1.5.	Cloning and sequence analysis of DLIM1 genomic DNA	77
2.	Subcellular localization of DLIM1	80
2.1.	Expression of DLIM1 as a GFP-fusion protein in <i>Dictyostelium</i>	80
2.1.1.	Subcellular localization of GFP-DLIM1 in vegetative cells	81
2.1.2.	Localization of GFP-DLIM1 fusion protein during pinocytosis	84
2.1.3.	Localization of GFP-DLIM1 during phagocytosis	85
2.1.4.	Localization of GFP-DLIM1 during exocytosis	89
2.1.5.	Localization of GFP-DLIM1 in motile cells	92
2.2.	N- and C-terminal DLIM1 deletion studies	93
3.	Generation of DLIM1 specific monoclonal antibodies	98
3.1.	Expression and purification of DLIM1 as a histidine-tagged protein	98
3.1.1.	Generation of monoclonal antibodies using histidine-tagged DLIM1 as an antigen	99
3.2.	Expression and purification of DLIM1 as a GST-fusion protein	100
3.2.1.	Generation of monoclonal antibodies using GST- DLIM1 fusion protein as an antigen	101
4.	<i>In vitro</i> binding of DLIM1 to F-actin	103
5.	Generation of DLIM1⁻ mutant cells	106
5.1.	Molecular biological analyses for screening of DLIM1 ⁻ mutant cells	106
5.1.1.	Southern blot analysis	106
5.1.2.	Northern blot analysis	106

Chapter	Description	Page(s)
6.	Characterization of DLIM1⁻ mutant	108
6.1.	Determination of cell size	108
6.2.	Quantitation of nuclei	108
6.3.	Growth of mutant cells in axenic medium	111
6.4.	Growth of mutant cells under stress conditions	111
6.4.1.	Growth under temperature stress	111
6.4.2.	Growth under osmotic stress	113
6.5.	Response to osmotic shock	115
6.6.	Growth on agar plates with bacteria as food source	117
6.7.	Development of mutant cells	117
6.7.1.	Development under submerged condition on plastic surface	117
6.7.2.	Development on agar plates	119
6.8.	Analysis of spore germination	121
6.9.	Cell-to-cell adhesion of mutant cells	121
6.10.	Qualitative phototaxis assay	122
IV.	DISCUSSION	124-136
1.	DLIM1 is a group 2 LIM domain protein	124
2.	Subcellular localization of DLIM1	125
2.1.	DLIM1 not only colocalizes with but also binds to actin	126
2.2.	DLIM1 is involved in the dynamic processes controlled by the actin cytoskeleton	127
3.	DLIM1⁻ mutant analyses	131
3.1.	Increase in cell-size and impaired cytokinesis	131
3.2.	Reduced growth under stress conditions and increased sensitivity to osmotic shock	132
3.3.	Defect in early development	133
4.	DLIM1: an overview	135
V.	SUMMARY/ZUSAMMENFASSUNG	137-140
	BIBLIOGRAPHY	i-ix
	Erklärung	x
	Curriculum Vitae/Lebenslauf	xi-xii

Abbreviations

AP	alkaline phosphatase
APS	ammonium persulphate
ATP	adenosine 5'-triphosphate
bp	base pair(s)
BCIP	5-bromo-4-chloro-3-indolylphosphate
BSA	bovine serum albumin
Bsr	blasticidin resistance cassette
cAMP	cyclic adenosine monophosphate
CCD	cooled charge-coupled device
cDNA	complementary DNA
CIAP	calf intestinal alkaline phosphatase
CRP	cysteine-rich protein
CRIP	cysteine-rich intestinal protein
dNTP	deoxyribonucleotide triphosphate
DABCO	diazobicyclooctane
DEPC	diethylpyrocarbonate
DMSO	dimethylsulphoxide
DNA	deoxyribonucleic acid
DNase	deoxyribonuclease
DTT	1,4-dithiothreitol
ECL	enzymatic chemiluminescence
EDTA	ethylenediaminetetraacetic acid
EGTA	ethyleneglycol-bis (2-amino-ethylene) N,N,N,N-tetraacetic acid
ELISA	enzyme linked immunosorbent assay
G418	geneticin
GFP	green fluorescent protein
GST	glutathione S-transferase
HEPES	N-[2-Hydroxyethyl] piperazine-N'-2-ethanesulphonic acid
HRP	horse radish peroxidase
IgG	immunoglobulin G
IPTG	isopropyl- β -D-thiogalactopyranoside
kb	kilo base pairs
MES	morpholinoethansulphonic acid
β -ME	beta-mercaptoethanol
MLP	muscle LIM protein
MOPS	Morpholinopropanesulphonic acid
Mw	molecular weight
NBT	nitrobluetetrazolium
NP-40	nonylphenylpolyethyleneglycol
pNPP	para-nitrophenyl phosphate
OD	optical density
ORF	open reading frame
PAGE	polyacrylamide gel electrophoresis
PCR	polymerase chain reaction

PEG	polyethyleneglycol
PIPES	piperazine-N,N'-bis [2-ethanesulphonic acid]
PMSF	phenylmethylsulphonylfluoride
RNA	ribonucleic acid
RNase	ribonuclease
rpm	rotations per minute
SDS	sodium dodecyl sulphate
TEMED	N,N,N',N'-tetramethyl-ethylendiamine
TRITC	tetramethylrhodamine isothiocyanate
U	unit
UV	ultra violet
vol.	volume
v/v	volume by volume
w/v	weight by volume
X-gal	5-bromo-4-chloro-3-indolyl- β -D-galactopyranoside

Units of Measure and Prefixes

<u>Unit</u>	<u>Name</u>
Ci	curie
°C	degree Celsius
D	Dalton
g	gram
h	hour
L	litre
m	meter
min	minute
s	sec
V	volt

<u>Symbol</u>	<u>Prefix (Factor)</u>
k	kilo (10^3)
c	centi (10^{-2})
m	milli (10^{-3})
μ	micro (10^{-6})
n	nano (10^{-9})
p	pico (10^{-12})

1. Introduction

1. The *Dictyostelium* actin cytoskeleton

The actin cytoskeleton of a cell is required for the establishment and maintenance of the cell morphology, motility, cell-cell and cell-substratum interactions, cytokinesis, intracellular transport processes, development and signal transduction. The multiplicity of these actin-related processes require the existence of actin in a variety of complex, dynamic structures, which are regulated by actin-binding proteins. Some of these actin-binding proteins facilitate the assembly of actin filaments into a three-dimensional meshwork by crosslinking or bundling the actin filaments, whereas others regulate filament turnover or remodel the actin cytoskeleton in response to external signals. *Dictyostelium discoideum*, an amoeboid cell is

an excellent model system for studying the macromolecular events coincident with and necessary for the reorganization of the actin network. It is a simple eukaryotic microorganism that lives as a natural phagocyte and feeds on yeast and bacteria. It divides as separate individuals as long as food is available. However, when starved, development is initiated and cells aggregate by chemotaxis in response to relayed cAMP signals to construct a slug, which further gives rise to a fruiting body consisting of spore cells resting on a slender stalk. The development of *Dictyostelium* is relatively simple and can be easily investigated with all the experimental techniques that are commonly used in developmental biology. Since the organism is haploid, mutants can easily be isolated and scored using the unique combination of the cell biological and molecular genetic approaches. Moreover, the actin cytoskeleton of *Dictyostelium* harbours essentially all classes of actin-binding proteins that had been found throughout eukaryotes making it valuable for investigating structures and functions of cytoskeleton proteins.

2. LIM domain: structure and function

In the last decade, a conserved cysteine rich sequence motif, LIM domain, has been identified in many different species in cytoskeleton-associated proteins as well as in a variety of other proteins including transcription factors and proto-oncogene products. The LIM motif was first identified in three developmentally regulated transcription factors, *Caenorhabditis elegans* Lin-11, rat Isl-1, and *C. elegans* Mec-3, from which the term LIM is derived (Freyd *et al.*, 1990, Karlsson *et al.*, 1990, Pfaff *et al.*, 1996, Way and Chalfie, 1988). The LIM domain displays the consensus amino acid sequence $CX_2CX_{16-23}HX_2CX_2CX_2CX_{16-21}CX_{2-3}(C/H/D)$ (Freyd *et al.*, 1990; Crawford *et al.*, 1994). Biochemical and biophysical data reveal that a LIM domain is a specific zinc-binding sequence that displays a striking structural similarity to the DNA-binding domains of the GR and GATA-1 transcription factors. The two zinc finger-like modules that constitute a LIM domain are responsible for binding to two zinc atoms via two tetrahedral metal coordinating centres established by the conserved cysteine, histidine and aspartic acid residues of the LIM consensus (Figure 1a). Zinc coordination is required to stabilize the secondary and the tertiary structure of the LIM domain to generate a binding interface for protein or nucleic acid (Kosa *et al.*, 1994; Michelsen *et al.*, 1994; Perez-Alvarado *et al.*, 1994). Although LIM domains bind zinc ions

and show structural similarity to zinc fingers, evidences available to date favour a role in protein-protein interactions rather than DNA binding (Feuerstein *et al.*, 1994; Sanchez-Garcia and Rabbitts, 1994; Schmeichel and Beckerle, 1994; Dawid *et al.*, 1995). LIM domains have been observed to function as modular protein-binding interfaces and, in this capacity, are thought to influence subcellular protein localization and regulate protein function (Schmeichel and Beckerle, 1994).

The NMR structure of the cysteine rich intestinal protein (CRIP), a single LIM domain containing protein is shown in Figure 1b. The two zinc fingers that constitute a LIM domain represent separate structural entities that are held together in a particular configuration by hydrophobic interactions. Both finger-like modules of the CRIP are constituted by two antiparallel β -sheets. The N-terminal module is followed by a tight turn that forms the linker to the following module. At the C-terminus of the second module, the β -sheets are followed by a short α -helix (Perez-Alvarado *et al.*, 1996). The solution structure of the C-terminal LIM domain of CRP2 is similar to that described for CRIP (Konrat *et al.*, 1997). Recently, the solution structures of the entire CRP1 and CRP2 molecules have been solved (Konrat *et al.*, 1998; Yao *et al.*, 1999). The solution structure of the CRP2 molecule is shown in Figure 1c. The structure of the N-terminal LIM domain within the whole protein is very similar to that of the isolated C-terminal segment (Konrat *et al.*, 1997; Konrat *et al.*, 1998). The two LIM domains form independent structural units that are held together by the linker region, which is disordered in solution, and there are no apparent interactions between the N- and C-terminal LIM domains. This characteristic confers both lateral and rotational freedom on the LIM domains and supports the notion that the proteins with multiple LIM domains may function as adapter molecules arranging two or more protein constituents into a macromolecular complex.

LIM domain proteins are widely distributed in nature differing in the number of LIM domains, position of the LIM domains and the presence of other functional domains besides the LIM domain, such as homeodomain, protein kinase domain and motifs involved in protein-protein interactions. Thus, the LIM domain is capable of functioning in a variety of molecular contexts.

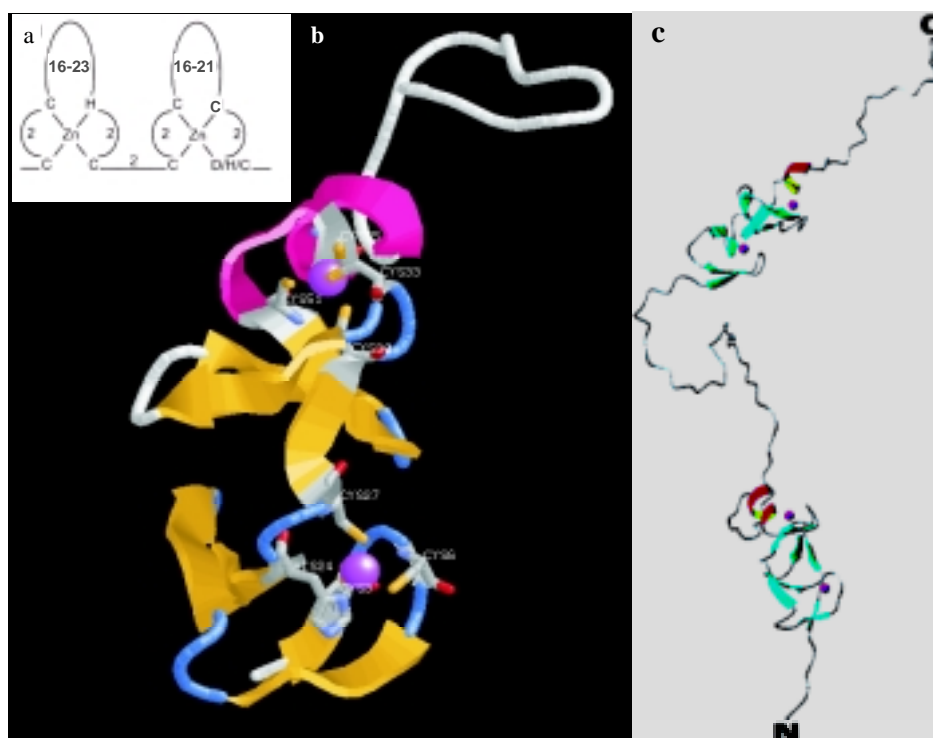


Figure 1. LIM domain structure. (a) Depicts the double-zinc finger motif of the LIM domain. (b) The solution structure of the cysteine rich intestinal protein, CRIP (Perez-Alvarado *et al.*, 1996). β -sheets are shown in yellow, α -helix in violet and the zinc-ions are depicted with violet balls. Positions of the conserved cysteine and histidine residues are indicated. (c) The solution structure of CRP2 (Konrat *et al.*, 1998). The two LIM domains of CRP2 form independent structural units that are held together by the linker region, which is disordered in solution, and there are no apparent interactions between the N- and C-terminal LIM domains. β -sheets are shown in green, α -helix in red and the zinc-ions are depicted with violet balls.

3. Classification of LIM proteins

The LIM domain proteins do not form a functional family, rather a variety of quite dissimilar proteins share domains that can be classified as similar by sequence comparison. The LIM domain proteins have been classified into 3 different groups (Figure 2) based on the sequence relationship among the LIM domains and on the overall structure of the proteins (Dawid *et al.*, 1998).

Group 1 proteins always contain paired LIM domains near the N-terminus. The N-terminal LIM domains fall into one sequence class (class A), while the second LIM domains form a

distinct sequence class (class B). Group 1 proteins include (i) LIM-only proteins, LMOs (Rhombotin/TTG), (ii) proteins that contain a DNA-binding homeodomain besides LIM domains (LHX proteins), and (iii) proteins possessing a kinase domain in addition to LIM domains (LIM-kinases or LIMKs). All the three founder LIM proteins Lin-11, Isl-1 and Mec-3 belong to the LHX subgroup of group 1 LIM proteins. The group 1 proteins are primarily nuclear, however, some can be found in the cytoplasm also, e.g., the LHX protein XLIM1/LHX1 and LIMKs (Smolich *et al.*, 1997; Dawid *et al.*, 1998).

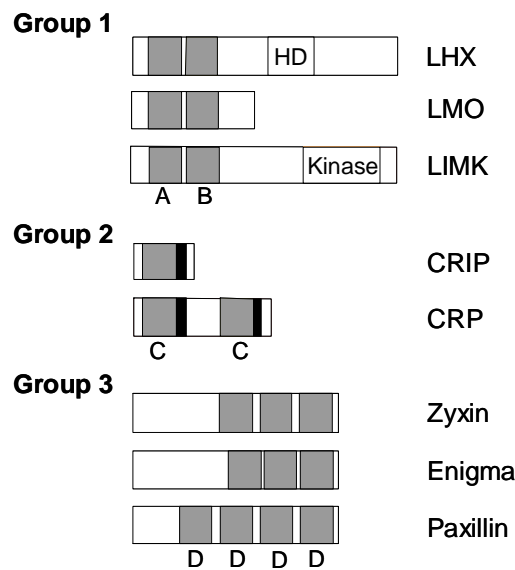


Figure 2. Classification of LIM domain proteins (Dawid *et al.*, 1998). LIM domains are shown in grey; glycine-rich regions in group 2 proteins are shown in black. HD represents the homeodomain region in LIM-homeodomain (LHX) proteins; kinase represents the kinase-domain in LIM-kinase proteins (LIMK). A, B, C and D are the different sequence classes of LIM domains.

Group 2 proteins consist of one or two copies of a single sequence type of LIM domain (class C) and the distance between the LIM domains is larger than found in the group 1 LIM proteins. These proteins are composed largely of LIM domains without additional structural or functional motifs; all, except a few, contain a short glycine-rich domain after each LIM domain. These proteins are primarily cytoplasmic, however, this distinction is not rigid. For example, CRPs are distributed in the nucleus and the cytoplasm (Arber and Caroni, 1996).

Group 3 proteins contain different numbers of LIM domains located at the C-terminus. The LIM domains of proteins included in this group are more heterogenous in sequence than group 1 and 2 LIM domains and most of the LIM domains in this group can be assigned to a

sequence class (class D). Members of this group include zyxin, paxillin and enigma. Group 3 proteins are also primarily cytoplasmic, however, zyxin is known to shuttle between the cytoplasm and the nucleus by virtue of its nuclear export signal (Beckerle, 1997; Nix and Beckerle, 1997).

LIM domain containing proteins are key players in organization of the cytoskeleton and a number of fundamental pathways controlling cell proliferation and differentiation (summarised in Figure 3). Discussed below are some of the cytoskeleton associated LIM domain containing proteins.

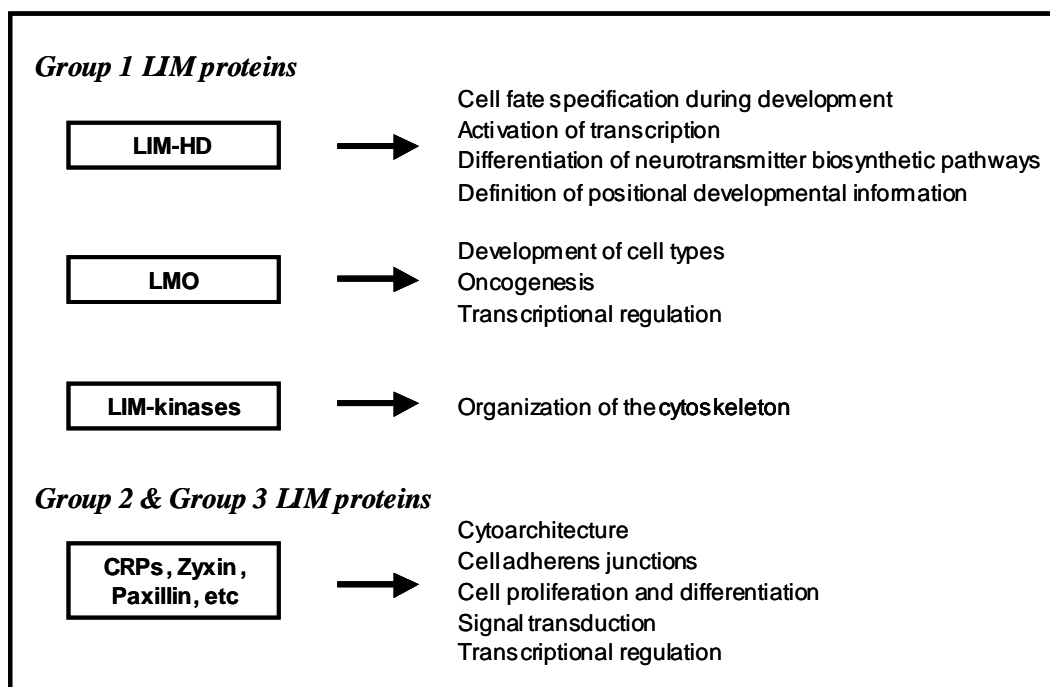


Figure 3. Role of different LIM domain containing proteins in various cellular processes (modified from Bach, 2000).

4. LIM proteins associated with the actin cytoskeleton

Two LIM-kinases, LIMK1 and LIMK2 have been identified in mammals so far (Okano *et al.*, 1995; Stanyon and Bernard, 1999). Experimental evidences available to date demonstrate a central cytoplasmic role of LIMK1 in the organization of the actin cytoskeleton. LIMK1 catalyses phosphorylation of a N-terminal serine residue of cofilin (a

small actin-binding protein of the actin-depolymerising-factor family), thereby inactivating its F-actin-depolymerising activity and leading to accumulation of actin filaments and aggregates (Arber *et al.*, 1998; Yang *et al.*, 1998). The N-terminal region of LIMK1 comprising LIM domains and a PDZ domain has been reported to influence the LIM-kinase activity (Edwards and Gill, 1999).

Several LIM domain containing proteins belonging to group 2 and 3 are associated with the cytoskeleton, for example CRPs, zyxin and paxillin. CRPs (CRP1, CRP2 and CRP3) have been shown to homodimerize, a reaction mediated by either of its two LIM domains, but not by an inter-LIM domain sequence fragment (Feuerstein *et al.*, 1994). Each of the three CRPs has been shown to be associated with elements of the actin cytoskeleton, as all are capable of directly interacting with an actin cross-linking protein α -actinin and zyxin (Sadler *et al.*, 1992; Schmeichel and Beckerle, 1994; Louis *et al.*, 1997; Pomies *et al.*, 1997). Both α -actinin and zyxin are important regulators of the organization of the actin cytoskeleton. The gene disruption studies in the mouse have confirmed the requirement for CRP3/MLP in cytoarchitectural organization. Mice that lack the CRP3/MLP gene show disruption of the cytoarchitecture of both cardiac and skeletal muscle and developed dilated cardiomyopathy with hypertrophy and heart failure after birth (Arber *et al.*, 1997). Zyxin, which exhibits an extensive proline-rich region at its N-terminus and three LIM domains at its C-terminus, is a low abundance phosphoprotein localized at the sites of integrin-dependent attachment to the extracellular matrix, that is, the adhesion plaque (Crawford and Beckerle, 1991; Sadler *et al.*, 1992). Protein-protein interactions mediated by CRP1 and zyxin at the adhesion plaques are depicted in Figure 4. It has been demonstrated that Zyxin interacts with members of the CRP family of LIM proteins by its most N-terminal LIM domain, indicating that LIM domains function as a unit mediating specific protein-protein interactions (Schmeichel and Beckerle, 1994). The sequence information required for α -actinin binding of CRP1 is confined to an 18 residue sequence occurring within the protein's N-terminal glycine-rich repeat that follows the N-terminal LIM domain of CRP1 (Harper *et al.*, 2000). However, the binding site for zyxin on CRP1 is not contained within a single contiguous sequence of amino acids, rather the interaction appears to rely on the coordinate action of sequences found in both of CRP1's component LIM domains (Schmeichel and Beckerle, 1998).

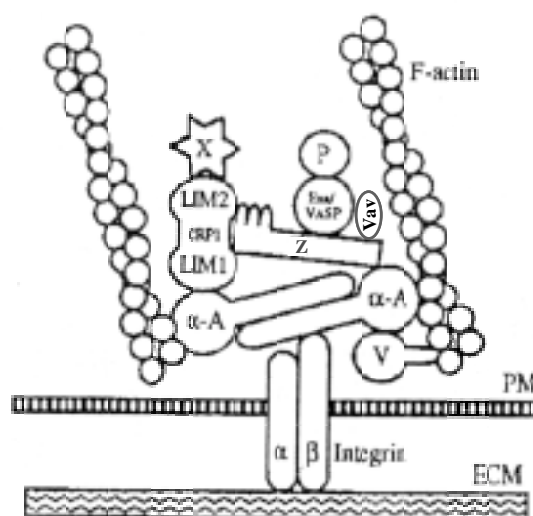


Figure 4. A schematic representation of the protein-protein interactions mediated by the LIM domain proteins at the adhesion plaque (model proposed by Pomies *et al.*, 1997, with slight modifications). Zyxin interacts with cysteine rich protein, α -actinin, Vav, and may recruit Ena/VASP family members and thus profilin and actin monomers to these sites; thus participating in the regulation of actin assembly dynamics. Abbreviations: (Z) zyxin; (CRP1) cysteine rich protein 1; (α -A) α -actinin; (P) profilin; (V) vinculin; (X) other CRP1 binding partners; (PM) plasma membrane; (ECM) extracellular matrix. LIM1 and LIM2 are the N- and C-terminal LIM domains of the CRP1, respectively.

Although, all the three CRPs reveal functional conservation since all are associated with elements of the actin cytoskeleton (zyxin and α -actinin), all show a divergent pattern of gene expression. CRP1 expression is detected in a variety of tissues enriched in smooth muscle, CRP2 expression is restricted to arteries and fibroblasts and CRP3 (also known as muscle LIM protein, MLP) is dominant in heart and skeletal muscle (Louis *et al.*, 1997). Therefore, the three CRP family members might perform similar functions in different muscle derivatives. Recently, CRP3/MLP has been demonstrated to specifically interact through its C-terminal LIM domain with the cytoskeletal protein β I-spectrin. Interestingly, the CRP3/MLP related proteins CRP1 and CRP2 do not bind spectrin, thereby providing an important distinction between the individual CRP family members (Flick and Konieczny, 2000).

Paxillin is another group 3 LIM domain protein found in focal adhesions. Paxillin exhibits four LIM domains at its C-terminus and a proline-rich domain at its N-terminus. Paxillin

also shows the presence of several potential phosphorylation sites. At its N-terminus, paxillin has binding sites for Vinculin, an adhesion complex molecule and for focal adhesion tyrosine kinase, FAK (Turner and Miller, 1994; Bellis *et al.*, 1995; Schaller and Parsons, 1995; Brown *et al.*, 1996). Although paxillin was initially believed to localize at focal adhesions through binding to Vinculin, recent reports indicate that LIM domains of paxillin regulate paxillin's focal adhesion localization (Brown *et al.*, 1996; Brown *et al.*, 1998). Brown *et al.* (1998) identified that LIM domains (LIM2 and LIM3) of paxillin have the capacity to serve as binding sites for, and substrates of serine/threonine protein kinases. Paxillin's LIM domain phosphorylation was observed to regulate the availability of paxillin to integrate into focal adhesions upon cell adhesion. In addition, constitutive LIM domain phosphorylation significantly potentiated the ability of cells to adhere to fibronectin, suggesting that paxillin may contribute directly to the transmittance of signals from the cytoplasm to the external environment (inside-out signalling) (Brown *et al.*, 1998). Thus paxillin functions as a unique adapter protein involved in regulating various functions of the focal adhesion.

5. LIM domain containing proteins of *Dictyostelium discoideum*

Recently, two LIM domain containing proteins DdLim and LIM2 have been isolated from *Dictyostelium* (Prassler *et al.*, 1998; Chien *et al.*, 2000). DdLim contains a single LIM domain at its N-terminus, whereas LIM2 exhibits five LIM domains at its C-terminus. The pattern of expression of DdLim and LIM2 is developmentally regulated, as both show elevated levels of transcription during early stages of development. Both the proteins have been observed to localize at the newly formed membrane extensions in motile cells. It is believed that DdLim acts as an adapter protein at the cytoskeleton-membrane interface where it is involved in a receptor mediated Rac1-signalling pathway that leads to actin polymerization and ultimately cell motility (Prassler *et al.*, 1998). LIM2 behaves as a regulatory protein that functions to control reorganization of the actin cytoskeleton during cell motility and chemotaxis, since *Dictyostelium* cells deficient in LIM2 protein aggregate poorly and arrest at the mound stage of development (Chien *et al.*, 2000). Thus the two known LIM domain proteins of *Dictyostelium* are playing important roles in the rearrangement of the actin cytoskeleton.

6. Overview

Ever increasing numbers of LIM proteins are being implicated in cytoskeletal regulation in many organisms. The biological roles of LIM proteins are highly diverse, however, the common theme of LIM domain function is the mediation of specific protein-protein interactions. It seems clear that the protein-protein interactions mediated by LIM domains are of fundamental and regulatory importance for many biological processes in the cell that require the formation of multiprotein complexes. Adhesion plaques are examples of such multiprotein complexes in which several LIM domain proteins have an important role. Much less is known about the specific biological functions of LIM domains. The identification and characterization of more LIM domain proteins in diverse cell systems and deciphering the cellular functions of these proteins will, undoubtedly, help in elucidating new and exciting basic biological mechanisms. As part of this approach we present characterization of DLIM1, a novel LIM domain containing protein of *Dictyostelium*, with the aim of understanding its cellular functions by investigating its subcellular localization and involvement in cytoskeleton-dependent processes using a green fluorescent protein (GFP)-tagged version of DLIM1; mapping domains that influence the subcellular localization of DLIM1; investigating its interaction with actin; and generating mutant cells that lack DLIM1 and characterizing phenotypes of the DLIM1⁻ cells.

2. Materials and Methods

1. Materials

1.1. Laboratory materials

Cellophane sheet, Dry ease	Novex
Centrifuge tubes, 15 ml, 50 ml	Greiner
Coverslips (glass), Ø 12 mm, Ø 18 mm, Ø 55 mm	Assistent
Corex tube, 15 ml, 50 ml	Corex
Cryo tube, 1 ml	Nunc
Electroporation cuvette, 2 mm electrode gap	Bio-Rad
Gel-drying frames	Novex
Hybridisation bag	Life technologies
Microcentrifuge tube, 1.5 ml, 2.2 ml	Sarstedt

Micropipette, 1-20 μ l, 10-200 μ l, 100-1,000 μ l	Gilson
Micropipette tips	Greiner
Multi-channel pipette	Finnigan
Needles (sterile), 18G–27G	Terumo, Microlance
Nitrocellulose membrane, BA85	Schleicher and Schuell
Nitrocellulose-round filter, BA85, \varnothing 82 mm	Schleicher and Schuell
Nylon membrane, Biotyne B	Pall
Parafilm	American National Can
Pasteur pipette, 145 mm, 230 mm	Brand, Volac
PCR softtubes, 0.2 ml	Biozym
Petri dish (35 mm, 60 mm, 100 mm)	Falcon
Petri dish (90 mm)	Greiner
Plastic cuvette, semi-micro	Greiner
Plastic pipettes (sterile), 1 ml, 2 ml, 5 ml, 10 ml, 25 ml	Greiner
Quartz cuvette, Infrasil	Hellma
Quartz cuvette, semi-micro	Perkin Elmer
Saran wrap	Dow
Scalpels (disposable), Nr. 10, 11, 15, 21	Feather
Slides, 76 x 26 mm	Menzel
Syringes (sterile), 1 ml, 5 ml, 10 ml, 20 ml	Ameffa, Omnifix
Syringe filters (Acrodisc), 0.2 μ m, 0.45 μ m	Gelman Sciences
Tissue culture flasks, 25 cm ² , 75 cm ² , 175 cm ²	Nunc
Tissue culture dishes, 6 wells, 24 wells, 96 wells	Nunc
Whatman 3MM filter paper	Whatman
X-ray film, X-omat AR-5, 18 x 24 mm, 535 x 43 mm	Kodak

1.2. Instruments and equipments

Centrifuges (microcentrifuges):	
Centrifuge 5417 C	Eppendorf
Centrifuge Sigma	B. Braun Biotech Instruments
Cold centrifuge Biofuge fresco	Heraeus Instruments
Centrifuges (table-top, cooling, low speed):	
Centrifuge CS-6R	Beckman
Centrifuge RT7	Sorvall
Centrifuge Allegra 21R	Beckman
Centrifuges (cooling, high speed):	
Beckman Avanti J25	Beckman
Sorvall RC 5C plus	Sorvall
Centrifuge-rotors:	
JA-10	Beckman
JA-25.50	Beckman
SLA-1500	Sorvall
SLA-3000	Sorvall
SS-34	Sorvall
Dounce homogeniser, 10 ml	B. Braun

Electrophoresis power supply, Power-pac-200, -300	Bio-Rad
Electroporation unit, Gene-Pulser	Bio-Rad
ELISA reader	Lab Systems
Freezer (-80°C)	Nunc
Freezer (-20°C)	Siemens, Liebherr
Gel-documentation unit	MWG-Biotech
Heating block, DIGI-Block JR	neoLab
Heating block, Dry-Block DB x 20	Techne
Hybridising oven	Hybaid
Ice machine	Ziegler
Incubators:	
CO ₂ -incubator, BBD 6220, BB 6220	Heraeus
CO ₂ -incubator, WTC Binder	Biotran
Incubator, microbiological	Heraeus
Incubator with shaker, Lab-Therm	Kuehner
Laminar flow, Hera Safe (HS 12)	Heraeus
Magnetic stirrer, MR 3001 K	Heidolph
Microscopes:	
Light microscope, CH30	Olympus
Light microscope, DMIL	Leica
Light microscope, CK2	Olympus
Fluorescence microscope, DMR	Leica
Fluorescence microscope, 1X70	Olympus
Confocal laser scan microscope, DM/IRBE	Leica
Stereomicroscope, SZ4045TR	Olympus
Oven, conventional	Heraeus
PCR machine, PCR-DNA Engine PTC-2000	MJ Research
pH-Meter	Knick
Refrigerator	Liebherr
Semi-dry blot apparatus, Trans-Blot SD	Bio-Rad
Shakers	GFL, Kuehner
Sonicator, Ultra turrax T25 basic	IKA Labortechnik
Sonicator (water bath), Sonorex RK 52	Bandelin
Speed-vac concentrator, DNA 110	Savant
Spectrophotometer, Ultraspec 2000, UV/visible	Pharmacia Biotech
Ultracentrifuges:	
Optima TLX	Beckman
Optima L-70K	Beckman
Ultracentrifuge-rotors:	
TLA 45	Beckman
TLA 100.3	Beckman
SW 41	Beckman
UV-crosslinker, UVC 500	Hofer
UV- transilluminator, TFS-35 M	Faust
Vortex, REAX top	Heidolph
Waterbath	GFL
X-ray-film developing machine, FPM-100A	Fujifilm

1.3. Kits

Nucleobond AX	Macherey-Nagel
NucleoSpin Extract 2 in 1	Macherey-Nagel
Nucleotrap	Macherey-Nagel
Original TA Cloning	Invitrogen
pGEM-T Easy	Promega
Qiagen Midi- and Maxi-prep	Qiagen
Stratagene Prime It II	Stratagene

1.4. Enzymes, antibodies, substrates, inhibitors and antibiotics

Enzymes used in the molecularbiology experiments:

Calf Intestinal Alkaline Phosphatase (CIAP)	Boehringer
Deoxyribonuclease I (DNase I)	Boehringer
Klenow fragment	Boehringer
Lysozyme	Sigma
Proteinase K	Sigma
Restriction endonucleases	Amersham, Life technologies, New England Biolabs
Reverse transcriptase, Superscript II	Life technologies
Ribonuclease H (RNase H)	Boehringer
Ribonuclease A (RNase A)	Sigma
S1-nuclease	Amersham
T ₄ DNA ligase	Boehringer
Taq-polymerase	Life technologies/Boehringer

Primary antibodies:

Goat anti-GST antibody	Pharmacia
Mouse anti-actin monoclonal antibody, Act 1-7	Simpson <i>et al.</i> , 1984
Mouse anti-GFP monoclonal antibody, K3-184-2	unpublished
Mouse anti-RGS(H) ₄ antibody	Qiagen
Rabbit anti-GFP antibody, Living colour peptide	Clontech

Secondary antibodies:

Goat anti-mouse IgG, peroxidase conjugated	Sigma
Goat anti-mouse IgG, alkaline phosphatase conjugated	Sigma
Goat anti-rabbit IgG, peroxidase conjugated	Sigma
Mouse anti-goat IgG, alkaline phosphatase conjugated	Sigma
Mouse anti-goat IgG, peroxidase conjugated	Sigma
Sheep anti-mouse IgG, Cy3 conjugated	Sigma

Substrates:

BCIP/NBT	Promega
pNPP, Sigma Fast tablet sets, 5ml, 20 ml	Sigma

Inhibitors:

Diethylpyrocarbonate (DEPC)	Sigma
Leupeptin	Sigma
Pepstatin	Sigma
Phenylmethylsulphonylfluoride (PMSF)	Sigma

Antibiotics:

Ampicillin	Gruenthal
Blasticidin S	ICN Biomedicals
Chloramphenicol	Sigma
Dihydrostreptomycinsulphate	Sigma
Geneticin (G418)	Life technologies
Kanamycin	Sigma, Biochrom
Tetracyclin	Sigma

1.5. Chemicals and reagents

Most of the chemicals and reagents were obtained either from Sigma, Fluka, Difco, Merck, Roche, Roth or Serva. Those chemicals or reagents that were obtained from companies other than those mentioned here are listed below:

Acetic acid (98-100%)	Riedel-de-Haen
Acrylamide (Protogel: 30:0,8 AA/Bis-AA)	National Diagnostics
Agar-Agar (BRC-RG)	Biomatic
Agarose (Electrophoresis Grade)	Life technologies
Caesium chloride	Biomol
Chloroform	Riedel-de-Haen
Dimethylformamide	Riedel-de-Haen
Ethanol	Riedel-de-Haen
Glycerine	Riedel-de-Haen
Glycine	Riedel-de-Haen
Isopropyl- β -D-thiogalactopyranoside (IPTG)	Loewe Biochemica
Methanol	Riedel-de-Haen
Morpholino propane sulphonic acid (MOPS)	Gerbu
N- [2-Hydroxyethyl] piperazine-N'-2-ethanesulfonic acid (HEPES)	Biomol
Peptone	Oxoid
Sodium hydroxide	Riedel-de-Haen
Yeast extract	Oxoid

Radiolabelled nucleotide:

α - ³² P-deoxyadenosine triphosphate, (10 mCi/ml)	Amersham
---	----------

1.6. Media and buffers

All media and buffers were prepared with deionised water filtered through an ion-exchange unit (Membra Pure). The media and buffers were sterilized by autoclaving at 120°C and antibiotics were added to the media after cooling to approx. 50°C. For making agar plates, a semi-automatic plate-pouring machine (Technomat) was used.

1.6.1. Media and buffers for *Dictyostelium* culture

AX2-medium, pH 6.7:

(Claviez *et al.*, 1982)

7.15 g yeast extract
14.3 g peptone (proteose)
18.0 g maltose
0.486 g KH_2PO_4
0.616 g $\text{Na}_2\text{HPO}_4 \cdot 2\text{H}_2\text{O}$
add H_2O to make 1 liter

Phosphate agar plates, pH 6.0:

9 g agar
add Soerensen phosphate buffer, pH 6.0 to make 1 liter

Salt solution:

(Bonner, 1947)

10 mM NaCl
10 mM KCl
2.7 mM CaCl_2

Starvation buffer, pH 6.5:

(Shaulsky *et al.*, 1998)

10 mM MES, pH 6.5
10 mM NaCl
10 mM KCl
1 mM CaCl_2
1 mM MgSO_4

SM agar plates, pH 6.5:

(Sussman, 1951)

9 g agar
10 g peptone
10 g glucose
1 g yeast extract
1 g $\text{MgSO}_4 \cdot 7\text{H}_2\text{O}$
2.2 g KH_2PO_4
1 g K_2HPO_4
add H_2O to make 1 liter

<u>3x HAT medium:</u>	572 ml Normal media 36 ml 50x HAT supplement (Biochrom)
<u>1x HAT medium:</u>	572 ml Normal media 12 ml 50x HAT supplement (Biochrom)
<u>1x HT medium:</u>	572 ml Normal media 12 ml 50x HT supplement (Biochrom)
<u>Normal media (NM):</u>	500 ml RPMI 1640 (Biochrom) 55 ml Foetal calf serum, heat-inactivated (Roche) 11 ml Kanamycin, 5 mg/ml 6 ml 1mM β -mercaptoethanol, freshly made
<u>RPMI 1640:</u>	Readymade RPMI 1640 medium (1x) containing 25 mM HEPES, 0.532 g/l L-glutamine, 5.5 g/l NaCl, 5 mg/l phenol-red and 2.0 g/l NaHCO ₃ was obtained from the company Biochrom.
<u>RPMI 1640 (w/o HEPES, w/o glutamine):</u>	Same as RPMI 1640 except that it is without HEPES and L-glutamine. It was obtained readymade (1x) from the company Biochrom.

1.6.4. Buffers and other solutions

The buffers and solutions that were commonly used during the course of this study are mentioned below-

<u>Hepes-phenol:</u>	1 kg phenol was melted at 60°C in a water-bath and equilibrated with 1 vol. of 1 M Hepes, pH 7.5. The equilibrated phenol was aliquoted in 50 ml Falcon tubes and stored at -20°C.
<u>10x MOPS (pH 7.0/ pH 8.0):</u>	41.9 g MOPS 16.7 ml 3 M sodium acetate 20 ml 0.5 M EDTA add H ₂ O to make 1 liter
<u>10x NCP-Puffer (pH 8.0):</u>	12.1 g Tris/HCl 87.0 g NaCl 5.0 ml Tween 20 2.0 g sodium azide add H ₂ O to make 1 liter

<u>PBG (pH 7.4):</u>	0.5 % bovine serum albumin 0.1 % gelatin (cold-water fish skin) in 1x PBS, pH 7.4
<u>1x PBS (pH 7.4):</u>	8.0 g NaCl 0.2 g KH ₂ PO ₄ 1.15 g Na ₂ HPO ₄ 0.2 g KCl dissolve in 900 ml deionised H ₂ O adjust to pH 7.4 add H ₂ O to make 1 liter, autoclave
<u>1.2 M Phosphate buffer (pH 6.8):</u>	1.2 M Na ₂ HPO ₄ , pH 9.1 was mixed with 1.2 M NaH ₂ PO ₄ , pH 4.02 in the ratio of 2:1.
<u>20x SSC (pH 7.0):</u>	3 M NaCl 0.3 M sodium citrate
<u>TE buffer (pH 8.0):</u>	10 mM Tris/HCl, pH 8.0 1 mM EDTA, pH 8.0
<u>Tris-phenol:</u>	1 kg phenol was melted at 60°C in a water-bath and equilibrated with 1 vol. of 1 M Tris/HCl, pH 8.0. The equilibrated phenol was aliquoted in 50 ml Falcon tubes and stored at -20°C.
<u>10x TAE buffer (pH 8.3):</u>	27.22 g Tris 13.6 g sodium acetate 3.72 g EDTA add H ₂ O to make 1 liter

1.7. Biological materials

Bacterial strains:

<i>E. coli</i> BL21 (DE)	Studier and Moffat, 1986
<i>E. coli</i> DH5 α	Hanahan, 1983
<i>E. coli</i> M15[pREP4]	Qiagen
<i>E. coli</i> MC1061	Wertman <i>et al.</i> , 1986
<i>E. coli</i> Y1088	Young and Davis, 1983
<i>E. coli</i> XL1 blue	Bullock <i>et al.</i> , 1987
<i>Klebsiella aerogenes</i>	Williams and Newell, 1976

Dictyostelium discoideum strain:

AX2-214	An axenically growing derivative of wild strain, NC-4 (Raper, 1935). Commonly referred to as AX2.
---------	---

1.8. Plasmids

pBsrΔBam	Adachi <i>et al.</i> , 1994
pCR-2.1	Kit: Invitrogen
pDEXRH	Faix <i>et al.</i> , 1992
pGEM-IRES-GFP-Stop	A gift from Dr. A. Hofmann
pGEM-T Easy	Kit: Promega
pGEX-2T	Pharmacia Biotech
pIC20H	Marsh <i>et al.</i> , 1984
pLITMUS29	New England Biolabs
pQE30	Qiagen

1.9. Oligonucleotide primers

The oligonucleotide primers were designed on the basis of sequence information available and ordered for synthesis to MWG Biotech company. Following is a list of the primers used for PCR or sequence analysis or both during the course of the present investigation. The position and orientation of the primers are indicated in the text when discussed.

Name	Sequence	Analysis
CLIM 5'	5'-CGGAATTCGGATCCACCAATTGTCCAAAATGTGGTAAG-3'	PCR & Seq.
CLIM 3'	5'-GGAATTCGATATCTTAATGTAAAATAATGCACCAGT-3'	PCR
CLIM-P 5'	5'-CGGAATTCGGATCCTATGATAGATTATTTAGACAAGC-3'	PCR
DLIM1 5'	5'-TCTGTCCAACATGCACTAAAAGAG-3'	PCR & Seq.
DLIM1 3'	5'-GGATCCATGTAAAATAATGCACCAGTATTGG-3'	PCR & Seq
DLIM1cDNA 5'	5'-GAAGATCTAAGCTTGGATCCATGAGTTCTATCTGTCCAACATG-3'	PCR
DLIM1cDNA 3'	5'-TTGGACAATTGGTTGGAATAATTG-3'	PCR
DLIM1-U	5'-TTCACATGCTTTAACAGCTTC-3'	Seq.
gDLIM1-I	5'-CCAATACTGGTGCATTAGTTTTACAT-3'	Seq.
M13 reverse	5'-CAGGAAACAGCTATGAC -3'	Seq.
NLIM 5'	5'-CGGAATTCGGATCCATGAGTTCTATCTGTCCAACA-3'	PCR
NLIM 3'	5'-GGAATTCGATATCTTAATCATAATCAGTTTTGCAATA-3'	PCR
NLIM-P 3'	5'-GGAATTCGATATCTTAATTGGTTGGAATAATTGAAC-3'	PCR
SP6 universal	5'-ATTTAGGTGACACTATAG-3'	Seq.
T7 universal	5'-TAATACGACTCACTATAGGG -3'	Seq.

2. Cell biological methods

2.1. Growth of *Dictyostelium*

2.1.1. Growth in liquid nutrient medium (Claviez *et al.*, 1982)

Dictyostelium discoideum AX2 and the derived transformants were grown in liquid AX2 medium containing dihydrostreptomycin (40 µg/ml) and other appropriate selective antibiotic (depending upon mutant) at 21°C either in a shaking-suspension in Erlenmeyer flask with shaking at 160 rpm or the cells were grown on petri dish. For all the cell biological works, culture was harvested at a concentration of 3-5 x 10⁶ cells/ml.

2.1.2. Growth on SM agar plates

In general, *Dictyostelium* cells were plated onto SM agar plates overlaid with *Klebsiella aerogenes* and incubated at 21°C for 3-4 days until *Dictyostelium* plaques appeared on the bacterial lawns. To obtain single clones of *Dictyostelium*, 50-200 cells were suspended in 100 µl Soerensen phosphate buffer and plated onto *Klebsiella*-overlaid SM agar plates. Single plaques obtained after incubation at 21°C for 3-4 days were picked up with sterile tooth-picks, transferred either to new *Klebsiella*-overlaid SM agar plates or to separate petri dishes in AX2 medium supplemented with dihydrostreptomycin (40 µg/ml) and ampicillin (50 µg/ml) to get rid of the bacteria and any other appropriate selective antibiotic (depending upon mutant).

2.2. Development of *Dictyostelium*

Development in *Dictyostelium* is induced by starvation. For analysis of development in suspension culture and on phosphate agar, cells grown to a density of 2-3 x 10⁶ cells/ml were pelleted by centrifugation at 2,000 rpm (Sorvall RT7 centrifuge) for 2 min at 4°C and were washed two times in equal volume of cold Soerensen phosphate buffer in order to remove all the nutrients present in the AX2 media.

2.2.1. Development in suspension culture

After washing twice in Soerensen phosphate buffer, the cells were resuspended in Soerensen phosphate buffer at a density of 1×10^7 cells/ml and were shaken at 160 rpm and 21°C for desired time periods.

2.2.2. Development on phosphate-buffered agar plates or water agar plates

Cells grown to a density of $2-3 \times 10^6$ cells/ml were washed twice with equal volumes of Soerensen phosphate buffer. 5×10^7 cells were then resuspended in 3 ml Soerensen phosphate buffer and evenly distributed onto phosphate-buffered agar plates (90 mm) or water agar plates (90 mm). The plates were air dried and any excess liquid was carefully aspirated without disturbing the cell layer. The plates were then incubated at 21°C. different stages of development were observed and the images were captured at indicated time points.

2.2.3. Development on plastic surface (DeLozanne and Spudich, 1987)

To observe the early stages of development of *Dictyostelium*, the cells were placed under starvation buffer on a plastic petridish. *Dictyostelium* cells were grown axenically to a density of $2-4 \times 10^6$ cells/ml. The cells were harvested and 2.8×10^6 cells were resuspended in 5 ml of fresh AX2 medium. The cell suspension was added to a 60 mm petridish (Falcon) and the cells were allowed to adhere to the plastic surface in a monolayer by incubating at 21°C for 6 h. After 6 h, the medium was carefully replaced by Soerensen phosphate buffer or SAP buffer. The plate was incubated at 21°C and different stages of early development were observed. The images were captured at indicated time points.

2.3. Preservation of *Dictyostelium*

2.3.1. Preservation of *Dictyostelium* cells

Dictyostelium cells were allowed to grow densely in AX2 medium to a concentration of $4-5 \times 10^6$ cells/ml. 9 ml of the densely grown culture was collected in a 15 ml Falcon tube on ice and supplemented with 1 ml Horse serum and 1 ml DMSO. The contents were mixed by

gentle pipetting, followed by preparing aliquots of 1 ml in cryotubes (1 ml, Nunc). The aliquots were incubated on ice for 60 min, followed by incubation at -20°C for at least 2 h. Finally, the aliquots were transferred to -80°C for long term storage.

For reviving the frozen *Dictyostelium* cells, the aliquot was taken out from -80°C and thawed immediately at 37°C in a waterbath. In order to remove DMSO, the cells were transferred to a falcon tube containing 30 ml AX2 medium and centrifuged at 2,000 rpm (Sorvall RT7 centrifuge) for 2 min at 4°C . The cell pellet was resuspended in 10 ml of AX2 medium and 200 μl of the cell suspension was plated onto SM agar plates overlaid with *Klebsiella*, while the remaining cell suspension was transferred into a 100-mm petri dish (Falcon) and antibiotics were added when appropriate. Cells in the petri dish were allowed to recover overnight at 21°C and the medium was changed the next day to remove the dead cells and the traces of DMSO, whereas, the SM agar plates coated with cell suspension and bacteria were incubated at 21°C until plaques of *Dictyostelium* cells started to appear.

2.3.2. Preservation of *Dictyostelium* spores

Dictyostelium cells were harvested and plated onto 90 mm phosphate-buffered agar plates as described above (Materials and Methods, 2.2.2.). The plates were incubated at 21°C till the mature fruiting bodies appeared. The spores were collected from the fruiting bodies, resuspended in Soerensen phosphate buffer to a density of 1×10^7 to 1×10^8 spores/ml and aliquoted 1 ml each in cryotubes (1 ml, Nunc). After immediately freezing the spores in liquid nitrogen, the aliquots were transferred to -80°C for long-term storage.

For germination of the frozen spores, one of the aliquots was taken out of -80°C and thawed quickly to room temperature. The spore suspension was resuspended in 30 ml of AX2 medium in an Erlenmeyer flask and incubated at 21°C and 160 rpm.

2.4. Transformation of *Dictyostelium* cells by electroporation

The electroporation method for transformation of *Dictyostelium* cells described by de Hostos *et al.* (1993) was followed with little modifications. *Dictyostelium discoideum* AX2 cells were grown axenically in suspension culture to a density of $2\text{-}3 \times 10^6$ cells/ml. Cell

suspension was incubated on ice for 20 min and centrifuged at 2,000 rpm (Sorvall RT7 centrifuge) for 2 min at 4°C to collect the cells. The cells were then washed with an equal volume of ice-cold Soerensen phosphate buffer followed by an equal volume of ice-cold Electroporation-buffer. After washings, the cells were resuspended in Electroporation-buffer at a density of 1×10^8 cells/ml. For electroporation, 20-25 µg of the plasmid DNA was added to 500 µl (5×10^7 cells) of the above cell suspension and the cell-DNA mixture was transferred to a pre-chilled electroporation cuvette (2 mm electrode gap, Bio-Rad). Electroporation was performed with an electroporation unit (Gene Pulser, Bio-Rad) set at 0.9 kV and 3 µF without the pulse controller. After electroporation, the cells were immediately spread onto a 100-mm petri dish (Falcon) and were allowed to sit for 10 min at 21°C. Thereafter, 1 ml of Healing-solution was added dropwise onto the cells and the petri dish was incubated at 21°C on a shaking platform at 50 rpm for 15 min. 10 ml of AX2 medium was added into the petri dish and the cells were allowed to recover overnight. The next day, the medium was changed to the selection medium containing appropriate antibiotic. To select stable transformants, selection medium was replaced after every 24-48 h until the control plate (containing cells electroporated without any DNA) was clear of live cells.

Electroporation-buffer:

100 ml 0.1 M potassium phosphate buffer
17.12 g sucrose
add distilled H₂O to make 1 litre
autoclave

0.1 M Potassium phosphate buffer:

170 ml 0.1 M KH₂PO₄
30 ml 0.1 M K₂HPO₄
adjust to pH 6.1

Healing-solution:

150 µl 0.1 M CaCl₂
150 µl 0.1 M MgCl₂
10 ml electroporation-buffer

2.5. Determination of cell size (Rivero *et al.*, 1996b)

Dictyostelium strain AX2 and derived mutant cells were grown to a density of 2×10^6 cells/ml. The cells were washed twice with cold Soerensen phosphate buffer and resuspended to a density of 1×10^7 cells /ml in Soerensen phosphate buffer supplemented with 20 mM EDTA. The cells were then transferred to an Erlenmeyer flask and incubated on a shaker (160 rpm, 21°C) for 1 h. After 1 h of incubation, essentially single spherical cells

were photographed using an inverted microscope (1X70, Olympus) equipped with a 40 x objective and a charge-coupled device (CCD) camera (CVM10, Progressive Scan, Japan). The diameters were determined from the prints.

2.6. Viability assay of osmotically shocked cells (Rivero *et al.*, 1996b)

Axenicly growing cells were harvested at a concentration of 3×10^6 cells/ml and washed once with cold Soerensen phosphate buffer. The cells were resuspended to a density of 3×10^7 cells/ml in Soerensen phosphate buffer and incubated at 21°C on a shaker at 160 rpm for 1 h. Thereafter, sorbitol was added to a final concentration of 0.4 M and the shaking was continued for another 2 h. After 2 h of incubation in hypertonic medium, cells were diluted in Soerensen phosphate buffer and 200 cells were plated onto SM plates in association with *K. aerogenes*. The plates were incubated at 21°C and after 2-4 days colonies appearing on plates were counted to assay the viability.

2.7. Spore germination assay (Ennis and Sussman, 1975)

Axenicly growing *Dictyostelium* cells were harvested, washed twice with equal volumes of Soerensen phosphate buffer and plated onto 90 mm phosphate-buffered agar plates as described in Materials and Methods (2.2.2.). The plates were incubated at 21°C till the mature fruiting bodies were visible. The spores were collected from the mature fruiting bodies and resuspended in Soerensen phosphate buffer at a concentration of 1×10^6 to 5×10^7 spores/ml. The spores were then activated by heating at 45°C for 30 min. After heat activation, spores were diluted in Soerensen phosphate buffer and 200 spores/plate were plated onto SM plates overlaid with *Klebsiella*. The plates were incubated at 21°C till the *Dictyostelium* colonies appeared.

2.8. Qualitative phototaxis assay (Wallraff and Wallraff, 1997)

Dictyostelium AX2 cells and derived mutants were cultivated on *Klebsiella* lawns on SM agar plates. Using sterile tooth picks, vegetative cells from edges of the colonies growing on *Klebsiella* lawns were transferred to 90 mm water agar plates. The application point for

phototaxis was located in the centre of the plate. The plates were wrapped in an opaque black plastic sheet with a slit of ~ 3 mm and incubated at 21°C. Approximately 72 h after inoculation, slime trails and cellular material were blotted to nitrocellulose filter (BA85, Ø 82 mm, Schleicher and Schuell) by keeping the filter on the plate for 1 h. Thereafter, filters were stained with staining solution for 5 min followed by incubation in destaining solution (with 2 changes) for 10-15 min to remove the excess stain. The filters exhibiting the stained slime trails were photographed using light microscope (Olympus) equipped with a CCD camera (CVM10, Progressive Scan, Japan).

Staining solution:

0.1 % amido black
25% isopropanol
10% acetic acid

Destaining solution:

25% isopropanol
10% acetic acid

2.9. Analysis of agglutination (Rivero *et al.*, 1999b)

Axenicly growing *Dictyostelium* AX2 cells and derived mutants were harvested, washed twice with equal volumes of Soerensen phosphate buffer and resuspended in Soerensen phosphate buffer to a density of 1×10^7 cells/ml. For strains with different cell size, cells were adjusted to the same total cell volume by resuspending them at an OD₆₀₀ of 0.9 in 10 ml Soerensen phosphate buffer. The cell suspension was then transferred to Erlenmeyer flask and incubated on a shaker at 160 rpm and 21°C. Samples were taken at the indicated time points and decrease in light scattering was measured at 600 nm.

3. Molecular biological methods

3.1. Purification of plasmid DNA

In general, for small cultures (1 ml) of *E. coli* transformants, the alkaline lysis method of Holmes and Quigley (1981) was used to extract plasmid DNA. This method is good for screening a large number of clones simultaneously for the desired recombinant plasmid. Briefly, single transformants were picked up from the culture plate and were grown overnight in 1 ml of LB media containing suitable antibiotic. Next day, the overnight grown

E. coli cells were pelleted by centrifugation at 6,000 rpm in a microcentrifuge for 3-5 min. The pellet was then resuspended completely in 250 μ l STET/lysozyme buffer and the suspension was incubated at the room temperature for 10 min to lyse the bacterial cells. The bacterial lysate was boiled at 100°C for 1 min and was then centrifuged in an eppendorf centrifuge at maximum rpm for 15 min at room temperature. The plasmid DNA present in the supernatant was precipitated by adding equal volume of isopropanol and incubating at room temperature for 10 min. The precipitated DNA was pelleted in the eppendorf centrifuge at 12,000 rpm for 15 min and the DNA pellet was washed with 70% ethanol, dried in the speed-vac concentrator and finally resuspended in 40 μ l TE, pH 8.0 containing RNase A at 1 μ g/ml.

STET/lysozyme buffer (pH 8.0):

50 mM Tris/HCl, pH 8.0

50 mM EDTA

0.5% Triton-X-100

8.0% Sucrose

Add lysozyme at 1 mg/ml at the time of use

Alternatively, for pure plasmid preparations in small and large scales, kits provided either by Macherey-Nagel (Nucleobond AX kit for small scale plasmid preparations) or by Qiagen (Qiagen Midi- and Maxi-Prep kit for large scale plasmid preparations). These kits were used when the pure plasmid DNA was required for sequencing, PCR or transformation. These kits follow basically the same approach: first overnight culture of bacteria containing the plasmid is pelleted and the cells are lysed by alkaline lysis. The freed plasmid DNA is then adsorbed on a silica matrix, washed with ethanol, and then eluted into TE, pH 8.0. This method avoids the requirement of caesium chloride or phenol-chloroform steps during purification.

3.2. Digestion with restriction enzymes

All restriction enzymes were obtained from NEB, Amersham or Life technologies and the digestions were performed in the buffer systems and temperature conditions as suggested by the manufacturers. The plasmid DNA was digested for 1-2 h and the chromosomal DNA for 12-16 h.

3.3. Generation of blunt ends in linearised plasmid DNA

For many cloning experiments, it was necessary to convert the 5' or 3' extensions generated by restriction endonucleases into blunt ends. Repair of 5' extensions was carried out by polymerase activity of the Klenow fragment, whereas repair of 3' extensions was carried out by the 3' to 5' exonuclease activity of the Klenow fragment.

Reaction-mix for 5' extensions:

1-4 µg linearised DNA
5 µl 10x High salt buffer
1 µl 50x dNTP-mix (each 4 mM)
2 U Klenow fragment
add H₂O to make 50 µl

Reaction-mix for 3' extensions:

1-4 µg linearised DNA
5 µl 10x High salt buffer
2 U Klenow fragment
add H₂O to make 50 µl

10x High salt buffer:

500 mM Tris/HCl, pH 7.5
1 M NaCl
100 mM MgCl₂
10 mM DTT

The reaction was carried out at 37°C for 25-30 min. After incubation, the reaction was immediately stopped by inactivating the enzyme by heating to 75°C for 10 min or by adding 1 µl 0.5 M EDTA. This was followed by phenol/chloroform extraction and precipitation of DNA with 2 vol. ethanol.

3.4. Dephosphorylation of DNA fragments

To avoid self-ligation of the vector having blunt ends or that has been digested with a single restriction enzyme, 5' ends of the linearised plasmids were dephosphorylated by calf-intestinal alkaline phosphatase (CIAP, Boehringer). Briefly, in a 50 µl reaction volume, 1-5 µg of the linearised vector-DNA was incubated with 1 U calf-intestinal alkaline phosphatase (CIAP) in CIAP-buffer (provided by the manufacturer) at 37°C for 30 min. The reaction was stopped by inactivating the enzyme by heating the reaction-mixture at 65°C for 10 min. The dephosphorylated DNA was extracted once with phenol-chloroform and precipitated with 2 vol. ethanol and 1/10 vol. 2 M sodium acetate, pH 5.2.

3.5. Setting up of ligation reaction

DNA fragment and the appropriate linearised plasmid were mixed in approximately equimolar amounts. T4 DNA ligase (Life technologies/Boehringer) and ATP were added as indicated below and the ligation reaction was left overnight at 10-12°C.

Ligation reaction:

Linearised vector DNA (200-400 ng)
DNA-fragment
4 µl 5x Ligation buffer
1 µl 0.1 M ATP
1.5 U T4 ligase
add H₂O to make 20 µl

5x Ligation buffer:

supplied along with the T4 ligase enzyme by the manufacturer

3.6. Isolation of *Dictyostelium* genomic DNA

Genomic DNA from *Dictyostelium* was prepared according to the method described by Nellen *et al.* (1987), with slight modifications. *Dictyostelium* cells were allowed to grow on *Klebsiella*-covered SM plates at 21°C. After 2-3 days, when the plates were covered with densely grown *Dictyostelium*, cells were collected in 15 ml ice-cold water, pelleted and washed twice with ice-cold water to get rid of *Klebsiella*. Alternatively, the pellet of 1×10^8 *Dictyostelium* cells grown in shaking suspension was washed twice with ice-cold Soerensen phosphate buffer. The pellet of *Dictyostelium* cells was finally resuspended in 5 ml cold Nucleolysis buffer. The nuclei fraction was obtained by centrifugation at 3,000 rpm (Sorvall RT7 centrifuge) for 10 min. The nuclear pellet obtained was carefully resuspended in 1 ml TE, pH 8.0, with 0.5% SDS and 0.1 mg/ml proteinase K and incubated at 37°C for 3-5 h. The genomic DNA was extracted twice with phenol/chloroform (1:1 v/v), precipitated by adding 2.5 vol. 96% ethanol and 1/10 vol. 3 M sodium acetate, pH 5.2. The DNA precipitate was carefully spooled with a Pasteur pipette, washed with 96% ethanol, air-dried and dissolved in the desired volume of TE, pH 8.0.

Nucleolysis buffer:

10 mM magnesium acetate
10 mM NaCl
30 mM HEPES, pH 7.5
10% sucrose
2% Nonidet P40

Estimation of DNA concentration:

1 O.D at 260 nm = 50 µg DNA

3.7. DNA agarose gel electrophoresis

Agarose gel electrophoresis was performed according to the method described by Sambrook *et al.* (1989) to resolve and purify the DNA fragments. Electrophoresis was typically performed with 0.7% (w/v) agarose gels in 1x TAE buffer submerged in a horizontal electrophoresis tank containing 1x TAE buffer at 1-5 V/cm. Only for resolving fragments less than 1,000 bp, 1% (w/v) agarose gels in 1x TAE buffer were used. DNA-size marker (Life technologies) was always loaded along with the DNA samples in order to estimate the size of the resolved DNA fragments in the samples. The gel was run until the bromophenol blue dye present in the DNA-loading buffer had migrated the appropriate distance through the gel. The gel was examined under UV light at 302 nm and was photographed using a gel-documentation system (MWG-Biotech)

DNA-size marker:

1 kb DNA Ladder (Life technologies): 12,216; 11,198; 10,180; 9,162; 8,144; 7,126; 6,108; 5,090; 4,072; 3,054; 2,036; 1,636; 1,018; 506; 396; 344; 298; 220; 201; 154; 134; 75 bp

3.8. Recovery of DNA fragments from agarose gel

DNA fragments from restriction enzyme digests or from PCR reactions were separated by agarose gel electrophoresis and the gel piece containing the desired DNA fragment was carefully and quickly excised while observing the ethidium bromide stained gel under a UV transilluminator. The DNA fragment was then purified from the excised gel piece using the Macherey-Nagel gel elution kit (NucleoSpin Extract 2 in 1), following the method described by the manufacturers.

3.9. Southern blotting

Southern blotting (Southern, 1975) is a technique used to transfer DNA from its position in an agarose gel to a nitrocellulose/nylon membrane. After transfer, the membrane can be hybridised with a radiolabelled probe to identify specific fragments. The ethidium bromide stained agarose gel was photographed using a scale under UV light to document migration of DNA fragments with respect to the DNA-size marker. DNA was depurinated by incubating

the gel in 2 vol. of 0.25 M HCl for 20 min at room temperature with gentle shaking. The gel was rinsed in deionised H₂O to remove excess HCl and was then incubated in 2 vol. of denaturation solution (0.5 M NaOH, 1.5 M NaCl) for 30 min in order to denature the DNA. Now the transfer was performed by capillary transfer technique. Briefly, the gel was transferred directly from the denaturation solution to a buffer reservoir containing a supporting wick (made up of Whatman 3MM paper) and 20x SSC. A dry nylon membrane (Biodyne B membrane, Pall) of the same size as the gel was then directly placed on the alkaline gel. Three pieces of Whatman 3MM paper followed by blotting pads, all cut to the same size as the gel, were placed on top of the nylon membrane. A glass plate supporting approximately 500 g weight was finally kept on top of the stack and transfer of DNA to the membrane was allowed to proceed for overnight. Next day, position of the wells and the orientation of the membrane was marked before removing the membrane from the gel surface. The transferred DNA was then immobilized onto the membrane by baking at 80°C for 1 h. After baking, the membrane was hybridised with a desired radiolabelled probe.

3.10. Isolation of total RNA from *Dictyostelium* cells

The pellet of 1×10^8 cells (harvested at growth or different stages of development) was washed with ice-cold DEPC-H₂O (0.1% DEPC, mixed by stirring for 5-6 h, autoclaved) and resuspended in 10 ml 50 mM Hepes buffer, pH 7.5. To the cell suspension, 100 μ l DEPC and 1 ml 10% SDS was added, mixed briefly, followed by immediately adding 1 vol. of phenol saturated with Hepes buffer, pH 7.5. The sample was then vortexed strongly and centrifuged at 3,000 rpm (Sorvall RT7 centrifuge) for 20 min at 4°C. The upper aqueous phase was collected carefully and was extracted with an equal volume of phenol/chloroform (1:1 v/v), till no interphase was visible. This was followed by an extraction with an equal volume of chloroform and finally the RNA present in the upper aqueous phase was precipitated by adding 2 vol. ethanol and 1/10 vol. 2 M sodium acetate, pH 5.2 and incubating the samples overnight at -20°C. Next day, the RNA was pelleted, washed with 70% ethanol, air-dried and dissolved in the desired volume of DEPC-H₂O. The concentration of RNA was determined by measuring the O.D₂₆₀ of the solution using a spectrophotometer. The RNA samples were stored at -80°C.

DEPC-H₂O:

0.1% DEPC in H₂O
mixed by stirring for 5-6 h
autoclaved

Estimation of RNA concentration:

1 O.D at 260 nm = 40 µg RNA

3.11. RNA formaldehyde-agarose gel electrophoresis

The formaldehyde-agarose denaturing electrophoresis (Lehrach *et al.*, 1977) is used for separation and resolution of single stranded RNA.

Sample preparation for electrophoresis:

In general, 30 µg of purified total RNA was mixed with an equal volume of RNA-sample buffer and denatured by heating at 65°C for 10 min. After denaturation, the sample was immediately transferred to ice and 1/10 vol. of RNA-loading buffer was added. Thereafter, the RNA samples were loaded onto a denaturing formaldehyde-agarose gel.

Formaldehyde-agarose gel preparation:

For a total gel volume of 150 ml, 1.8 g agarose (final concentration 1.2%) was initially boiled with 111 ml DEPC-H₂O in an Erlenmeyer flask, cooled to 60°C and then 15 ml of RNA-gel-casting buffer, pH 8.0 and 24 ml of 36% formaldehyde solution were added. The agarose solution was mixed by swirling and poured into a sealed gel-casting chamber of the desired size. After the gel was completely set, denatured RNA samples were loaded and the gel was run in 1x RNA-gel-running buffer, pH 7.0, at 100 V until the bromophenol blue dye had migrated the appropriate distance through the gel. A test gel was sometimes run with 5 µg of total RNA to check the quality of the RNA samples. In such a case, 10 µg/ml ethidium bromide was added to the RNA-sample buffer during sample preparation and after electrophoresis the gel was examined under UV light at 302 nm and was photographed using the gel-documentation system.

10x RNA-gel-casting buffer (pH 8.0):

200 mM MOPS
50 mM sodium acetate
10 mM EDTA
adjust pH 8.0 with NaOH
autoclaved

10x RNA-gel-running buffer (pH 7.0):

200 mM MOPS
50 mM sodium acetate
10 mM EDTA
adjust pH 7.0 with NaOH
autoclaved

RNA-sample buffer:

50% formamide
6% formaldehyde
in 1x RNA-gel-casting buffer, pH 8.0

RNA-loading buffer:

50% sucrose, RNase free
0.25% bromophenol blue
in DEPC-H₂O

Internal RNA-size standard:

26S rRNA (4.1 kb)
17S rRNA (1.9 kb)

3.12. Northern blotting

After electrophoresis, the RNA formaldehyde agarose gel was rinsed in sufficient amount of deionised H₂O for 5 min and then equilibrated in 10x SSC for 25 min. The resolved RNA was then transferred from the gel to the nylon membrane (Biodyne B membrane, Pall) using the transfer setup as described for Southern blotting (see Materials and Methods 3.9.). After overnight transfer with 20x SSC, the transferred RNA was immobilised by baking the membrane in an oven at 80°C for 1 h.

3.13. Radiolabelling of DNA

Prime-it kit (Stratagene) was used for radiolabelling of DNA fragments following the method suggested by the manufacturers. Briefly, 0.1-0.3 µg DNA sample was suspended in 24 µl ddH₂O (final volume). Then 10 µl of random-oligonucleotide-primer (supplied along with the kit) was added and the DNA template was denatured at 95°C for 5 min. After denaturation, 10 µl of 5x dATP-primer buffer (supplied along with the kit), 5 µl of α-³²P-ATP (Amersham) and 1 µl Klenow enzyme (5 U/µl, supplied along with the kit) was added and the reaction-mixture was incubated at 37°C for 10 min. After 10 min the reaction was immediately stopped by adding 2 µl stop-mix (supplied along with the kit). Now the reaction-mixture was diluted with 100 µl TE, pH 8.0 to increase the reaction volume and the reaction-mixture was overlaid on a 0.9 ml Sephadex G-50 spin column (see Materials and Methods 3.13.1.). The free nucleotides present in the reaction-mixture were separated by centrifugation at 3,000 rpm (Sorvall RT7 centrifuge) for 2 min through the Sephadex G-50 spin column and the radiolabelled DNA probe was collected in a 1.5 ml eppendorf tube. The purified radiolabelled DNA probe was denatured by heating at 100°C for 10 min, cooled on ice and used for hybridisation of Southern- or northern-blot.

3.13.1. Chromatography through Sephadex G-50 spin column

This technique (Sambrook *et al.*, 1989), which employs gel filtration to separate high-molecular weight DNA from smaller molecules, was used to segregate radiolabelled DNA from unincorporated α -³²P-ATP. 30 g of Sephadex G-50 (Pharmacia) was slowly added to 250 ml of TE, pH 8.0, in a 500-ml bottle and the beads were allowed to swell overnight at room temperature. Next day, the supernatant was decanted and was replaced with an equal volume of TE, pH 8.0. The beads were autoclaved and stored in a screw-capped bottle at 4°C. For preparation of Sephadex G-50 spin column, the swollen Sephadex G-50 beads were packed in a disposable 1-ml syringe plugged with sterile glass wool and the column was spun at 3,000 rpm (Sorvall RT7 centrifuge) for 2 min. Sephadex G-50 was added until the packed column volume was 0.9 ml. The column was then used for segregation of radiolabelled DNA probe.

3.13.2. Hybridisation of Southern- or northern-blot with radiolabelled DNA probe

Southern- or northern-blots were rinsed briefly with 2x SSC and incubated in a heat-sealable hybridisation-bag (Life technologies) in 15-20 ml of pre-hybridisation buffer for 1h at 37°C on a shaking platform. After pre-hybridisation, the denatured radiolabelled DNA probe was added directly to the pre-hybridisation-buffer in the hybridisation-bag and the hybridisation was performed by incubating the blot overnight at 37°C. After hybridisation, the blot was washed twice with 2x SSC/0.1% SDS for 10 min each at room temperature with gentle shaking followed by two washings with wash buffer for 30 min each at 37°C with gentle shaking. The blot was then wrapped in a plastic wrap and autoradiography was performed by exposing the blot to X-ray film at -70°C for the desired time.

Pre-hybridisation/Hybridisation buffer:

50% formamide
1% sodium lauryl sarcosinate
0.2% SDS
2 mM EDTA, pH 7.2
0.12 M phosphate buffer, pH 6.8
2x SSC
4x Denhardt's reagent

Wash buffer:

same contents as Pre-hybridisation/
hybridisation buffer except without
4x Denhardt's reagent

100x Denhardt's reagent:

2% ficoll 400
2% polyvinylpyrrolidone
2% bovine serum albumin

3.14. PCR-mediated screening of *Dictyostelium* transformants

A PCR approach was used for screening of the DLIM1⁻ mutant cells. Briefly, AX2 cells were transformed with the DLIM1 gene replacement vector (see Materials and Methods, 3.19.4.) and the transformants were selected for resistance to blasticidin (3.5 µg/ml). Single cell transformants were then obtained by spreader dilution of the whole pool of transformants onto SM plates overlaid with *Klebsiella*. Thereafter, the single transformants were picked up and grown in separate wells in a 24 well tissue culture plate in the selection medium (as above) that has been supplemented with streptomycin (40 µg/ml) and ampicillin (50 µg/ml) to get rid of the bacteria.

Preparation of DNA for PCR reaction:

After the cells had grown to confluency in the wells, cells were suspended in the medium present in the wells and transferred to a 1.5 ml microcentrifuge tube. The cells were then pelleted by centrifugation in a microcentrifuge at maximum speed for 15 s. The cells were washed twice with 1 ml of ice-cold H₂O and resuspended in 100 µl of lysis buffer. The cells were then incubated at 56°C for 45 min followed by incubation at 95°C for 10 min to liberate the genomic DNA.

PCR conditions:

15 µl of the processed cell suspension containing the liberated genomic DNA was used as a template for PCR. Reaction programme and composition of the reaction-mix are indicated:

Lysis buffer:

0.5% Nonidet P-40
0.05 mg/ml proteinase K
in 1x PCR buffer

10x PCR buffer:

100 mM Tris/HCl
500 mM KCl
15 mM MgCl₂
adjust to pH 8.3

Reaction-mix (50µl final volume):

15 µl template
2.5 µl DLIM1 5' primer (2 pmol/µl)
2.5 µl DLIM1 3' primer (2 pmol/µl)
1.0 µl dNTP-mix (10 mM each)
5.0 µl 10x PCR buffer
1.0 µl Taq polymerase (1 U/µl)
23 µl H₂O

Reaction programme:

1-step 92°C for 3 min
2-step 35 cycles of-
92°C for 1 min
54°C for 1 min
72°C for 3 min
3-step 72°C for 10 min
4-step 4°C till end

3.15. Transformation of *E. coli*

3.15.1. Transformation of *E. coli* cells by the CaCl₂ method

Preparation of CaCl₂-competent *E. coli* cells:

Overnight grown culture of *E. coli* (0.5 ml) was inoculated into 50 ml LB medium and incubated at 37°C, 250 rpm until an OD₆₀₀ of 0.4-0.6 was obtained. The bacteria were then pelleted at 4°C for 10 min at 4,000 rpm (Beckman Avanti J25, rotor JA-25.50) and the bacterial pellet was resuspended in 20 ml of ice-cold 0.1 M CaCl₂ and incubated on ice for 15 min. The bacterial cells were again pelleted and resuspended in 2 ml of ice-cold 0.1 M CaCl₂. These CaCl₂-competent cells were stored at 4°C for up to 1 week. Alternatively, the pellet of CaCl₂-competent *E. coli* cells was resuspended in 0.1 M CaCl₂/20% glycerol and then aliquoted 200 µl/tube. The aliquots were then quickly frozen in a dry ice/ethanol bath and immediately stored at -80°C.

Transformation of CaCl₂-competent *E. coli* cells:

Plasmid DNA (~50-100 ng of a ligase reaction or ~10 ng of a supercoiled plasmid) was mixed with 100-200 µl of CaCl₂-competent *E. coli* cells and incubated on ice for 30 min. The cells were then heat-shocked at 42°C for 45 s and immediately transferred to ice to cool for 2 minutes. The cells were then mixed with 1 ml of pre-warmed (at 37°C) SOC medium and incubated at 37°C with shaking at ~150 rpm for 45 min. Finally, 100-200 µl of the transformation mix, or an appropriate dilution, was plated onto selection plates and the transformants were allowed to grow overnight at 37°C.

3.15.2. Transformation of *E. coli* cells by electroporation

Preparation of electroporation-competent *E. coli* cells

An overnight grown culture (5 ml) was inoculated into 1,000 ml of LB medium and incubated at 37°C with proper aeration and shaking at 250 rpm until an OD₆₀₀ of 0.4-0.6 was obtained. The culture was then incubated on ice for 15-20 min. Thereafter, the culture was transferred to pre-chilled 500-ml centrifuge bottles (Beckman) and the cells were pelleted by centrifugation at 4,200 rpm (Beckman Avanti J25, rotor JA-10) for 20 min at 4°C. The bacterial pellet was washed twice with an equal volume of ice-cold water and the cells were

resuspended in 40 ml of ice-cold 10% glycerol, transferred to a pre-chilled 50-ml centrifuge tube and centrifuged at 4,200 rpm (Beckman Avanti J25, rotor JA-25.50) for 10 min at 4°C. Finally, the cells were resuspended in equal volume of 10% chilled glycerol and aliquoted (50-100 µl) in 1.5-ml eppendorf tubes that have been placed in a dry ice/ethanol bath. The frozen aliquots were immediately transferred to –80°C for long-term storage.

Transformation of electroporation-competent *E. coli* cells

Plasmid DNA (~20 ng dissolved in 5-10 µl ddH₂O, no salts) was mixed with 50-100 µl electroporation-competent *E. coli* cells. The transformation mix was transferred to a 2 mm BioRad electroporation cuvette (pre-chilled) and the cuvette was incubated on ice for 10 min. The DNA was then electroporated into competent *E. coli* cells using an electroporation unit (Gene Pulser, BioRad) set at 2.5 kV, 25 µF, 200 Ω. Immediately after electroporation, 1 ml of pre-warmed (37°C) SOC medium was added onto the transformed cells and the cells were incubated at 37°C with shaking at ~150 rpm for 45 min. Finally, 100-200 µl of the transformation mix, or an appropriate dilution, was plated onto selection plates and the transformants were allowed to grow overnight at 37°C.

3.16. Glycerol stock of bacterial culture

Glycerol stocks of all the bacterial strains/transformants were prepared for long-term storage. The culture was grown overnight in LB medium with or without the selective antibiotic (depending upon the bacterial transformant). 850 µl of the overnight grown culture was added to 150 µl of sterilized glycerol in a 1.5 ml microcentrifuge tube, mixed well by vortexing and the tube was frozen on dry ice and stored at –80°C.

3.17. DNA colony blot for screening of *E. coli* transformants

The method of Sambrook *et al.* (1989) was used to screen many bacterial colonies simultaneously. After the bacterial colonies had grown to a diameter of 0.1-0.2 mm, the plates were removed from the 37°C incubator and stored at 4°C for 1-2 h in an inverted position. Thereafter a dry nitrocellulose filter (BA85, Ø82 mm, Schleicher and Schuell) was labelled with a ball-point pen and placed with the numbered side down, on the surface of the agar medium in contact with the bacterial colonies until the filter was completely wet. The

filter and underlying agar were then marked in three or more asymmetric locations by stabbing through it with a 18-gauge needle. The filter was then carefully peeled off and the plates were incubated at 37°C for 4-8 h until the colonies had regenerated. The bacteria adhering to the filter were immediately lysed by placing the filter, colony side up, for 5 min on a sheet of 3MM Whatman paper that had been saturated with denaturing solution. The filter was then transferred to a second sheet of 3MM Whatman paper that had been saturated with neutralizing solution. After 5 min, the filter was transferred to a third sheet of 3MM Whatman paper that had been saturated with 2x SSC and placed for 5 min. While transferring filters from one sheet to another, care was taken to remove as much fluid as possible from the underside of the filter by briefly placing the filter on a dry paper towel. Now the filter was laid, colony side up, on a sheet of dry 3MM Whatman paper and was allowed to dry at room temperature for 30-60 min. Thereafter, the liberated DNA was immobilised onto the filter by baking the filter for 2 h at 80°C in an oven. After baking, the filter was floated and submerged for 5 min in 2x SSC, followed by incubation in pre-wash solution at 50°C for 30 min. Loose bacterial debris or any fragments of agarose were removed during incubation in the pre-wash solution by gently scrapping on the colony surface. Thereafter, the filter was transferred to pre-hybridisation solution with 50% formamide and incubated at 42°C for 1-2 h with gentle shaking, followed by hybridisation with denatured radiolabelled probe as described above (Materials and Methods 3.13.2.). After hybridisation, the filter was washed twice with 2x SSC/0.1% SDS for 5-10 min each at room temperature with gentle shaking followed by two washings with 1x SSC/0.1% SDS for 30 min each at 37°C with gentle shaking. The filter was then wrapped in a saran wrap and autoradiography was performed by exposing the filter to an X-ray film for the desired time at -70°C. The individual colonies giving positive hybridisation signals were picked and grown.

Denaturing solution:

0.5 M NaOH
1.5 M NaCl

Neutralizing solution:

1.5 M NaCl
0.5 M Tris/HCl, pH 8.0

Pre-wash solution:

5x SSC
0.5% SDS
1 mM EDTA

Pre-hybridisation solution:

same as described in Materials and Methods (3.13.2.)

3.18. DNA sequencing

Sequencing of the PCR-amplified product or plasmid DNA was performed at the sequencing facility of the Centre for Molecular Medicine, University of Cologne, Cologne by modified dideoxy nucleotide termination method using a 'Perkin Elmer ABI prism 377' DNA sequencer.

3.19. Construction of vectors

3.19.1. Amplification and cloning of the partial DLIM1 cDNA

Partial DLIM1 cDNA (536 bp) was amplified employing RT-PCR approach. Total RNA isolated from axenically growing *Dictyostelium* was initially treated with reverse transcriptase enzyme (Superscript II, Life technologies) to synthesize cDNA template. 3 µg of RNA was taken in a nuclease-free microcentrifuge tube and 2 µl of the oligonucleotide primer, p(dN)₆ (50 µM) was added to it in a total volume of 12 µl. The mixture was heated to 70°C for 10 minutes to break the secondary structures within the template, followed by cooling on ice to prevent secondary structures from reforming. To the above mixture, 7 µl of RT-mix was added and incubated at 42°C for 2 min. Then 1 µl of reverse transcriptase (200 U/µl) was added to the tube, mixed gently by flickering and incubated further for 50 min at 42°C followed by heating at 70°C for 15 min and cooling on ice. The mixture was then treated with 1 µl of RNase H for 20 min at 37°C.

For amplification of cDNA synthesized by reverse transcription, 1 µl of the above mixture was used as a template for PCR. DLIM1 cDNA was amplified using DLIM1 5' and DLIM1 3' primers (Material and methods 1.9.), which were designed on the basis of the sequence information (Figure 6). DLIM1 3' primer was designed with an engineered BamHI site to facilitate subcloning. Reaction mix and reaction programme for PCR are indicated below. After amplification, the PCR product was directly cloned into the pCR2.1 vector (Invitrogen) as suggested by the manufacturer. The resultant vector was verified by sequencing both the strands using M13 reverse and T7 universal primers and designated as pCR-DLIM1.

10x PCR buffer (Life technologies):

100 mM Tris/HCl, pH 8.3
500 mM KCl

RT-mix:

4 μ l 5x RT buffer (Promega)
2 μ l 0.1 mM DTT
1 μ l dNTP-mix (10 mM each)

Reaction-mix:

1 μ l Template
2.5 μ l DLIM1 5' primer (2 pmol/ μ l)
2.5 μ l DLIM1 3' primer (2 pmol/ μ l)
5 μ l 10x PCR buffer (Life technologies)
3 μ l 25 mM MgCl₂
1 μ l dNTP-mix (10 mM each)
1 μ l Taq polymerase (1 U/ μ l)
add H₂O to make 50 μ l

Reaction programme:

1-step 92°C for 5 min
2-step 35 cycles of-
92°C for 1 min
54°C for 1 min
72°C for 50 s
3-step 72°C for 10 min
4-step 4°C till end

3.19.2. Cloning of full length DLIM1 cDNA

In order to obtain a full length DLIM1 cDNA, a λ gt11 cDNA library derived from growth phase *Dictyostelium* cells was screened. The DNA from the positive phages was isolated and subcloned.

3.19.2.1. Screening of λ gt11 cDNA library (Sambrook *et al.*, 1989)

Preparation of plating bacteria:

A single bacterial colony of Y1088 cells was inoculated into 50 ml of LB medium supplemented with 0.2% maltose and 10 mM MgSO₄. The bacteria were allowed to grow overnight at 37°C on a shaker.

Plating bacteriophage λ gt11 cDNA library:

The stock of the recombinant bacteriophage (λ gt11 cDNA library) was appropriately diluted in SM. 1 μ l and 10 μ l of the bacteriophage suspension was mixed with 100 μ l of the plating bacteria and incubated in a water-bath at 37°C for 20 min. Now each aliquot of the infected bacteria was mixed with 4 ml of melted top agarose (at 50°C) in a test tube and spread evenly onto pre-warmed 90 mm LB plates (at 37°C). The plates were allowed to stand for 5 min at room temperature to allow the top agarose to harden. The plates were then incubated at 37°C for overnight or until the plaques reach a diameter of ~ 1.5 mm. The plates should not show confluent lysis. The plates were then transferred to 4°C for at least an hour.

SM (medium for phage storage and dilution):

100 mM NaCl

10 mM MgSO₄·7H₂O

50 mM Tris/HCl, pH 8.0

0.01% gelatin

The solution was sterilized by autoclaving and stored at 4°C

Screening bacteriophage plaques by hybridisation:

The DNA from the bacteriophage plaques was transferred to nitrocellulose filter (BA85, Ø82 mm, Schleicher and Schuell) and the filters were hybridised to a ³²P labelled partial DLIM1 cDNA probe essentially according to the method described for DNA colony blot for screening of the bacterial transformants (Materials and Methods, 3.17.). The only exception being that the filters were immersed in solutions (denaturing solution followed by neutralization solution and 2x SSC) kept in separate trays instead of placing the filters on 3MM Whatman papers saturated with each of these solutions as described in case of the DNA colony blot for screening of bacterial transformants.

Picking plaques:

The plaques giving positive hybridisation signals were picked using a Pasteur pipette equipped with a rubber bulb. The hard agar beneath the selected plaque was stabbed by the Pasteur pipette and by applying mild suction the plaque, together with the underlying agar, was drawn into pipette. The fragments of agar were transferred into 500 µl of SM in a microcentrifuge tube and incubated at room temperature for at least 2 h (or overnight at 4°C) to allow the bacteriophage particles to diffuse out of the agar. An aliquot of the bacteriophages that elute from the agar was replated and rescreened by hybridisation until a single, well-isolated, positive plaque was obtained.

3.19.2.2. Isolation and cloning of DLIM1 cDNA from bacteriophagesExtraction of bacteriophage λ DNA:

The bacteriophage λ was initially purified from infected bacterial culture (<1 L volume) following essentially the 'Equilibrium centrifugation in caesium chloride' protocol for small-scale preparations of bacteriophage described by Sambrook *et al.* (1989). The DNA from six

independent purified bacteriophage preparations was then extracted according to the method described by Sambrook *et al.* (1989) and finally resuspended in desired volume of TE buffer.

Isolation and cloning of DLIM1 cDNA:

The bacteriophage λ DNA (from six independent phage plaques) was digested with EcoRI to liberate the cDNA inserts. The digested bacteriophage λ DNA was resolved on a 0.7% agarose gel, the cDNA inserts were eluted from the gel and cloned at the EcoRI site in the pIC20H vector. The resultant plasmids were sequenced using T7 universal and M13 reverse oligonucleotide primers to obtain the sequence of full length DLIM1 cDNA. One of these plasmids, pIC-DLIM1cDNA-2, that contains the entire DLIM1 cDNA sequence was selected for further molecular biological work.

3.19.3. Cloning of genomic DLIM1 DNA

Genomic DNA of *Dictyostelium* AX2 cells was isolated and 60 μ g of the DNA was digested overnight with EcoRI+NdeI restriction enzymes in a reaction volume of 400 μ l. The digested genomic DNA was subjected to 15% sucrose density gradient ultracentrifugation at 30,000 rpm (Optima L-70K, SW41 rotor, Beckman) at 15°C for overnight. Fractions of 1 ml were collected after ultracentrifugation and precipitated with ethanol and finally resuspended in 50 μ l of TE buffer, pH 8.0. Out of 50 μ l of DNA suspension, 15 μ l was resolved in a 0.7% agarose gel and transferred onto nylon membrane. The membrane was hybridised using the partial DLIM1 cDNA (536 bp) as a probe under high stringency conditions (see Materials and Methods, 3.13.2.). The fraction containing a ~ 4.3 kb genomic fragment of interest was ligated into a pGEM-IRES-GFP-Stop vector (a gift from Dr. A. Hofmann) that had been digested with EcoRI and NdeI restriction enzymes and gel-eluted. EcoRI+NdeI digestion of the pGEM-IRES-GFP-Stop vector releases the insert 'IRES-GFP-Stop' and facilitates the elution from gel of the pGEM 5zf(+) vector backbone (Promega) from which the pGEM-IRES-GFP-Stop vector is derived. The ligated mixture was precipitated, resuspended in 10 μ l H₂O and used for transformation of competent *E. coli* MC1061 cells. The bacterial clones were screened by colony blotting (see Materials and Methods, 3.17.) using the partial DLIM1 cDNA as a probe. The positive clone obtained was designated as pgDLIM1 and sequenced using a combination of forward and reverse primers as indicated in Figure 9a..

3.19.4. DLIM1 gene replacement vector

For disruption of DLIM1 gene in the wild type AX2 cells, a DLIM1 gene replacement vector was constructed using the plasmid, pgDLIM1 containing the genomic DLIM1 fragment (Materials and Methods, 3.19.3.). Sequence and restriction analyses of the pgDLIM1 plasmid revealed the presence of two HincII restriction sites, one located at 145 bp downstream of the DLIM1 translation start codon, another located upstream of the DLIM1 coding region but within the genomic fragment. For construction of the DLIM1 gene replacement vector, a blasticidin resistance cassette was inserted at the HincII site located downstream of the DLIM1 translation start codon (Figure 30a). To achieve this, the pgDLIM1 plasmid was partially digested with HincII restriction enzyme for 6-7 min at 37°C, followed by EcoRI digestion and subsequently treated with Klenow enzyme to generate blunt ends. The blunt-ended vector was self-ligated to destroy the HincII site located upstream of the DLIM1 coding region and was designated as pgDLIM1 Δ HincII. Now the pgDLIM1 Δ HincII plasmid was digested with HincII restriction enzyme, the 5' overhangs generated were filled-in using Klenow enzyme, and the blunt-ended vector was treated with alkaline phosphatase. A blunt-ended 1.4 kb blasticidin resistance cassette (obtained as HindIII-XbaI fragment from pBsr Δ Bam vector) was then ligated into the linearised and blunt-ended pgDLIM1 Δ HincII plasmid. *E. coli* DH5 α cells were transformed with the ligation mixture and the clones obtained were checked for the desired insertion by colony blotting using the blasticidin resistance cassette as a probe. The positive clone obtained was verified by restriction analysis and was designated as pgDLIM1-k/o (or DLIM1 gene replacement construct). The DLIM1 gene replacement construct was then used for gene disruption in *Dictyostelium* wild type AX2 cells (Figure 30a).

3.19.5. Vector for expression of DLIM1 as a GFP-fusion protein

A vector for expression of DLIM1 as a GFP-DLIM1 fusion protein in *Dictyostelium* under the control of actin-15 promoter and actin-8 terminator was constructed using the vector pDEXRH (Faix *et al.*, 1992). To facilitate subcloning in the pDEXRH vector, the full length DLIM1 cDNA was obtained from pIC-ModDLIM1cDNA (Materials and Methods, 3.19.7.) as a XbaI+SacI fragment and cloned in the XbaI+SacI restricted pLITMUS29 vector (New

England Biolabs). The resultant plasmid was named as pLit-ModDLIM1cDNA. Now the full length DLIM1 cDNA was obtained from the pLit-ModDLIM1cDNA plasmid as a EcoRI fragment and was subcloned in-frame at the EcoRI site located at the C-terminus of the coding region of the green fluorescent protein (GFP) in the pDEXRH expression vector. The resulting plasmid was verified by sequencing using DLIM1-U primer (see figure 5 for orientation and position of the primer) and designated as pGFP-DLIM1.

3.19.6. N- and C-terminal DLIM1 deletion constructs

The N- and C-terminal DLIM1 deletion constructs were generated via a PCR based approach. Oligonucleotide primers were generated (depicted in Figure 20) to amplify DLIM1 cDNA sequences corresponding to a) NLIM (a.a. 1-58); b) NLIM and P-rich sequence (a.a. 1-111), which we refer to as NLIM-P; c) CLIM (a.a. 110-182) and d) CLIM and P-rich sequence (a.a. 57-182), which we refer to as CLIM-P. The primers were designed such that each amplified fragment was supplemented with an in-frame stop codon as well as flanking suitable restriction sites to facilitate subcloning (Materials and Methods, 1.9.). For amplification, pIC-ModDLIM1cDNA plasmid (Materials and Methods, 3.19.7.) containing the full-length DLIM1 cDNA was used as a template. The composition of the reaction mix as well as the reaction programme for PCR is similar to that described in Materials and Methods (3.19.1.). After amplification, the PCR product was cloned directly into the pGEM-T Easy vector (Promega) as described by the manufacturer. The NLIM, NLIM-P, CLIM and CLIM-P DNA fragments were subsequently obtained from the resultant vectors (named pGEM-NLIM, pGEM-NLIM-P, pGEM-CLIM and pGEM-CLIM-P, respectively) as EcoRI fragments and subcloned in-frame at the EcoRI site located at the C-terminus of the coding region of GFP in the pDEXRH expression vector. The resultant vectors were designated pGFP-NLIM, pGFP-NLIM-P, pGFP-CLIM and pGFP-CLIM-P.

3.19.7. Vector for expression of DLIM1 as a histidine-tagged protein

Expression of DLIM1 as a N-terminal hexa-histidine fusion-protein in *E.coli* was achieved by subcloning the DLIM1 cDNA sequence in-frame at the multiple cloning site of the pQE30 expression vector (Qiagen). To achieve this, the DLIM1 cDNA sequence was modified using a PCR-mediated approach employing DLIM1cDNA 5' and DLIM1cDNA 3'

primers (Materials and Methods, 1.9.). The DLIM1cDNA 5' primer was designed with engineered BglII, HindIII and BamHI restriction enzyme sites to facilitate subcloning. The DLIM1cDNA 3' primer corresponds to the region of the DLIM1 cDNA sequence with an internal MunI site (Figure 5). For amplification, pIC-DLIM1cDNA-2 plasmid DNA (Materials and Methods, 3.19.2.) was used as a template. The composition of the reaction mix as well as the reaction programme for PCR is similar to that described in Materials and Methods (3.19.1.). The amplified PCR product was digested with BglII+MunI restriction enzymes and the digested fragment was subcloned in a BamHI+MunI digested pIC-DLIM1cDNA-2 plasmid. The resultant plasmid containing the modified DLIM1 cDNA sequence was verified by sequencing using M13 reverse primer and designated as pIC-ModDLIM1cDNA. Now the full-length DLIM1 cDNA was obtained from the pIC-ModDLIM1cDNA plasmid as a BamHI-HindIII fragment and subcloned in a BamHI+HindIII digested pQE30 expression vector (Qiagen). The resultant plasmid that allows the expression of DLIM1 as a N-terminal hexa-histidine fusion protein was verified by sequencing with DLIM1-U primer and designated as pQE30-DLIM1.

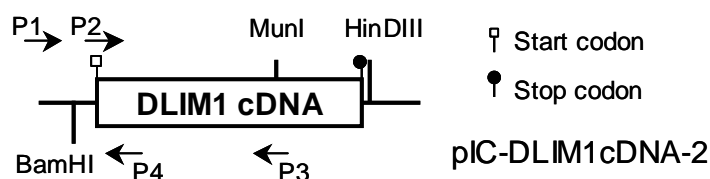


Figure 5. Schematic representation of the PCR strategy used for generation of restriction enzyme sites at the 5' end of the DLIM1 cDNA. The position as well as the orientation of the primers used for PCR- (P2 and P3) and sequencing- (P1 and P4) analyses are indicated by arrows. The location of relevant restriction enzymes in the DLIM1 cDNA sequence and the vector backbone are also indicated. Abbreviations used for primers: P1, M13 reverse; P2, DLIM1cDNA 5'; P3, DLIM1cDNA 3'; P4, DLIM1-U. Putative start and stop codons of the DLIM1 cDNA are depicted. Sequence of the individual primers is mentioned in Materials and Methods (1.9.).

3.19.8. Vector for expression of DLIM1 as a GST-fusion protein

For expression of DLIM1 as a GST-fusion protein, pGEX-2T, a GST expression vector was used. The full length cDNA of DLIM1 was obtained from pIC-ModDLIM1cDNA plasmid as a BamHI+EcoRI fragment and subcloned in-frame in a BamHI+EcoRI restricted pGEX-2T vector. The obtained pGEX-DLIM1 expression vector was verified by sequencing using

the DLIM1-U primer and electroporated into *E. coli* XL1 blue cells for expression of GST-DLIM1 fusion protein.

4. Biochemical methods

4.1. Preparation of total protein from *Dictyostelium*

1×10^7 to 5×10^8 *Dictyostelium* cells obtained from growth as well as different stages of development were washed once in Soerensen phosphate buffer. Total protein was prepared by lysing the pellet of cells in 500 μ l 1x SDS sample buffer. For detection of the protein expression in different cell lines, equal amount of protein (equivalent to 2×10^5 cells/lane to 1×10^7 cells/lane) was loaded onto a discontinuous SDS-polyacrylamide gel to allow for a quantitative comparison.

4.2. SDS-polyacrylamide gel electrophoresis

SDS-polyacrylamide gel electrophoresis was performed using the discontinuous buffer system of Laemmli (1970). Discontinuous polyacrylamide gel (10-15% resolving gel, 5% stacking gel) was prepared using glass-plates of 10 cm x 7.5 cm dimensions and spacers of 0.5 cm thickness. A 12-well comb was generally used for formation of the wells in the stacking gel. The composition of 12 resolving and 12 stacking gels is given in the table below:

Components	<u>Resolving gel</u>			<u>Stacking gel</u>
	10 %	12 %	15 %	5%
Acrylamide/Bisacrylamide (30:0.8) [ml]:	19.7	23.6	30	4.08
1.5 M Tris/HCl, pH 8.8 [ml]:	16	16	16	-
0.5 M Tris/HCl, pH 6.8 [ml]:	-	-	-	2.4
10 % SDS [μ l]:	590	590	590	240
TEMED [μ l]:	23	23	23	20
10 % APS [μ l]:	240	240	240	360
Deionised H ₂ O [ml]:	23.5	19.6	13.2	17.16

Protein solutions were mixed with suitable volumes of 2x SDS sample buffer, whereas protein pellets were resuspended in a suitable volume of 1x SDS sample buffer. The samples

were denatured by heating at 95°C for 5 min and loaded into the wells in the stacking gel. A molecular weight marker, which was run simultaneously on the same gel in an adjacent well, was used as a standard to establish the apparent molecular weights of proteins resolved on SDS-polyacrylamide gels. The molecular weight markers were prepared according to manufacturer's specifications. After loading the samples onto the gel, electrophoresis was performed in 1x gel-running buffer at a constant voltage of 100-150 V until the bromophenol blue dye front had reached the bottom edge of the gel or had just run out of the gel. After the electrophoresis, the resolved proteins in the gel were either observed by Coomassie blue staining or transferred onto a nitrocellulose membrane.

SDS-sample buffer:

<u>1x</u>	<u>2x</u>	
50	100	(mM) Tris/HCl, pH 6.8
2	4	(% v/v) SDS
10	20	(% v/v) glycerine
0.1	0.2	(% v/v) bromophenol blue
2	4	(% v/v) β -mercaptoethanol

Molecular weight markers:

LMW-Marker (Pharmacia)-
94, 67, 43, 30, 20.1, 14.4 kD

SeeBlue pre-stained marker (Novex)-
250, 98, 64, 50, 36, 30, 16, 6, 4 kD

Pre-stained marker (Bio-Rad)-
208, 115, 79.5, 49.5, 34.8, 28.3, 20.4, 7.2 kD

10x Gel-running buffer:

1.9 M glycine
0.25 M Tris/HCl, pH 8.8
1% SDS

4.2.1. Coomassie blue staining of SDS-polyacrylamide gels

After electrophoresis, the resolved proteins were visualised by staining the gel with Coomassie blue staining solution. The gel to be stained was placed in the Coomassie blue staining solution immediately after electrophoresis and the gel was allowed to stain at room temperature with gentle agitation for at least 30 min. After staining, the staining solution was poured off and destaining solution was added. The gel was then destained at room temperature with gentle agitation. For best results, the destaining solution was changed with fresh destaining solution several times until protein bands were clearly visible.

Coomassie blue staining solution:

0.1% Coomassie blue R250
50% ethanol
10% acetic acid
filter the solution before use

Destaining solution:

7% acetic acid
20% ethanol

4.2.2. Drying of SDS-polyacrylamide gels

After destaining, the gel was immersed in gel-dry buffer for 10-15 min at room temperature. Two sheets of cellophane (Novex), slightly bigger than the size of the gel, were also immersed in gel-dry buffer. The gel was then carefully placed between two moistened sheets of cellophane avoiding trapping of air-bubbles, clamped between the gel-drying frames (Novex) and dried overnight at room temperature.

Gel-drying buffer:

25% ethanol
5% glycerine

4.3. Western blotting using the semi-dry method

The proteins resolved by SDS-polyacrylamide gel electrophoresis (SDS-PAGE) were electrophoretically transferred from the gel to a nitrocellulose membrane by using the method described by Towbin *et al.* (1979) with little modifications. The transfer was performed using Towbin's buffer in a semi-dry blot apparatus (Bio-Rad) at a constant voltage of 10 V for 35-45 min. The instructions provided along with the semi-dry apparatus were followed in order to set up the transfer.

Towbin's buffer (transfer buffer):

39 mM glycine
48 mM Tris/HCl, pH 8.3
0.0375% SDS
20% methanol or ethanol

4.3.1. Ponceau S staining of western blots

To check for the transfer of proteins onto the nitrocellulose membrane, the membrane was stained in 10-15 ml of Ponceau S solution for 2-5 min at room temperature. After staining,

the membrane was removed from the Ponceau S solution and rinsed with deionised water to destain until bands of proteins were visible and the background was clear. The position of the constituent proteins of the molecular weight marker and/or the protein of interest was marked and the membrane was again washed with several changes of deionised water to completely remove the stain. Now the membrane carrying the transferred proteins was used for immunodetection (see Materials & Methods, 4.4.) of specific protein.

Ponceau S solution:

1 ml Ponceau S concentrate (Sigma)
19 ml distilled H₂O

Ponceau S concentrate (Sigma):

2% w/v Ponceau S in 30% w/v TCA
and 30% w/v sulfosalicylic acid

4.4. Immunodetection of membrane-bound proteins

The western blot was immersed in blocking buffer (1x NCP) and the blocking was performed with gentle agitation either overnight at room temperature or for 2-3 h at room temperature with several changes of 1x NCP. After blocking, the blot was incubated at room temperature with gentle agitation with either commercially available primary antibodies at a proper dilution (in 1x NCP) for 1-2 h, or hybridoma-supernatant for overnight. After incubation with primary antibody, the blot was washed 5-6 times with 1x NCP at room temperature for 5 min each with repeated agitation. Following washings, the blot was incubated for 1 h at room temperature with a proper dilution (in 1x NCP) of enzyme conjugated secondary antibody directed against the primary antibody. The secondary antibody was conjugated with either Horse radish peroxidase (HRP) or alkaline phosphatase (AP). After incubation with secondary antibody, the blot was washed as described above. After washings, substrate reaction was carried out depending upon the enzyme coupled to the secondary antibody. Enzymatic chemi-luminescence (ECL) detection system (see Materials & Methods 4.4.1.) was used for blots incubated with HRP-conjugated secondary antibody, whereas, the BCIP/NBT colour development substrate reaction was used for blots incubated with AP-conjugated secondary antibody (see Materials & Methods 4.4.2.).

4.4.1. Enzymatic chemi-luminescence (ECL) detection system

The blot was incubated in ECL-detection-solution for 1-2 min and then wrapped in a saran wrap after removing the excess ECL-detection-solution. Now an X-ray film was exposed to

the wrapped membrane for 1-30 min and the film was developed to observe the immunolabelled protein.

ECL-detection-solution:

2 ml 1 M Tris/HCl, pH 8.0
200 μ l 250 mM 3-aminonaphthylhydrazide in DMSO
89 μ l 90 mM p-Coumaric acid in DMSO
18 ml deionised H₂O
6.1 μ l 30% H₂O₂ (added just before using)

4.4.2. BCIP/NBT colour development substrate reaction

The blot was developed using 5-bromo-4-chloro-3-indolyl-phosphate (BCIP) as a substrate and nitro blue tetrazolium (NBT) as a colour indicator. The blot was incubated in 10 ml of BCIP/NBT substrate solution at room temperature with gentle agitation for 5 min or until sufficient colour development has occurred. The reaction was stopped by washing the membrane several times with deionised water and the membrane was allowed to dry on a piece of blotting paper.

BCIP/NBT substrate solution:

66 μ l 50mg/ml NBT (Promega)
33 μ l 50mg/ml BCIP (Promega)
10 ml 0.1M Na₂CO₃, pH 10.0

4.5. Expression and purification of histidine-tagged DLIM1

E. coli strain M15[pREP4] cells (obtained from Qiagen) were transformed with expression vector pQE30-DLIM1 (Materials and Methods, 3.19.7.) for expression of DLIM1 as a histidine-tagged protein. Single colonies (5-10) of recombinant cells were picked and grown overnight in 10 ml of LB medium containing ampicillin (100 μ g/ml) and kanamycin (25 μ g/ml) at 37°C and 250 rpm. 5 ml of the overnight grown culture was inoculated into 45 ml of fresh LB medium containing ampicillin (100 μ g/ml) and kanamycin (25 μ g/ml). The culture was then allowed to grow at 37°C till an OD₆₀₀ of 0.5-0.6 was obtained. Now the induction of expression was initiated by adding IPTG. In order to standardise the conditions of maximum expression of the fusion protein, induction was performed with varying

concentrations of IPTG (0.5 mM, 1.0 mM and 2 mM final concentration) at two different temperature conditions (30°C and 37°C). Samples of 1 ml were withdrawn at different hours of induction (0 h, 1 h, 2 h, 3 h, 4 h, 5 h and 6 h), the cells were pelleted and resuspended in 100 µl of 1x SDS sample buffer. The samples were denatured by heating at 95°C for 5 min and 10 µl of each sample were checked on a 12% SDS-polyacrylamide gel. Expression of the histidine-tagged DLIM1 protein was analysed by Coomassie staining of the SDS-polyacrylamide gel as well as by western blotting using anti-RGS(H)₄ antibody (Qiagen). On the basis of these results large-scale expression (in 1-2 L culture volume) of histidine-tagged DLIM1 protein was performed. The histidine-tagged DLIM1 protein was purified from the soluble bacterial extracts after 5 h of induction with 2 mM IPTG at 37°C under denaturing conditions using a Ni-NTA agarose column as recommended by the manufacturer (Qiagen).

4.6. Expression and purification of GST-DLIM1 fusion protein

E. coli strain XL1 blue cells were transformed with expression vector pGEX-DLIM1 (Materials and Methods, 3.19.8.) for expression of DLIM1 as a glutathione S-transferase (GST)-fusion protein under the control of tac promoter.

4.6.1. Small-scale protein expression

Small-scale expression of GST-DLIM1 fusion protein was performed to check the efficiency of expression of various recombinant clones as well as to standardise the conditions of expression before proceeding for the large-scale expression and purification of GST-DLIM1 fusion protein. Single colonies (5-10) of recombinant cells were picked and grown overnight in 10 ml of LB medium containing ampicillin (100 µg/ml) at 37°C and 250 rpm. 5 ml of the overnight grown culture was inoculated into 45 ml of fresh LB medium containing ampicillin (100 µg/ml). The culture was then allowed to grow at 37°C till an OD₆₀₀ of 0.5-0.6 was obtained. Now the induction of expression was initiated by adding IPTG. In order to standardise the conditions of maximum expression of the fusion protein, induction was performed with varying concentrations of IPTG (0.1 mM, 0.5 mM and 1.0 mM final concentration) at two different temperature conditions (30°C and 37°C). Samples of 1 ml were withdrawn at different hours of induction (0 h, 1 h, 2 h, 3 h, 4 h and 5 h), the cells were

pelleted and resuspended in 100 μ l of 1x SDS sample buffer. The samples were denatured by heating at 95°C for 5 min and 10 μ l of each sample were checked on a 12% SDS-polyacrylamide gel. Expression of the GST-DLIM1 fusion protein was analysed by Coomassie staining of the SDS-polyacrylamide gel as well as by western blotting using anti-GST antibody.

4.6.2. Large-scale protein expression

Large-scale expression of GST-DLIM1 fusion protein was performed on the basis of results obtained with small-scale expression procedures as described above. Overnight culture was started with a recombinant clone, showing maximum level of expression, in 50 ml LB medium containing ampicillin (100 μ g/ml) at 37°C and 250 rpm. The next day, 50 ml of the overnight grown culture was inoculated into 450 ml fresh LB medium containing ampicillin (100 μ g/ml) and the culture was allowed to grow at 37°C till an OD₆₀₀ of 0.5-0.6 was obtained. Now the induction of expression was initiated by adding 100 mM IPTG to a final concentration of 1.0 mM and the induction was performed for 3 h at 37°C and 250 rpm.

4.6.3. Preparation of cell homogenate

After the induction, the culture was transferred to a 500 ml centrifuge bottle (Beckman) and the cells were collected by centrifugation at 4,000 rpm (Beckman Avanti J25, rotor JA-10) for 10 min at 4°C. The pellet was resuspended in 10 ml of ice-cold lysis buffer containing lysozyme (1 mg/ml) and Triton X-100 (0.5%) and supplemented with fresh protease inhibitors, collected in a 50 ml tube and incubated on ice for 20 min. Incubation in lysis buffer was followed by a brief sonication (3 pulses of 10 s each with a 15 s rest between each pulse), keeping the tube immersed in ice. Sonication was followed by homogenisation using a Dounce homogeniser for 2-3 min in order to ensure complete and efficient cell lysis. The lysate was transferred to a pre-cooled fresh 50 ml centrifuge tube and centrifuged at 5,000 rpm (Beckman Avanti J25, rotor JA-25.50) for 10 min at 4°C. The supernatant was transferred to a fresh chilled tube and was directly used for elution of the fusion protein. Both the pellet as well as the supernatant were analysed for the presence of fusion protein by SDS-PAGE analysis and/or western blotting using anti-GST antibody. The pellet was

resuspended in 10 ml of lysis buffer and 100 μ l of this pellet fraction was added to 100 μ l of 2x SDS sample buffer. Likewise, 100 μ l of the supernatant was added to 100 μ l of 2x SDS sample buffer. The samples were then denatured by heating at 95°C for 5 min and 10 μ l of each sample was checked on a 12 % SDS-polyacrylamide gel.

Lysis buffer:

50 mM Tris/HCl, pH 7.5
100 mM NaCl
5 mM MgCl₂
0.5 % Triton X-100
add fresh before use-
1 mM DTT
1 mg/ml lysozyme
1 mM DTT
protease inhibitors

Protease inhibitors:

1 mM PMSF
1.4 μ g/ml pepstatin
5.0 μ g/ml leupeptin

4.6.4. Elution of GST-DLIM1 fusion protein by affinity chromatography

GST-DLIM1 fusion protein was purified from the supernatant of the cell-lysate (see Materials and Methods, 4.6.3.) using affinity chromatography. The supernatant (~10 ml) was supplemented with fresh protease inhibitors and then incubated with 500 μ l of a 50% slurry (v/v in PBS) of glutathione agarose beads at 4°C on a rotary wheel for 1-2 h. After incubation, the beads were pelleted by centrifugation at 3,000 rpm (Sorvall RT7) for 5 min at 4°C and the supernatant was collected in a separate tube for later SDS-PAGE analysis. The beads were carefully washed 4-5 times with 5 ml of cold wash buffer and finally resuspended in 1 ml of cold wash buffer and transferred to a 1.5 ml centrifuge tube. The beads were again pelleted at maximum speed in a microcentrifuge at 4°C for 15-20 s and the supernatant was carefully removed. Now the GST-DLIM1 fusion protein was eluted from the beads by incubating the beads with 500-700 μ l of release buffer on a rotary wheel at 4°C for 5 min. After 5 min of incubation with the release buffer, the beads were pelleted as described above and the supernatant containing the eluted GST-DLIM1 fusion protein was carefully collected. The elution of GST-DLIM1 fusion protein from the beads was repeated 3-4 times and the elute-fractions were collected in separate 1.5 ml centrifuge tubes and stored at -20°C. Each of the elute-fractions was analysed by SDS-PAGE and/or western blotting using anti-GST antibody. 20 μ l of 2x SDS sample buffer was added to 20 μ l of each

elute-fractions. The sample was denatured by heating at 95°C and 20 µl of the sample was loaded onto a 12% SDS-polyacrylamide gel.

Release buffer:

50 mM Tris/HCl, pH 8.0
150 mM NaCl
5 mM MgCl₂
add fresh before use-
1 mM DTT
10 mM reduced glutathione

Wash buffer:

50 mM Tris/HCl, pH 7.5
100 mM NaCl
5 mM MgCl₂

50% slurry (v/v) of glutathione-agarose beads:

200 mg of glutathione-agarose beads (Sigma)
add 20 ml PBS
incubate on a rotary wheel at 4°C for 1-2 h
wash twice with PBS (3,000 rpm, 5 min, 4°C)
finally add equal volume of PBS to swollen beads
store at 4°C

4.6.5. Lyophilization of eluted GST-DLIM1 fusion protein

The elute fractions containing the GST-DLIM1 fusion protein were pooled and dialysed overnight against 100 vol. 10 mM ammonium bicarbonate solution, pH 8.0, with several changes of dialysis buffer. The next day, the dialysate was aliquoted in five 1.5 ml tubes, quickly frozen on dry-ice/ethanol and lyophilized overnight in a lyophilizer (Lyovac GT 2-E, Finn Aqua). The lyophilised protein was dissolved in a suitable buffer before use.

4.7. Expression and purification of GST

GST protein was expressed in order to screen hybridoma clones secreting antibodies specific to the GST protein as well as for the selection of the hybridoma clones secreting antibodies specific to the DLIM1 part of the GST-DLIM1 fusion protein. Purified GST protein was also used as a control in other biochemical assays performed with GST-DLIM1 fusion protein. *E. coli* strain BL21 (DE) was transformed with a GST expression vector pGEX-2T (Pharmacia) and the GST protein was expressed and purified essentially according to the method described above (Materials and Methods, 4.6.1. to 4.6.4.).

4.8. Quantification of protein

Colorimetric method described by Lowry *et al.* (1951) was used for quantification of protein. Protein sample (5-50 μ l) and different concentrations of BSA (1-25 μ g) were taken in separate 1.5 ml tubes and diluted with solution I to bring the final volume to 1 ml in each tube. After incubating the tubes at room temperature for 10 min, 100 μ l of solution II was added to each tube, the contents in the tubes were immediately mixed by brief vortexing and the tubes were allowed to stand at room temperature for 20 min. Thereafter, OD of the sample was measured at 660 nm and the concentration of protein in the sample was estimated from a standard curve obtained by plotting OD₆₆₀ values of 1-25 μ g BSA.

Solution I (freshly prepared):

0.2 ml 2% CuSO₄·5H₂O
0.2 ml 4% potassium sodium tartrate
9.6 ml 3% Na₂CO₃ in 0.1 N NaOH

Solution II (freshly prepared):

1 vol. Folin-Ciocalteu reagent
2 vol. distilled H₂O

4.9. Triton X-100 extraction of *Dictyostelium* cells (Prassler *et al.*, 1997)

Growth phase GFP-DLIM1 expressing *Dictyostelium* cells were washed and resuspended in two volumes of lysis buffer [80 mM PIPES, pH 6.8, 30% glycerol, 0.5 mM DTT, 5 mM EGTA, 5 mM MgCl₂, 1 mM PMSF, Protease inhibitor cocktail (10 μ g/ml of each inhibitor)] and lysed with 1% Triton X-100 for 5 min at room temperature. Cytoskeleton associated proteins that are largely insoluble were pelleted at 4°C for 3 min at 14,000 x g. The supernatant was carefully collected and the pellet was washed twice with lysis buffer without detergent and finally resuspended in original volume of lysis buffer without detergent. Proteins of the Triton X-100-soluble and -insoluble fractions were extracted in 2x SDS sample buffer and resolved on a 12% SDS-polyacrylamide gel. The resolved proteins were either stained with Coomassie blue or blotted onto a nitrocellulose membrane and the blot was subsequently labelled with anti-GFP antibody (Clontech).

4.10. Actin-sedimentation assays (Prassler *et al.*, 1997)

Actin from *D. discoideum* AX2 cells was procured from Prof. Noegel, actin purified from rabbit skeletal muscle was obtained from Dr. E. Korenbaum and α -actinin was a kind gift of

Prof. Schleicher. GST-DLIM1, GST and α -actinin proteins were dialyzed overnight at 4°C against 20 mM imidazole buffer (pH 7.0) containing 100 mM KCl and 2 mM MgCl₂. All the proteins were centrifuged at ~ 1,25,000 x g (45,000 rpm in a TLA 45 rotor; Optima TLX ultracentrifuge, Beckman) for 30 min at 4°C to remove aggregates. The actin-sedimentation assay was performed in a total volume of 100 μ l with 60-80 μ g of GST-DLIM1 fusion protein (or 20 μ g of GST) added to each assay mixture. G-actin (23 μ g) from *D. discoideum* or rabbit skeletal muscle was polymerised in the presence or absence of GST-DLIM1 (or GST) by the addition of 10x concentrated polymerisation buffer (same as dialysis buffer plus 10 mM EGTA or 2 mM CaCl₂) for 1 h at room temperature. For some experiments, pre-cleared α -actinin (40 μ g) was also added to the assay mixture. Binding to F-actin was determined by high-speed centrifugation at ~ 1,25,000 x g (45,000 rpm in a TLA 45 rotor; Optima TLX ultracentrifuge, Beckman) for 30 min at 15°C. 80 μ l of the supernatant was carefully collected from the top and mixed with 20 μ l of 5x SDS sample buffer. The pellet was carefully washed with 100 μ l of 1x polymerisation buffer, resuspended in 100 μ l of 1x polymerisation buffer and mixed with 25 μ l of 5x SDS sample buffer. Proteins in the supernatant and pellet fractions were separated by SDS-PAGE and stained with Coomassie blue.

5. Immunological methods

5.1. Generation of monoclonal antibodies

5.1.1. Immunization of mice

Immunization of mice with histidine-tagged DLIM1 protein:

The partially-purified histidine-tagged DLIM1 (~ 100 μ g) was resolved on a 12% SDS-PAGE gel. The gel was immersed in a chilled 0.1 M KCl solution for 30-60 min at 4°C to visualise the histidine-tagged DLIM1 protein. The gel-slice containing the histidine-tagged DLIM1 protein was cut out and homogenised in PBS. Two female BALB/c mice (6-7 weeks old) were immunized intraperitoneally with this gel suspension. The mice were boosted three weeks after the first immunization with the freshly prepared gel suspension as described

above. Two weeks later and three days before the fusion, the mice were again boosted by injecting the freshly prepared gel suspension.

Immunization of mice with GST-DLIM1 fusion protein:

Two female BALB/c mice (7 weeks old) were immunized intraperitoneally with purified GST-DLIM1 fusion protein (see Materials and Methods 4.6.5.). The first injection was performed with a 1:1 emulsion (200 μ l/mouse) of 20 mM Tris, pH 8.0, containing \sim 100 μ g of the GST-DLIM1 antigen and complete Freund's adjuvant. The mice were boosted three weeks after the first immunization by injecting an emulsion (200 μ l/mouse) of equal volumes 20 mM Tris, pH 8.0, containing \sim 50 μ g of the GST-DLIM1 antigen and incomplete Freund's adjuvant. Two weeks later and three days before the fusion, the mice were again boosted by injecting 50 μ g of the antigen in 200 μ l of PBS.

5.1.2. Preparation of mouse feeder cells for fusion and cloning

One day prior to seeding of hybridomas from cell fusion or cloning procedures, mouse feeder cells (macrophages and other cells) were isolated. In general, 3-5 BALB/c mice per fusion were sacrificed for the isolation of peritoneal feeder cells. The mouse was sacrificed by cervical dislocation, disinfected with 70% ethanol and then laid on a dissecting board. The peritoneal cavity of the mouse was exposed by snipping its skin at diaphragm level and pulling the skin back. Now 10 ml of cold Normal medium (NM) was injected into the peritoneal cavity using a 10 ml syringe and an 18 G needle and the peritoneal feeder cells were harvested by withdrawing as much solution as possible into the syringe. This step was repeated two more times and the feeder cells were collected in a pre-cooled 50 ml centrifuge tube. The feeder cells were then pelleted by centrifugation at 1,000 rpm for 5 min at 4°C (Beckman CS-6R) and the pellet was washed twice with 25 ml NM. The feeder cells were finally resuspended in an appropriate volume of NM or 1x HT medium.

5.1.3. Fusion

Three days after the last immunization, spleen cells were harvested from the immunized mouse and fused with myeloma cells. Two different myeloma cell lines, PAIB₃Ag81 (PAI) and X63-Ag8.653 (Ag8) were used for fusion. On the day of fusion, both the myeloma cell

lines were harvested in their log phase of growth and collected in two separate 50 ml sterile centrifuge tubes. The cells were pelleted by centrifugation at 1,500 rpm for 5 min (Beckman CS-6R) and washed twice with 25 ml RPMI 1640 medium (w/o HEPES, w/o glutamine). After washings, both types of myeloma cells were resuspended separately at a density of 2.5×10^6 cells/ml in 10 ml of RPMI 1640 (w/o HEPES, w/o glutamine).

For isolation of spleen cells, one of the immunized mice was sacrificed by cervical dislocation and disinfected by immersing in 70% ethanol. The spleen was then aseptically removed according to standard protocols and transferred into a 60 mm petri dish containing 5 ml of cold RPMI 1640 (w/o HEPES, w/o glutamine). Now the spleen in petridish was taken to a sterile hood. The surface fats and other tissues adhering to the spleen were carefully removed using a sterile forceps and scissors and during this process, the spleen was transferred 2-3 times into a fresh 60 mm petri dish containing 5 ml of cold RPMI 1640 (w/o HEPES, w/o glutamine). After complete removal of adipose tissues and other adhering tissues, the spleen was transferred to a fresh 60 mm petri dish containing 5 ml of cold RPMI 1640 (w/o HEPES, w/o glutamine). Now the spleen was cut into small pieces with sterile scissors, followed by shearing the small pieces with sterile forceps. Now the cell suspension was collected, leaving the larger spleen pieces in the petri dish, and filtered through a sterile cotton-plugged syringe (10 ml). The left-over larger spleen pieces were again resuspended in 5 ml of cold RPMI 1640 (w/o HEPES, w/o glutamine) and were gently homogenised in a sterile homogeniser. The homogenised suspension was then filtered through the sterile cotton-plugged syringe and the filtrate containing the spleen cells was collected in a 50 ml centrifuge tube. The spleen cells were then pelleted by centrifugation at 1,500 rpm for 5 min (Beckman CS-6R) and the supernatant was aspirated with a sterile pasteur pipette. The spleen cells were then washed twice with 25 ml of RPMI 1640 (w/o HEPES, w/o glutamine) and finally resuspended in 10 ml of RPMI 1640 (w/o HEPES, w/o glutamine) at a density of $\sim 1 \times 10^7$ cells/ml.

For fusion, the spleen cells were divided into two halves and mixed with the two different myeloma cells (spleen cells : myeloma = 2 : 1) in separate tubes and centrifuged at 1,500 rpm for 5 min (Beckman CS-6R). The supernatant was carefully aspirated and the pellet was loosened by gentle tapping and then mixed with a heat-closed Pasteur pipette. To the pellet, 0.5 ml of pre-warmed (37°C) PEG 4,000 solution (Sigma) was added and the tube was

incubated at 37°C in a waterbath with gentle shaking for exactly 1 min. Thereafter, the tube was incubated at room temperature for 1 min and over the next 5 min, 10 ml of RPMI 1640 (w/o HEPES, w/o glutamine) was slowly added to the tube with gentle shaking at 37°C in a waterbath. Now the tube was incubated on ice for 10-15 min in order to stabilise the fused cells. The fused cells were then pelleted by centrifugation at 1,500 rpm for 5 min (Beckman CS-6R) and the pellet was resuspended in 125 ml NM. Now the fused cells were added (0.5 ml/well) to 24-well tissue culture plates that have been coated with mouse feeder cells 24 h prior to fusion. The plates were incubated in a CO₂ incubator at 37°C with 5% CO₂ and 95% relative humidity. The next day, selection of hybridoma cells was started by adding 0.5 ml of 3 x HAT medium to each well and the plates were incubated for another 2 days. Thereafter, the medium was changed every alternate day with 1x HAT medium (1 ml/well) and the hybrids were grown in 1x HAT medium for 2 weeks after fusion. After 2 weeks, the medium was changed to HT medium and the hybrids were grown in HT medium until the completion of cloning procedures.

5.1.4. Screening of hybridoma clones

When the hybridoma cell growth had covered 10% to 50% of the surface areas of the wells, the hybridoma-supernatants were collected and screened for DLIM1 specific antibody production. Screening of hybridoma clones obtained from spleen cells of mice immunized with GST-DLIM1 fusion protein was performed initially by indirect enzyme linked immunosorbent assay (indirect ELISA) and those which gave a positive reaction in ELISA were further confirmed by immunoblotting. The hybridoma clones obtained from spleen cells of mice that were immunized with histidine-tagged DLIM1 were screened directly by stripe test (immunoblotting).

5.1.4.1. Indirect ELISA for screening of hybridoma clones

The purified GST-DLIM1 fusion protein was diluted to 0.4 µg/ml in carbonate buffer and 100 µl of this antigen solution was coated into each well of the 96-well ELISA plate (Nunc). The plate was incubated overnight at 4°C. The next day, unbound antigen was washed out by inverting the plate and flicking the wells, followed by 3 washings with wash buffer for 10 min each. Now the residual binding capacity of the wells was blocked by adding 100 µl of

blocking buffer to each well and incubating the plates at room temperature for 1 h. After blocking, the plate was washed 3 times with wash buffer for 10 min each and after each washing, the residual liquid in the plate was removed by gently flicking the plate face down onto several paper towels lying on the benchtop. Now the hybridoma-supernatants to be evaluated were added to the wells in duplicate (100 µl/well) and the plate was incubated at room temperature for 2 h. The incubation with hybridoma-supernatants was followed by 4 washings with wash buffer as described above. After usual washings, 100 µl of alkaline phosphatase conjugated goat anti-mouse IgG (diluted 1:10,000 in blocking buffer) was added to each well and the plate was again incubated at room temperature for 1 h. Following incubation in secondary antibody, the plate was again washed 4 times with wash buffer as described above and 100 µl of the chromogenic substrate, p-nitro phenyl phosphate (pNPP, Sigma) solution, was added to each well and the plate was incubated in the dark for 30 min to 1 h at room temperature. Hydrolysis of the pNPP substrate was detected by the appearance of a yellow colour and was quantitatively monitored with an ELISA-plate reader using a 405 nm filter.

Blocking buffer:

5% bovine serum albumin
0.05% Triton X-100
0.02% NaN₃
in 1x PBS, pH 7.4

Carbonate buffer, pH 9.4:

1.59 g Na₂CO₃
0.2 g NaN₃
2.93 g NaHCO₃
adjust to pH 9.4
add deionised H₂O to make 1 liter

Wash buffer:

0.05% Triton X-100
0.02% NaN₃
in 1x PBS, pH 7.4

pNPP substrate solution:

Sigma Fast tablet sets for 5 ml or 20 ml solution were used according to manufacturer's specifications.

5.1.4.2. Stripe test for screening of hybridoma clones

Whole cell homogenate of the *E. coli* cells expressing the GST-DLIM1 fusion protein and the GST protein alone or the histidine-tagged DLIM1 protein (see Materials and Methods, 4.5., 4.6. and 4.7.) were loaded onto a 12% SDS-polyacrylamide gel (front-running) and after resolving, the proteins were transferred onto a nitrocellulose membrane. After overnight blocking in 1x NCP buffer, the immunoblotting was performed as described in Materials and Methods (4.4.) except that the membrane containing the transferred protein

was cut into several small stripes (~30 stripes/mini-gel) and then each stripe was separately incubated with the hybridoma-supernatants at room temperature for overnight. The next day, stripes were washed 4 times with 1x NCP for 5 min each and then incubated with alkaline phosphatase conjugated goat anti-mouse IgG (1:5,000 in 1x NCP buffer). After usual washings, BCIP/NBT colour development substrate reaction was carried out.

5.1.5. Cloning of hybridoma cells

Hybridoma cells that were positive by ELISA and immunoblotting were selected for cloning in order to establish a single hybridoma cell line. The day before cloning, mouse feeder cells were isolated (Materials and Methods, 5.1.2.) and checked for possible contamination by incubating 100-200 μ l of the feeder cells in a 96 well microtiter plate for overnight in a CO₂ incubator at 37°C with 5% CO₂ and 95% relative humidity. For cloning, 96 well microtiter plate was prepared by adding 3-4 drops of 1x HT medium or NM (depending upon the type of medium in which the hybridoma cells to be cloned are present) in A1 to A4 wells of the microtiter plate. Hybridoma cells to be cloned were grown to log phase in 24 well plates and were resuspended in 1 ml fresh 1x HT medium or NM. A drop of the hybridoma cell suspension was then added to the A1 well of the microtiter plate using a sterile cotton-plugged pasteur pipette, mixed well by gentle pipetting and then transferred a drop from the well A1 to A2. Likewise, serial dilutions of the hybridoma cells were prepared in the wells A1 to A4 and then observed under the inverted microscope. The well showing 20-25 cells/microscopic field was selected for cloning. Using a sterile cotton-plugged pasteur pipette, a drop of the cell suspension was carefully placed in the centre of each well of the microtiter plate (maximum 2-3 rows at a time to avoid drying of the drops) and the wells containing the drop were immediately observed under the inverted microscope. The wells that exhibited only one hybridoma cell/well (or per drop) were marked and filled with mouse feeder cell suspension. This procedure of cloning was repeated till at least 20 single-cells per hybridoma cell line were cloned. The microtiter plates were then covered with saran wrap and incubated in a CO₂ incubator (37°C, 5% CO₂, 95% relative humidity). After 1.5 to 2 weeks, the wells exhibiting 10-50% confluent cell growth were assayed for specific antibody by checking their hybridoma supernatants by immunoblotting (Materials and Methods, 5.1.4.2.) and fresh medium (NM or 1x HT medium) was added to the wells. The positive

subclones from each clone were expanded by transferring into a 24 well plate (2-3 subclones/24 well plate to avoid cross-contamination) and the plates were incubated in a CO₂ incubator (37°C, 5% CO₂, 95% relative humidity). Medium in the 24 well plate was changed every second day and when the cell-growth in the well was >50% confluent, cells were either frozen in a cryotube (Materials and Methods, 5.1.6.) or transferred to a 25 cm² tissue culture flask (in 5 ml NM). From 25 cm² tissue culture flask, the cells were transferred to a 75 cm² tissue culture flask (in 10 ml NM) and then to a 175 cm² tissue culture flask (in 50 ml NM), each time when the cell-growth in the flask was >50% confluent. Every alternate day, the hybridoma supernatant was collected and fresh medium was added.

5.1.6. Freezing and recovery of hybridoma cell lines

Freezing of hybridoma cell lines:

Hybridoma cells to be frozen were, in general, harvested in the log phase of growth. When the cell-growth in a 24 well plate or a 25 cm² tissue culture flask was >50% confluent, the hybridoma supernatant was replaced with the fresh medium (1 ml/well or 5 ml/flask) in order to remove the dead cells. Cells were then resuspended in the medium, collected in a sterile 15 ml centrifuge tube and incubated on ice. After 30 min of incubation on ice, the cells were pelleted by centrifugation at 1,200 rpm (Beckman CS-6R) for 5 min at 4°C. The supernatant was aspirated and the pellet was resuspended in equal volume of cold freezing medium. Aliquots of 1 ml/cryotube (Nunc) were prepared and incubated overnight at -80°C in a thermal box to freeze the cells slowly (~2°C/min). The next day, the frozen aliquots were transferred to liquid nitrogen for long-term storage.

Recovery of frozen cell lines:

The cryotubes were taken out of the liquid nitrogen and immediately thawed at 37°C in a waterbath. In order to remove DMSO, the cells were transferred to a 15 ml centrifuge tube containing 12 ml of NM and centrifuged at 1,200 rpm for 5 min at 4°C. The supernatant was aspirated and the cell pellet was resuspended in 1 ml NM and transferred to a well in 24 well plate. The plate was incubated overnight at 37°C in a CO₂ incubator with 5% CO₂ and 95% relative humidity. The next day, dead cells and traces of DMSO were removed by changing the medium in the well. Thereafter, the cells were propagated as described earlier.

5.2. Indirect immunofluorescence of *Dictyostelium* cells

5.2.1. Preparation of *Dictyostelium* cells

Dictyostelium cells were grown in shaking culture to a density of $2-4 \times 10^6$ cells/ml. Desired amount of cells were collected in a centrifuge tube, washed once with Soerensen phosphate buffer and finally resuspended in Soerensen phosphate buffer at 1×10^6 cells/ml. 400 μ l of the cell suspension was then pipetted onto a 18 mm acid-washed glass coverslip lying on a parafilm-covered glass-plate resting in a humid-box. Cells were allowed to attach to the glass coverslip for 15 min. Thereafter, cells attached onto the coverslip were fixed immediately by one of the fixation techniques described below.

5.2.2. Fixation of *Dictyostelium* cells

Described below are two fixation techniques that work well for preserving cytoskeletal elements in *Dictyostelium*.

5.2.2.1. Methanol fixation

After the cells have attached to the coverslip, the supernatant was aspirated and the coverslip was dipped instantaneously into the pre-chilled (-20°C) methanol in a petri dish and incubated at -20°C for 10 min. The coverslip was then taken out from methanol and placed on the parafilm in the humid-box with the cell-surface facing upwards, followed by 3 washings (each with 500 μ l of PBG, pH 7.4, for 5 min at room temperature) and immunolabelling as described in Materials and Methods (5.2.3.).

PBG (pH 7.4):

- 0.5 % bovine serum albumin
- 0.1 % gelatin (cold-water fish skin)
- in 1x PBS, pH 7.4

5.2.2.2. Picric acid-paraformaldehyde fixation

After the cells have attached to the glass coverslips, the supernatant was gently aspirated from the edge of the coverslip and 200 μ l of freshly prepared picric acid-paraformaldehyde

solution was directly added onto the cell-surface of the coverslip and incubated at room temperature for 30 min. After incubation, the picric acid-paraformaldehyde solution was aspirated and the coverslip was washed once with Soerensen phosphate buffer for 5 min at room temperature. The coverslip was then picked up with a fine forceps and swirled in 10 mM PIPES buffer, pH 6.0, followed by blotting off the excess solution from the coverslip with a tissue paper. Now the coverslip was swirled in PBS/glycine and placed on a parafilm-covered glass-plate resting in a moist chamber with the cell-surface facing upwards. The coverslip was then washed with 500 μ l PBS/glycine for 5 min followed by post-fixation with 500 μ l 70% ethanol for 10 min. This was followed by 2 washings with 500 μ l PBS/glycine for 5 min each followed by 2 washings with 500 μ l of PBG for 15 min each. After washings, the cells were immunolabelled as discussed in Materials and Methods (5.2.3.).

PBS/glycine:

500 ml PBS
3.75 g glycine
filter sterilized
store at -20°C

20 mM PIPES buffer, pH 6.0:

0.605 g PIPES
in 100 ml distilled H_2O
adjust to pH 6.0
filter sterilized

Picric acid-paraformaldehyde solution:

0.4 g paraformaldehyde was dissolved in 5 ml dd H_2O by stirring at 40°C and adding 3-4 drops of 2M NaOH. After dissolving, the volume was adjusted to 7 ml with dd H_2O . To this paraformaldehyde solution, 10 ml of 20 mM PIPES buffer, pH 6.0, and 3 ml of saturated picric acid was added and the pH was finally adjusted to 6.5.

5.2.3. Immunolabelling of fixed cells

The coverslip containing the fixed cells were incubated with 400 μ l of the desired dilution (in PBG) of primary antibody for 1-2 h in the humid-box at room temperature. After incubation, the excess unattached antibody was removed by washing the coverslip 6 times with PBG for 5 min each. Now the coverslip was incubated for 1 h with 400 μ l of a proper dilution (in PBG) of Cy3-conjugated secondary antibody. Following the incubation with secondary antibody, two washings with PBG for 5 min each followed by three washings with PBS for 5 min each were performed. After washings, the coverslip was mounted onto a glass slide (see Materials and Methods, 5.2.4.).

5.2.4. Mounting of coverslips

After immunolabelling of the fixed cells, the coverslip was swirled once in deionised water and the extra water was soaked off on a soft tissue paper. Now a drop of gelvatol was placed to the middle of a clean glass slide and the coverslip was mounted (with the cell-surface facing downwards) onto the drop of gelvatol taking care not to trap any air-bubble between the coverslip and the glass slide. Mounted slides were then stored in the dark at 4°C for overnight. Thereafter, the mounted slides were observed under a fluorescence microscope or confocal laser scan microscope.

Gelvatol:

2.4 g of polyvinyl alcohol (Mw 30,000-70,000; Sigma) was added to 6 g of glycerol in a 50 ml centrifuge tube and mixed by stirring. To the mixture, 6 ml of distilled H₂O was added and the mixture was incubated at room temperature. After several hours of incubation at room temperature, 12 ml of 0.2 M Tris/HCl, pH 8.5, was added and the mixture was heated to 50°C for 10 min with occasional mixing to completely dissolve polyvinyl alcohol. The solution was centrifuged at 5,100 rpm for 15 min. After centrifugation, 2.5% of diazobicyclo octane (DABCO), an anti-oxidant agent was added to reduce the bleaching of the fluorescence. The solution was aliquoted in small volumes in 1.5 ml microcentrifuge tubes and stored at -20°C.

5.3. DAPI and phalloidin staining of fixed cells

DAPI staining of *Dictyostelium* nuclei and phalloidin staining of *Dictyostelium* F-actin was performed simultaneously. Staining of F-actin with phalloidin demarcated the cell-boundary, which facilitated in determining the number of DAPI stained nuclei within a particular cell. Cells were harvested and the coverslips coated with cells were prepared as explained in Materials and Methods (5.2.1.). Cells were then fixed onto the coverslip by picric acid-paraformaldehyde fixation method as discussed in Materials and Methods (5.2.2.2.). After fixation and usual washings, coverslips were incubated for 30 min with 400 µl of PBG containing DAPI (1:1,000 dil.) and TRITC-phalloidin (1:200 dil.). Thereafter, the coverslip was washed twice with 400 µl of PBG for 5 min each followed by three washings with 400 µl of PBS for 5 min each. After washings, the coverslips were mounted onto the glass slides

(see Materials and Methods, 5.2.4) for observation under a fluorescence microscope or confocal laser scan microscope.

5.4. Immunolabelling of GFP-DLIM1 expressing *Dictyostelium* cells fixed during phagocytosis

To correlate the localization of DLIM1 with the organization of the actin cytoskeleton during the process of phagocytosis, GFP-DLIM1 expressing cells were fixed during phagocytosis and immunolabelled with anti-actin monoclonal antibody (Act 1-7). Briefly, cells were prepared as explained in Materials and Methods (5.2.1.). After the cells had adhered to the glass coverslip, the Soerensen phosphate buffer on the coverslip was replaced with 400 μ l of the solution containing heat-killed yeast cells diluted 1:10 in Soerensen phosphate buffer. Cells were incubated with yeast for different time intervals (5 min, 10 min, 15 min and 20 min). Thereafter, the buffer on the coverslips was carefully aspirated and the cells were immediately fixed onto the coverslip by methanol fixation method (see Materials and Methods, 5.2.2.1.). After fixation and usual washings, either the coverslip was directly mounted onto a glass slide or the cells were first immunolabelled with anti-actin monoclonal antibody (Act 1-7) as described in Materials and Methods (5.2.3.), before mounting onto a glass slide.

Preparation of heat-killed yeast cells:

Five grams of dry yeast *Saccharomyces cerevisiae* (Sigma) was suspended in 50 ml of PBS in a 100 ml Erlenmeyer flask and incubated for 30 min in a boiling waterbath with stirring. After boiling, the yeast cells were washed five times with PBS, followed by two washings with Soerensen phosphate buffer. The yeast cells were then finally resuspended in Soerensen phosphate buffer at a concentration of 1×10^9 yeast cells/ml. Aliquots of 1 ml and 20 ml were made and stored at -20°C .

6. Microscopy

For conventional immunofluorescence microscopy, DAPI staining and phalloidin staining, the cells were observed under a fluorescence microscope (Leica DNR) equipped with a 100x

Neofluar objective. The images were captured by a cooled charge-coupled device (CCD) camera (SensiCam, PCO). Various stages of development of *Dictyostelium* cells were also visualized using the fluorescence microscope (Leica DNR) equipped with a 2.5x or 5.0x objective and images were captured by a cooled CCD camera (SensiCam, PCO). Visual inspection of GFP-DLIM1 expressing *Dictyostelium* cells was performed using an inverted fluorescence microscope (Olympus 1X70). For studying the localization of GFP-DLIM1 fusion protein in live cells during cell locomotion, phagocytosis and endocytosis, an inverted confocal laser scanning microscope (Leica DM/IRBE) equipped with a 40x PL Fluotar 1.25 oil immersion objective or a 63x PL Fluotar 1.32 oil immersion objective was used. The 488-nm band of an argon-ion laser was used for excitation, and a 510-525-nm band-pass filter was used for emission. Confocal images of immunolabelled specimens were obtained with confocal laser scanning microscope (Leica DM/IRBE) equipped with 488-nm argon-ion laser for excitation of GFP fluorescence and a 568-nm krypton-ion laser for excitation of Cy3 fluorescence. For simultaneous acquisition of GFP and Cy3 fluorescence, the green and red contributions to the emission signal were separated by using a band-pass filter of 510-525-nm and a long-pass filter of 570-nm, respectively. The images from green and red channels were independently attributed with colour codes and then superimposed using the accompanying software and converted to the TIFF format after the experiment.

6.1. Live cell imaging of GFP-DLIM1 expressing *Dictyostelium* cells

To record the distribution of GFP-DLIM1 in living cells, GFP-DLIM1 expressing cells were grown to a density of $2-3 \times 10^6$ cells/ml, washed in Soerensen phosphate buffer and resuspended at a density of 1×10^7 cells/ml. The cells were then starved for about 1 h with shaking. Starvation facilitated observation as it allowed the cells to digest endocytosed nutrient medium, which is autofluorescent. For observation, cells were initially diluted in Soerensen phosphate buffer at 1×10^6 cells/ml and then 500 μ l of the cell suspension (5×10^5 cells) were transferred onto a 18 mm glass coverslip glued to a plastic rim of the same size. Cells were allowed to adhere to the glass coverslip for 10-15 min and confocal images were obtained and processed as described above (Materials and Methods, 6.).

6.2. Imaging distribution of GFP-DLIM1 during pinocytosis

For analysis of dynamics of GFP-DLIM1 during fluid phase endocytosis, coverslips containing GFP-DLIM1 expressing cells were prepared as described (Materials and Methods, 6.1.). After the cells had attached to the glass coverslip, the buffer was carefully aspirated and was replaced with Soerensen phosphate buffer containing 1 mg/ml TRITC-dextran (Mw 70,000; Sigma). Confocal sections were obtained by scanning at different intervals in one plane using a 488-nm argon-ion laser for GFP fluorescence and a 568-nm krypton-ion laser for TRITC fluorescence. Details of imaging and image processing have been discussed in Materials and Methods (6.).

6.3. Imaging distribution of GFP-DLIM1 during phagocytosis

For analysis of dynamics of GFP-DLIM1 during phagocytosis, coverslips containing GFP-DLIM1 expressing cells were prepared as described above (Materials and Methods, 6.). After the cells had adhered to the glass coverslips, 5-10 μ l of the heat-killed, TRITC-labelled/unlabelled yeast cells (1×10^9 yeast cells/ml) was carefully added from one edge of the coverslip. Immediately after the yeast cells had settled (in 2-5 min), confocal images were obtained as explained above (Materials and Methods, 6.).

Heat-killed, TRITC-labelled yeast cells :

For labelling, the pellet of 2×10^{10} heat-killed unlabelled yeast cells (Materials and Methods, 5.4.) was resuspended in 20 ml of 50 mM Na_2HPO_4 , pH 9.2, containing 2 mg of TRITC (Sigma) and incubated for 30 min at 37°C on a rotary shaker. After washing twice with 50 mM Na_2HPO_4 , pH 9.2, and four times with Soerensen phosphate buffer, aliquots of 1×10^9 yeast cells/ml were frozen at -20°C .

6.4. Imaging distribution of GFP-DLIM1 in aggregation-competent cells

GFP-DLIM1 expressing cells grown to a density of $2-3 \times 10^6$ cells/ml were washed twice in equal volume of Soerensen phosphate buffer and resuspended at a density of 1×10^7 cells/ml. The cells were then starved for 6 h with shaking at 250 rpm in order to make them aggregation-competent. Aggregation-competent cells have a typical elongated shape with a

well defined front and tail. After starvation for 6 h, 50 μ l of the cell-suspension (5×10^5 cells) was transferred onto a 18 mm glass coverslip (glued to a plastic rim of the same size) that had been pre-loaded with 200-300 μ l Soerensen phosphate buffer. Cells were allowed to adhere to the glass coverslip for 10-15 min. After the cells had elongated, confocal images were obtained as explained above (Materials and Methods, 6.).

7. Computer analyses

Analyses of the sequences and homology searches were performed using the 'University of Wisconsin' GCG software package (Devereux *et al.*, 1984) and different gene bank databases and *Dictyostelium discoideum* gene databases. Structural predictions and multiple alignment of the protein sequences were made using Expasy Tools software, accessible on the world-wide web. For processing images, Corel Draw version 8, Corel Photopaint, Adobe Illustrator, Adobe Photoshop and Microsoft Powerpoint softwares were used. Graphs and histograms were prepared using the Microsoft Excel software.

3. Results

1. Analyses of the DLIM1 gene

1.1. Cloning and sequence analysis of DLIM1 cDNA

Sequence information for a *Dictyostelium* cDNA was obtained from the Tsukuba CSM cDNA sequencing project, University of Tsukuba, Japan (accession number SSC 504). Analysis of the deduced amino acid sequence revealed that the clone SSC 504 contains incomplete sequence information, since its start codon was missing (Figure 6). Analysis of the deduced amino acid sequence, however, revealed the existence of two LIM domains, hence the name DLIM1.

```

1   cggtttttttttttttttaattaatctgtcattataataacttattctt
                                     * *
                                     DLIM1 5' →
51  aataaaaaaatgagtttctaTCTGTCCAACATGCACTAAAAGAGTTTATGC
      M S S I (C) P T (C) T K R V Y A 14
101 AGCTGAAGCTGTTAAAGCATGTGAAAAACAATATCATAAATTATGTCTTC
      A E A V K A C E K Q Y (H) K L (C) L Q 31
151 AATGTTTCCATTGTCATAAAAATCCTTCAATTAGGTCAATACTCTGAACGT
      (C) F H (C) H K I L Q L G Q Y S E R 47
201 GATGGTCAACCATATTGCAAAACTGATTATGATAGATTATTTAGACAAGC
      D G Q P Y (C) K T (D) Y D R L F R Q A 64
251 AGGTTACAGAGGTGGTGGTGTGTTGCAGACAGTTTTGAACCAGCACCAA
      G Y R G G G V V A D S F E P A P K 81
301 AAGTTGAAACTACAACCTCCAGTCGAACCAACCCACCTCCAACCTTTTTTA
      V E T T T P V E P T P P P T F L 97
351 ACACCAACTGAAGAAGTTAAAGTTCAATTATTCCCAACCAATTGTCCAAA
      T P T E E V K V Q L F P T N (C) P K 114
401 ATGTGGTAAGAAAGCATACTTTAATGAACTTAAAGTTTATAACTCTCGTG
      (C) G K K A Y F N E L K V Y N S R D 131
451 ATTGGCATAAGACTTGTTCGCTTGTTCATGTAATAAAAACTTAGTA
      W (H) K T (C) F A (C) F S (C) N K N L V 147
501 AGTGGTCAATACAGTGAAAAAGAAGTTTAATTTATTGTCCAAGATGTTA
      S G Q Y S E K E G L I Y (C) P R (C) Y 164
551 TCAATCTAAATTTGGTCCAAGTGGTTACACCAATACTGGTGCATTAGTTT
      Q S K F G P S G Y T N T G A L V L 181
601 TACATTAAAAATAaaatcaaaaaaaaaaataaaatcaaaaaaaaa
      H * 182
651 aaaaacg

```

Figure 6. Nucleotide sequence and deduced amino acid sequence of DLIM1 cDNA. The clone SSC 504 (Japanese cDNA sequencing project) provided incomplete sequence information (upper case letters) as the start codon was missing. The full length DLIM1 cDNA was obtained on screening a λ gt11 cDNA library derived from growth phase *Dictyostelium* cells. Lower case letters represent the sequences that were missing in the clone SSC 504. The nucleotide sequence shows the presence of a start codon at position 60. The start and stop codons are shown in bold letters. The presence of two in-frame stop codons (indicated by asterisks) immediately upstream of the ATG, and two putative polyadenylation signals (shown in boxes) following the TAA stop codon, suggests that the coding region is complete. The deduced amino acid sequence (shown below the corresponding coding sequence) suggests the presence of two LIM domains, one each at its N- and C-terminus spanning from amino acid residues 5–56 and 112–163, respectively. The conserved cysteine and histidine residues of the N-terminal (bold, encircled letters) and C-terminal (bold, shaded and encircled letters) LIM domain are shown. The intervening sequence between the two LIM domains is rich in proline residues (bold and underlined letters). The position and orientation of oligonucleotide primers DLIM1 5' and DLIM1 3' used for the PCR amplification are indicated by the arrows above the nucleotide sequences.

In order to obtain a full length DLIM1 cDNA, a λ gt11 cDNA library derived from growth phase *Dictyostelium* cells was screened. To achieve this, DLIM1 partial cDNA was amplified by RT-PCR (Materials and Methods, 3.19.1.) using total RNA isolated from *Dictyostelium* AX2 cells as a template and DLIM1 specific 5' and 3' oligonucleotide primers (depicted in Figure 6). The PCR amplified product containing 536 bp partial DLIM1 cDNA was directly cloned into pCR2.1 (TA cloning vector, Invitrogen) and verified by sequencing both the strands using M13 reverse and T7 universal primers. Subsequently, the 536 bp partial DLIM1 cDNA was used as a probe to screen a λ gt11 cDNA library derived from growth phase *Dictyostelium* cells (Materials and Methods, 3.19.2.1.). Six positive phage-plaques were observed. DNA from the positive phages was isolated and the cDNA inserts were subcloned at the EcoRI site into the pIC20H vector (Materials and Methods, 3.19.2.2.). Sequencing was performed in both orientations using T7 universal and M13 reverse oligonucleotide primers. The longest cDNA clone is 657 bp long with an open reading frame encompassing 564 bp (Figure 6). The first ATG is located at 60 bp and most likely serves as a putative translation initiation codon since the sequence preceding this ATG is unusually rich in A and T bases, common for non-translated regions of the *Dictyostelium* genome (Kimmel and Firtel, 1983). Moreover, the sequence immediately upstream of the ATG exhibits two in-frame stop codons located at nucleotides 36 and 39. The coding region is terminated by a stop codon at nucleotide position 606, which is followed by two polyadenylation signals AATAAA located 4 bp and 25 bp after the stop codon.

1.2. Amino acid sequence of DLIM1

The full length DLIM1 cDNA (549 bp) codes for a polypeptide of 182 amino acid residues with an estimated molecular weight of 20 kD. Analysis of the deduced polypeptide sequence of DLIM1 reveals the existence of two LIM domains, one each at its N- and C-terminus (Figure 6), spanning from amino acid residues 5-56 and 112-163, respectively. The LIM motif is characterized by conserved cysteine and histidine residues that exhibit a consensus amino acid sequence $[CX_2CX_{16-23}HX_2C]-X_2-[CX_2CX_{16-21}CX_2(C/H/D)]$ (Freyd *et al.*, 1990; Sadler *et al.*, 1992). The positions of cysteine and histidine residues are invariant in this sequence, but the length of the loops may span from 16 to 23 amino acids. The amino acid sequence of the two LIM domains of DLIM1 can be represented as $(CX_2CX_{17}HX_2C)-X_2-$

(CX₂CX₁₇CX₂D/C). The N-terminal LIM domain has an aspartic acid residue at position 56, whereas the C-terminal LIM domain has a cysteine residue at position 163 (Figure 6). The presence of two LIM domains in DLIM1 that are separated by an intervening sequence of 55 amino acids identifies DLIM1 as a group 2 LIM protein according to the classification of LIM domain proteins (Dawid *et al.*, 1998). According to their classification, group 2 proteins contain 1 or 2 copies of a single sequence type of LIM domains, whereas group 1 proteins always contain paired LIM domains near the N-terminus and group 3 proteins consist of multiple LIM domains localized at the C-terminus. In addition, the LIM domains of DLIM1 conform exactly to the organization of the LIM domains of other members of the group 2 LIM proteins (CRPs and CRIP), with an intervening sequence of 17 amino acids in both the loops of the LIM domains of these proteins (Stronach *et al.*, 1996). A glycine-rich region that normally follows the LIM domain in group 2 LIM proteins (CRPs and CRIP) is, however, not present in the DLIM1 protein. In DLIM1, only 4 and 3 glycine residues follow the N-terminal and C-terminal LIM domains, respectively. Interestingly though, the sequence between the two LIM domains of DLIM1 is proline-rich with 9 of the total 14 proline residues in DLIM1 residing in this region. The functional significance of this proline-rich region is not known.

Comparison of the entire amino acid sequence of DLIM1 to the protein databases revealed the highest degree of homology to members of the cysteine-rich protein (CRP) family CRP1, CRP2 and CRP3 (Figure 7a). Members of the CRP family have been shown to be associated with elements of the actin cytoskeleton as all are capable of directly interacting with α -actinin (an actin crosslinking protein) and zyxin (a LIM domain containing adhesion plaque protein) (Sadler *et al.*, 1992; Schmeichel and Beckerle, 1994; Louis *et al.*, 1997; Pomies *et al.*, 1997). The full length DLIM1 sequence exhibits 29-31% identity and 43-45% similarity to the three CRPs. The N-terminal LIM domain of DLIM1 is 33-35% identical to the N-terminal LIM domains of the three CRPs, whereas the C-terminal LIM domain of DLIM1 exhibits a slightly higher identity (42-44%) to the C-terminal LIM domains of the three CRPs. Cysteine-rich intestinal protein (CRIP), a single LIM domain containing protein belonging to group 2 (Perez-Alvarado *et al.*, 1996), exhibits a high homology to the N-terminal region (1-77) of DLIM1 (38% identity and 55% similarity). Moreover, the LIM domains of DLIM1 (N-terminal) and CRIP are 44% identical (Figure 7b).

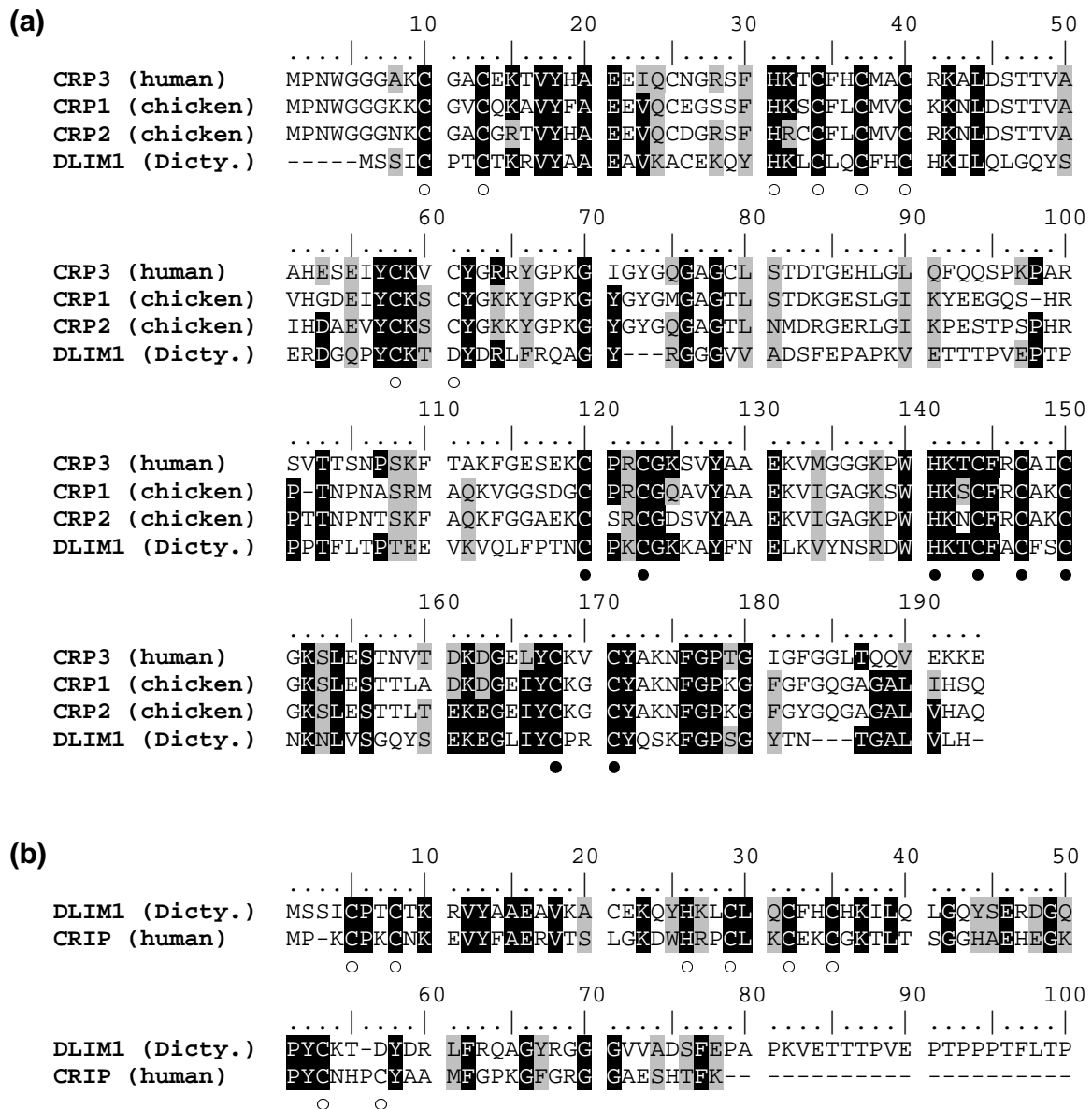


Figure 7. Alignment of the DLIM1 amino acid sequence with several group 2 LIM domain containing proteins. (a) Alignment of the DLIM1 amino acid sequence with members of the CRP family. Residues that are identical between DLIM1 and any of the other members of the CRP family are shadowed in dark grey, and residues that are similar are shadowed in grey. Open and filled circles below the aligned sequences indicate the N- and C-terminal LIM consensus, respectively. (b) Alignment of the N-terminal region of DLIM1 with CRIP. Residues that are identical between DLIM1 and CRIP are shadowed in dark grey, and residues that are similar are shadowed in grey. Open circles below the aligned sequences indicate the N-terminal LIM consensus. Sequences were aligned using the Clustal W programme (Wisconsin package version 9.0). Dashes indicate gaps introduced in the sequence for optimal alignment. Gene bank accession numbers: CRP1, P32965; CRP2, P50460; CRP3, NP_003467; CRIP, 1633212.

1.3. Southern blot analysis of DLIM1 gene

Southern blot analysis of restricted genomic DNA using the 536 bp partial DLIM1 cDNA as a probe was performed under high stringency conditions (Materials and Methods, 3.13.2.) to determine the number of copies of the DLIM1 gene as well as to check the presence of other related genes in the *Dictyostelium* genome. Genomic DNA of *Dictyostelium* was digested with various restriction enzymes (BglII, ClaI, EcoRI, NdeI, XbaI, XhoI), which do not have any internal restriction site in the DLIM1 cDNA. Presence of only one strong hybridisation signal in all the lanes suggests that DLIM1 is encoded by a single copy gene and no other related gene is present in the *Dictyostelium discoideum* genome (Figure 8a).

1.4. Expression of DLIM1 specific RNA during development

Dictyostelium cells grow vegetatively as unicellular amoebae when nutrients are available. Depletion of nutrients triggers a 24 h developmental programme leading to the formation of a multicellular fruiting body. This transition of cells from growth phase to the developmental phase is a consequence of stage specific expression that involves activation of certain genes and repression of others. Therefore, northern blot analysis was performed to study the DLIM1 gene expression during transition from single cell growth phase to multicellular fruiting body formation in *Dictyostelium* (Materials and Methods, 3.10.-3.13.). Hybridisation under stringent conditions with 536 bp partial DLIM1 cDNA probe revealed that DLIM1 transcripts are more abundant during growth and early development of *Dictyostelium* and strongly decline once tight aggregates have formed (Figure 8b).

1.5. Cloning and sequence analysis of DLIM1 genomic DNA

In order to obtain a genomic fragment containing the entire DLIM1 gene sequences, ~ 4.3 kb EcoRI-NdeI restricted DLIM1 genomic DNA, which was assumed to contain the entire DLIM1 genomic sequence, was purified by sucrose density gradient centrifugation and cloned (Materials and Methods, 3.19.3.). This assumption was based on the facts that Southern blot analysis performed with EcoRI+NdeI restricted genomic DNA revealed a

single band of ~ 4.3 kb upon hybridisation with the 536 bp partial DLIM1 cDNA, which does not have any internal EcoRI and NdeI site (Figure 8a) and that most of the *Dictyostelium discoideum* genes are not bigger than 4.0 kb.

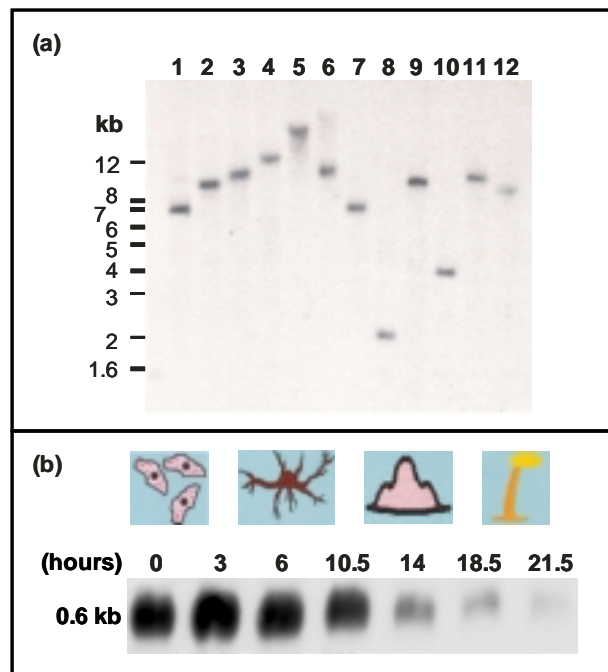
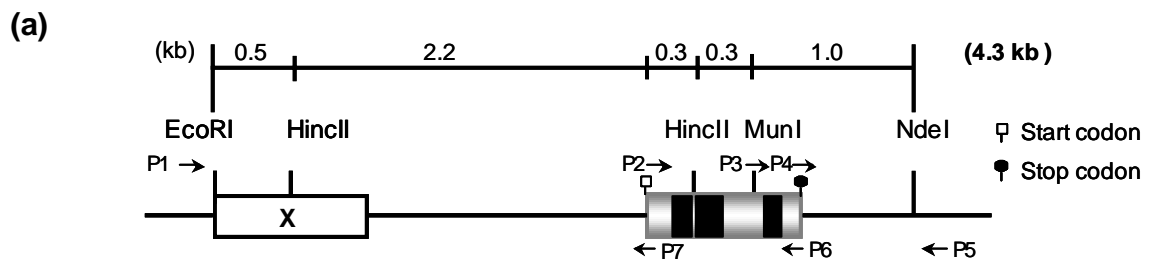


Figure 8. Southern and northern blot analyses. (a) The Southern blot probed with the 536 bp partial DLIM1 cDNA under high stringency conditions indicates the presence of a single copy of the gene. For lanes 1-12, wild-type *Dictyostelium* genomic DNA was digested with BglII (1), ClaI (2), EcoRI (3), NdeI (4), XbaI (5), XhoI (6), BglII + EcoRI (7), BglII + NdeI (8), EcoRI + ClaI (9), EcoRI + NdeI (10), EcoRI + XbaI (11), EcoRI + XhoI (12). (b) Northern blot showing the expression of DLIM1 during the development of *Dictyostelium*. Same amount (30 μ g) of total RNA (isolated from different hours of development on phosphate-buffered agar plates) was loaded in each lane. DLIM1 transcripts are most abundant during growth and early development.

The plasmid containing the DLIM1 genomic DNA was named pgDLIM1 and sequenced using a set of primers as indicated in Figure 9a. Analyses of deduced sequences reveal that the coding region of the DLIM1 gene spans 962 bp and is interrupted by three introns of 130 bp, 168 bp and 118 bp, respectively (Figure 9b). Comparison of the DLIM1 genomic and cDNA sequences allowed confirmation of the intron-exon boundary. In addition, all the three introns are 86-93% AT-rich, a common feature exhibited by most *Dictyostelium* introns. Moreover, all the three introns display a consensus sequence of GTA and TAG at

their 5' and 3' ends, respectively, which is essentially similar to the 5' and 3' consensus splice sites for *Dictyostelium* introns as proposed by Csank *et al.* (1990). Two potential polyadenylation signals are located 4 bp and 25 bp after the stop codon. The coding region is flanked by sequences containing extensive homopolymeric A/T-rich stretches. Upstream of the DLIM1 gene locus is an ORF, which has been found homologous to an unclassified *Dictyostelium* gene in the database. The 5' intergenic region is ~ 1.5 kb long and contains the DLIM1 promoter (Figure 9a). Some of the potential regulatory elements of the DLIM1 promoter are indicated in Figure 9b. We could, however, not identify a potential TATA box in the DLIM1 promoter.



(b)

```

-446      taaaaa attttaggtt taatttttagg ttttaaacct ttccattttt
-400  taaaggggac caattttttt tttttttttt tttttttttt ttttgaacc
-350  ttttttttta aaaagtaata ttaataatat gattttcaaa taaattatgc
-300  ctttgggcat aacccaaaaa gggcaaagag gattattttt gatcaaatag
-250  cttttttcct tgaaaatttt cccaaataaa acctcgctaa aaaaaaaaaa
-200  aaaaaaaaaa taaaaaaaaa ataaaaaaaa ggcttttggg gggataaatt
-150  tttcatcaaa aacatcgcta aaaaaaatca aaatattaat aaaaaaatt
-100  aaaaattaaa aaaaaaaaaa aaaaaaaaaa atcaaaatca attttatttt
-50   tttttttttt tatttatctg tcattattat aacttattct taataaaaaa
  1   ATGAGTTCTA TCTGTCCAAC ATGCACTAAA AGAGTTTATG CAGCTGAAGC
  51  TGTTAAAGCA TGTGAAAAAC AATATCATAA ATTATGTCTT CAATGTTTCC
 101  ATTGTCATAA AATCCTTCAA TTAGGTCAAg taagtatcac aatcatttta
 151  attaaaaaaaa aaaaaataaa taaaaaaaaa aaataaaaaa aataaaaaata
 201  aatcgctaac atttttttatt tttattttta tttttatttt tattttttatt
 251  tttatttagT ACTCTGAACG TGATGGTCAA CCATATTGCA AAAGTgtaaa
 301  ttatcaaaaa aaaaaaaaaa aaaaaaaaaa aaaaaaaaga aaaaaaaaaa
 351  gaaaaaaaaa aaaaagaatt taaaacaat ttttactaa ggaaatacca
 401  aattttttta atgaaaaaaaa taaaaccaa aaaaaccaa ccaaacc
 451  aaccaataaa tagGATTATG ATAGATTATT TAGACAAGCA GGTACAGAG
 501  GTGGTGGTGT TGTTCAGAC AGTTTTGAAC CAGCACCAA AGTTGAAACT
 551  ACAACTCCAG TCGAACCAAC CCCACCTCCA ACTTTTTTAA CACCAACTGA
 601  AGAAGTTAAA GTTCAATTAT TCCCAACCAA TTGTCCAAA TGTGGTAAGA
 651  AAGCATACTT TAATGAACCT AAAGTTTATA ACTCTCGTGA TTGGCATAAG
 701  ACgtatgtac tttttattta tttattttatt tcaatttatt ttcaaaaata
 751  aaatcaaaa aaaaaaaaaa aaattttatt aatcaaaaaa taaaatata
 801  aaatataaaa taaatattag TTGTTTCGCT TGTTCCTCAT GTAATAAAAA

```


(.....*Figure continued from the previous page*)

```

851 CTTAGTAAGT GGTC AATACA GTGAAAAAGA AGGTTTAATT TATTGTCCAA
901 GATGTTATCA ATCTAAATTT GGTCCAAGTG GTTACACCAA TACTGGTGCA
951 TTAGTTTTAC ATTAAaaaaa a ataaaatcaa aaaaaaaaaa ataaaaatca
1001 aaaaacaaga ataaaatatg tgctataaaa aaataataat atttatttaa
1051 ataaataata aaaataaaaa atcaaaaata aaaaaaaatt aaaaaaatct
1101 aatataatat tttaaaatga ttaattttaa aataaagggg ggatgaggcg
1151 gatatTTTTT tTTTTTTgac atctaaaaat aaacaatgcc atatTTTTT
1201 ttaatTTTTT tTTTTTTTT tttcaatcct tctttctttt tTTTTTctt
1251 ctttcctttt caaaaaaatt ccctaaatt tccccagggg ccaatTTTTT
1301 tttat

```

Figure 9. Organization of the DLIM1 gene locus. (a) Schematic representation of the DLIM1 gene locus. Restriction sites and estimated size of the fragments are indicated. The box representing the DLIM1 coding sequence is shaded and three black boxes within the DLIM1 coding sequence represent the intron sequences. The start and stop codons are indicated. X represents an unclassified open reading frame located upstream of the DLIM1 coding sequences. The position and orientation of oligonucleotide primers used for sequencing, T7 universal (P1), DLIM1 5' (P2), CLIM 5' (P3), gDLIM1-I (P4), SP6 universal (P5), DLIM1 3' (P6), DLIM1-U (P7) are indicated by arrows. (b) Sequence of the DLIM1 gene. The open reading frame (upper case letters) of the DLIM1 gene is interrupted by three introns (lower case letters). Putative start and stop codons are indicated in bold upper case letters. Two potential polyadenylation signals following the stop codon are shown in boxes. The 5'- and 3'- flanking sequences are shown in lower case letters. Putative regulatory sequences in the 5' flanking region are underlined.

2. Subcellular localization of DLIM1

To investigate the subcellular localization of DLIM1 in *Dictyostelium*, two strategies were planned: i, expression of DLIM1 as a green fluorescent protein (GFP)-fusion protein in *Dictyostelium*, which also allows to follow the cellular dynamics of DLIM1 *in vivo*; ii, generation of DLIM1 specific monoclonal antibodies to perform immunofluorescence studies.

2.1. Expression of DLIM1 as a GFP-fusion protein in *Dictyostelium*

Full length DLIM1 cDNA was subcloned in frame at the C-terminus of GFP in the pDEXRH vector, a GFP expression vector, under the control of actin-15 promoter (Materials and Methods, 3.19.5.; Figure 10a). The resulting vector was introduced into *Dictyostelium* AX2

cells by electroporation and the stable transformants were selected for growth in the presence of 20 µg/ml G418 (Geneticin). The transformants were confirmed by visual inspection under a fluorescence microscope and were used for localization studies *in vivo*.

2.1.1. Subcellular localization of GFP-DLIM1 in vegetative cells

GFP-DLIM1 expressing cells were grown axenically and prepared for imaging under a confocal laser scan microscope (Leica DM/IRBE) as described in Materials and Methods (6.1.). The confocal fluorescence microscopic studies of the GFP-DLIM1 expressing cells clearly indicate a preferential localization of the GFP-DLIM1 fusion protein at the cell cortex but the distribution is not uniform (Figure 10b). A diffused fluorescence of GFP-DLIM1 in the cytoplasm is also observed that likely manifests free GFP-DLIM1. In addition, we observed a significant accumulation of GFP-DLIM1 at the leading edges of the motile GFP-DLIM1 expressing cells (Figure 11). Occasional localization of GFP-DLIM1 in the nucleus was also observed (Figure 10b), the significance of which is not known. This pattern of distribution contrasts with the one of GFP that being evenly distributed throughout the cytoplasm shows no particular accumulation at specific sites (Maniak *et al.*, 1995, Westphal *et al.*, 1997). The observed accumulation of GFP-DLIM1 can, therefore, be attributed to the DLIM1 moiety of the fusion protein rather than the GFP-moiety.

To correlate the localization of DLIM1 with the organization of the actin cytoskeleton, GFP-DLIM1 expressing cells were fixed with cold methanol and immunostained with anti-actin monoclonal antibody (Act 1-7) followed by staining with Cy3 conjugated goat-anti mouse IgG as the secondary antibody as described in Materials and Methods (5.2.). After immunolabelling, the fixed cells were observed under the confocal laser scan microscope and the images were captured (Materials and Methods, 6). For most areas of the cells, the pattern of GFP-DLIM1 fluorescence coincides with that of the actin staining (Figure 12).

The colocalization of GFP-DLIM1 and actin prompted us to analyse the association of DLIM1 with the actin cytoskeleton by extracting the *Dictyostelium* cells expressing GFP-DLIM1 fusion protein with Triton X-100 (Materials and Methods, 4.9.). Triton X-100 treatment of cells solubilizes a substantial proportion of intracellular proteins, whereas the

insoluble fraction is enriched in cytoskeletal proteins (Prassler *et al.*, 1998). Figure 13b shows an immunoblot of the Triton X-100 soluble and insoluble fractions of GFP-DLIM1 expressing *Dictyostelium* cells labelled with anti-GFP antibodies (Living color peptide antibody, Clontech). Surprisingly, the GFP-DLIM1 fusion protein is observed in the Triton X-100 soluble fraction of the cell. A similar Triton X-100 soluble behaviour has been reported for mammalian gelsolin, an actin binding protein (Barkalow *et al.*, 1996; Wang *et al.*, 1997). To address the localization of GFP-DLIM1 with respect to actin, we next investigated the dynamics of GFP-DLIM1 distribution in those cellular processes in which the actin cytoskeleton plays a major role like pinocytosis, phagocytosis and motility.

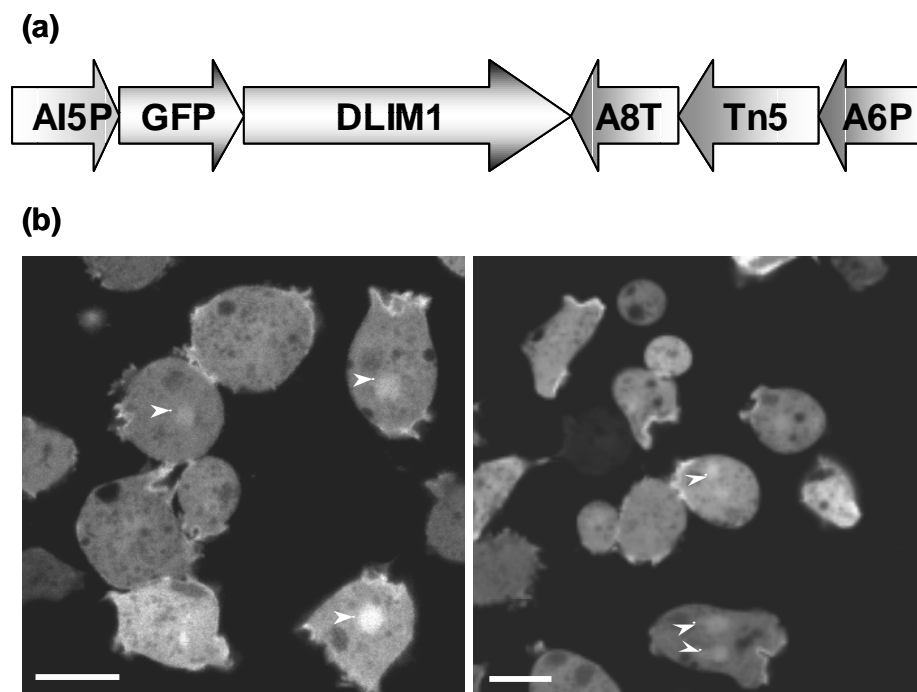


Figure 10. Expression of DLIM1 as a GFP-DLIM1 fusion protein in *Dictyostelium*. (a) Schematic representation of the vector allowing expression of DLIM1 as a GFP-fusion protein in *Dictyostelium*. DLIM1 was cloned in frame at the C-terminus of GFP in a pDEXRH vector under the control of actin-15 promoter. The actin-6 promoter controls the expression of Tn5 (G418 resistance gene), and the actin-8 terminator region is located downstream of the Tn5 coding sequence as well as the DLIM1 coding sequence. (b) Subcellular localization of GFP-DLIM1 fusion protein in GFP-DLIM1 expressing cells. The GFP-DLIM1 fusion protein accumulates to high levels at the cell cortex. Occasional localization of GFP-DLIM1 in the nucleus was also observed (marked with arrowheads). Bars, 10 μ m.

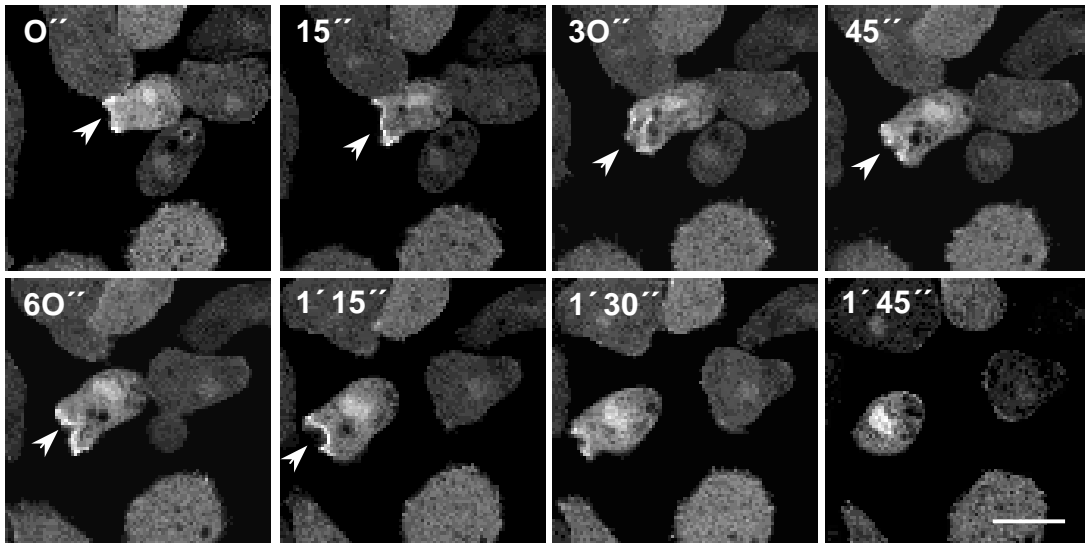


Figure 11. Localization of DLIM1 on the leading edge of the motile cell. Confocal sections were taken at the times indicated. The series of confocal sections indicate that GFP-DLIM1 accumulates to high levels on the leading edge (marked with arrowheads) of the motile cell. Bar, 10 μ m.

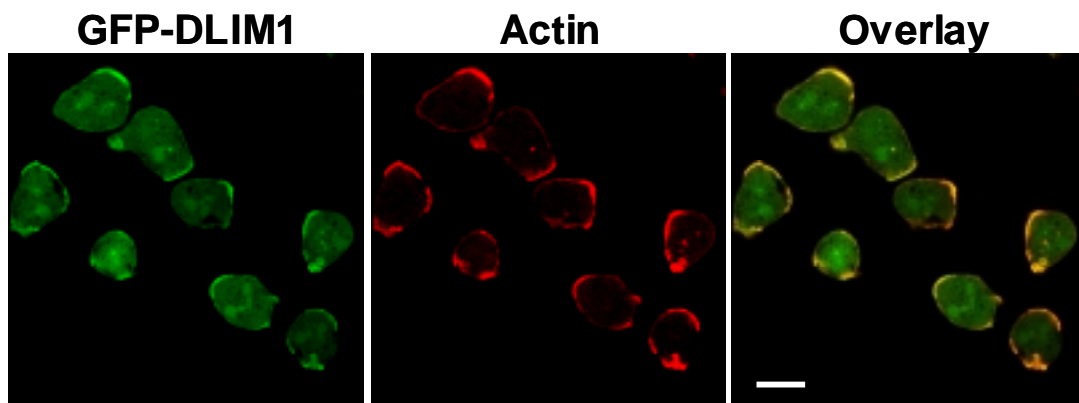


Figure 12. Colocalization of GFP-DLIM1 fusion protein and actin in the cell cortex. Immunofluorescence studies performed with GFP-DLIM1 expressing cells exhibit that the fluorescence pattern of GFP-DLIM1 fusion protein coincides with that of the actin staining for most areas of these cells. The cells were fixed with methanol and immunolabelled with anti-actin monoclonal antibody (Act 1-7). The GFP fluorescence pattern and the corresponding actin-staining images are shown. Overlay image show the colocalization of GFP-DLIM1 fluorescence with the actin staining in the cell-cortex. Bar, 10 μ m.

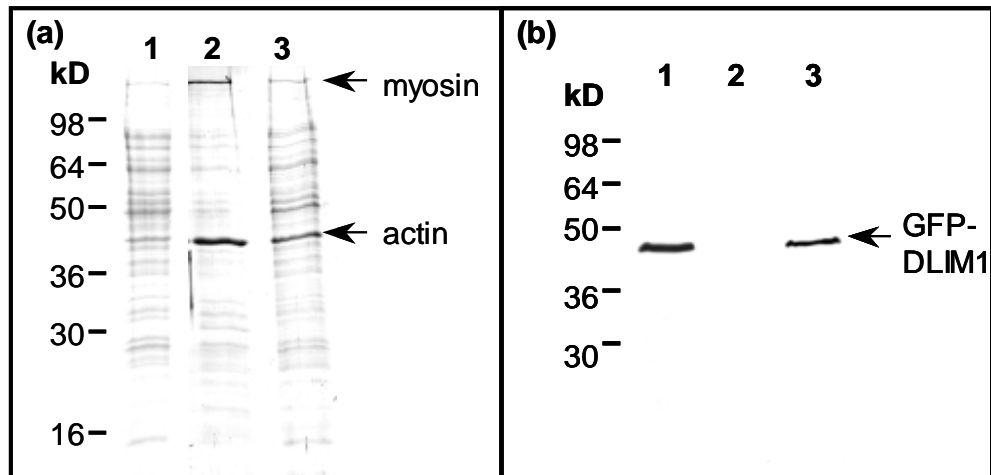


Figure 13. Triton X-100-soluble and -insoluble fractions of GFP-DLIM1 expressing *Dictyostelium* cells. *Dictyostelium* cells expressing GFP-DLIM1 fusion protein were lysed with 1% Triton X-100 in the presence of cytoskeleton-stabilizing buffer (80 mM PIPES, pH 6.8, 30% glycerol and 5 mM MgCl₂). Triton X-100-soluble and -insoluble fractions were separated by centrifugation at 14,000 x g for 3 min and extracted in 2x SDS sample buffer, (a) A Coomassie stained 12% SDS-polyacrylamide gel and (b) Immunoblot demonstrating the association of GFP-DLIM1 fusion protein with Triton X-100-soluble fraction. For both (a) and (b), proteins of the Triton X-100-soluble (lane 1), -insoluble (lane 2) fraction, and whole cell homogenate of GFP-DLIM1 expressing cells (lane 3) were resolved on a 12% SDS-polyacrylamide gel. For (b), the resolved proteins were blotted onto a nitrocellulose membrane and the blot was labelled with anti-GFP antibody (Living color peptide antibody, Clontech). Association of actin and myosin with the Triton X-100-insoluble fraction can be seen in the Coomassie stained gel (a).

2.1.2. Localization of GFP-DLIM1 fusion protein during pinocytosis

In *Dictyostelium* cells, macropinocytosis accounts for most of the fluid-phase uptake and depends on the integrity of the actin cytoskeleton, as shown by treatment of cells with cytochalasin A, an actin depolymerising drug (Hacker *et al.*, 1997). We were, therefore, interested in investigating the dynamics of GFP-DLIM1 distribution in *Dictyostelium* cells during fluid-phase endocytosis. *Dictyostelium* cells expressing GFP-DLIM1 fusion protein were allowed to adhere to glass coverslip, supernatant was replaced with phosphate buffer containing TRITC-dextran (Sigma) and confocal images were obtained to follow the distribution of GFP-DLIM1 fluorescence during uptake of TRITC-dextran (Materials and Methods, 6.2.).

Figure 14 represents a time series of endocytosis stages in a *Dictyostelium* cell expressing GFP-DLIM1 fusion protein. The cortical enrichment of GFP-DLIM1 is clearly apparent in this cell. The redistribution of GFP-DLIM1 during formation of a macropinosome can be followed at the site of the cell marked with an arrow. At the beginning of the sequence, a GFP-DLIM1 rich membrane invaginates (6 s). The protrusion of the GFP-DLIM1 rich membrane progresses (12 s through 36 s) until the edges of the protrusions fuse to form a macropinosome containing a portion of the surrounding liquid that is surrounded by a coat containing GFP-DLIM1 (42 s). Thereafter, GFP-DLIM1 gradually dissociates from the macropinosome (48 s through 1 min 18 s) to liberate the macropinosome into the cytoplasm. In the end (1 min 24 s and 1 min 30 s), GFP-DLIM1 completely dissociates from the macropinosome, though the vesicle is still present. This process is highly suggestive of an involvement of DLIM1 at early stages of endocytosis; on maturation of the endosome, DLIM1 dissociates from the endosome and returns to the cortex or remains in the cytoplasm. In general, GFP-DLIM1 dissociates completely from the endosome within <1 min of the internalisation of the endosome.

2.1.3. Localization of GFP-DLIM1 during phagocytosis

Phagocytosis is initiated by adhesion of a particle to the surface of a *Dictyostelium* cell. A phagocytic cup is formed at the cell surface around the particle that like fluid-phase endocytosis involves active rearrangement of the actin cytoskeleton. The rim of the cup extends around the particle resulting in the internalisation of the particle. In an attempt to study the dynamics of GFP-DLIM1 during phagocytosis, GFP-DLIM1 expressing cells were allowed to sit on a glass coverslip and challenged with TRITC-labelled yeast cells (Materials and Methods, 6.3.). The dynamics of GFP-DLIM1 redistribution during phagocytosis was followed by observing under a confocal laser scan microscope.

In the sequence shown in Figure 15, a GFP-DLIM1 expressing *Dictyostelium* cell phagocytosing a yeast cell is followed. GFP-DLIM1 fusion protein was observed to accumulate to high levels at the phagocytic cup (0 s). Cup progression (6 s) leads to the formation of a coat around the yeast cell that is enriched in GFP-DLIM1 (12 s), resulting in engulfment of the yeast cell. Immediately after the yeast cell has been successfully ingested,

GFP-DLIM1 is gradually removed from the phagosome (18 s through 48 s). Like fluid-phase endocytosis, GFP-DLIM1 dissociates completely from the phagosomes within <1 min of the yeast uptake and returns to the cortex or remains in the cytoplasm.

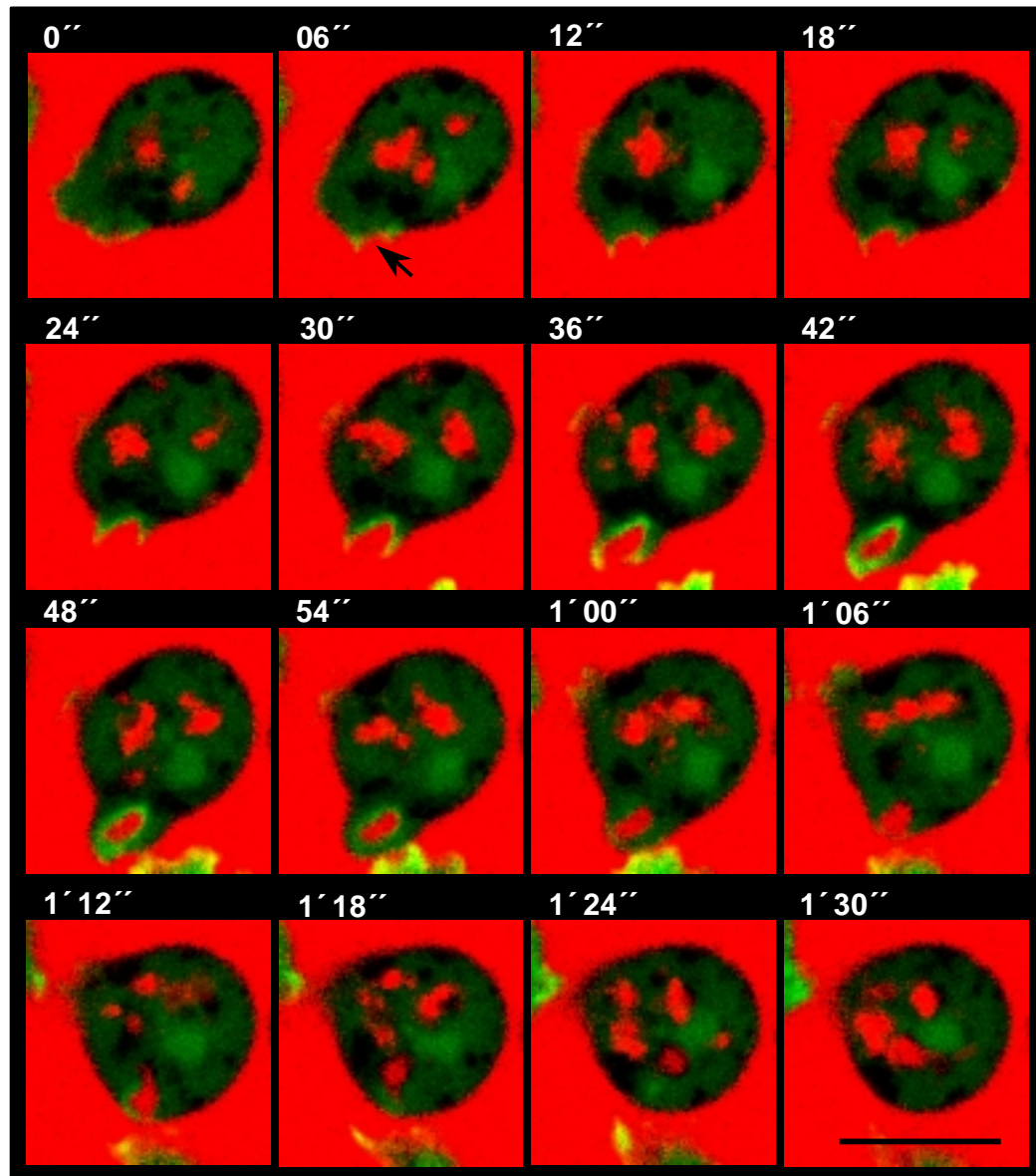


Figure 14. Dynamics of GFP-DLIM1 redistribution during pinocytosis. GFP-DLIM1 cells were allowed to adhere to glass coverslips and then the supernatant was replaced by phosphate buffer containing TRITC-dextran. Confocal sections were taken at the times indicated. Note the strong enrichment of GFP-DLIM1 at the cell-cortex, and the redistribution of GFP-DLIM1 during the formation of the pinocytotic vesicle. An arrow in the second panel (06 s) indicates the site of formation of a pinocytotic vesicle as seen in subsequent images. Bar, 10 μ m.

In the series of confocal images shown in Figure 16, attachment of a yeast cell to a GFP-DLIM1 expressing *Dictyostelium* cell (0 s) leads to the accumulation of GFP-DLIM1 in the phagocytic cup (30 s). At the same time (30 s), a GFP-DLIM1 rich membrane invaginates from the cell at an area opposite to the attached yeast cell leading to the formation of a macropinosome rich in GFP-DLIM1 (1 min). Even during the formation of a macropinosome opposite to the site of attachment of the yeast cell, the phagocytic cup progression proceeds (1 min through 1 min 30 s). However at 1 min 30 s, the area where the macropinosome has formed turns into a leading edge and the phagocytic cup progression ceases. The accumulated GFP-DLIM1 dissociates completely from the phagocytic cup (2 min) and the phagocyte detaches from the yeast cell (3 min 30 s), suggesting that relocalization of DLIM1 in phagocytic cups does not irreversibly influence the process of phagocytosis. The series of events shown in Figure 16 also indicate that a phagocytic cup, a macropinosome and a leading edge can coexist in a cell.

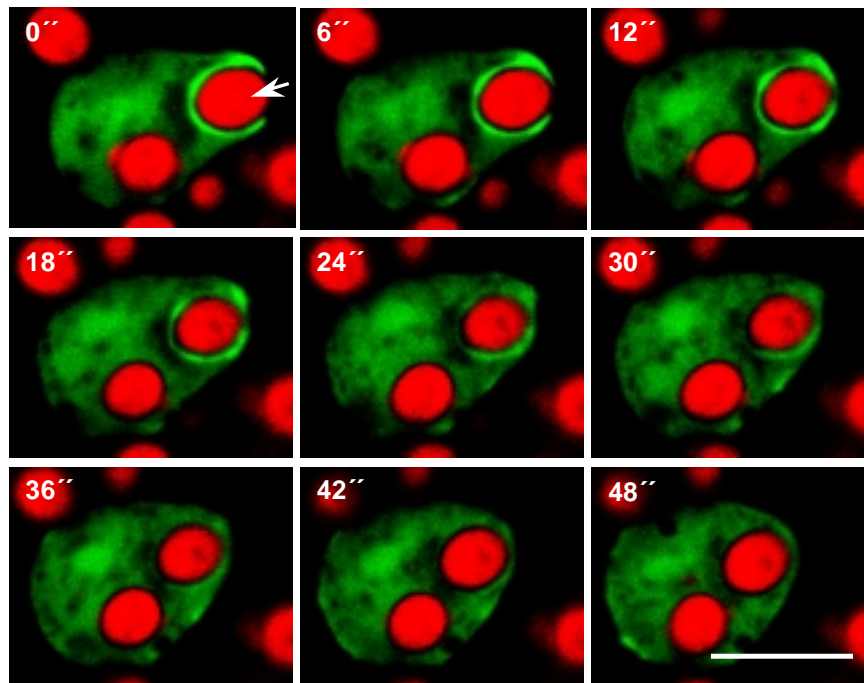


Figure 15. Dynamics of GFP-DLIM1 redistribution during phagocytosis. GFP-DLIM1 cells were incubated with TRITC-labelled, heat-killed yeast cells. Confocal sections were taken at the times (in seconds) indicated. The series of confocal sections indicate that GFP-DLIM1 accumulates to high levels in the phagocytic cups, which progresses to form a coat around the yeast particle. After engulfment of the yeast particle the fusion protein gradually dissociates from the phagosome. An arrow in the first image (0 s) shows the yeast cell of interest. Bar, 10 μ m.

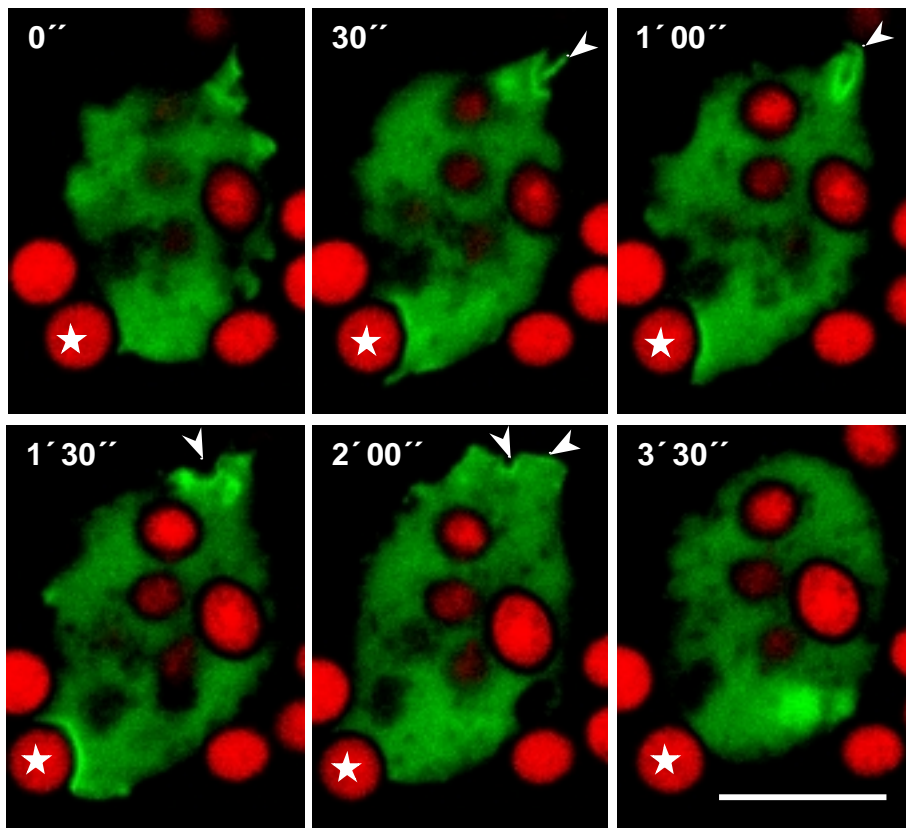


Figure 16. Dynamics of GFP-DLIM1 redistribution during unsuccessful ingestion. Confocal sections were obtained at the times indicated as described in the legend of Figure 15. The series of confocal sections exhibit formation and regression of the phagocytic cup. Upon cessation of the phagocytic cup-progression, the accumulated GFP-DLIM1 dissociates completely from the cup, and the phagocyte detaches from the yeast cell. Asterisk represents the yeast cell of interest. Arrowhead represents the site of formation of a macropinosome (30 s and 1 min) or a leading edge (1 min 30 s and 2 min). Bar, 10 μm .

To investigate the localization of GFP-DLIM1 with respect to actin during phagocytosis, *Dictyostelium* cells expressing GFP-DLIM1 fusion protein were incubated with heat-killed yeast cells for 10 min on a glass coverslip and immunolabelled after methanol fixation with anti-actin monoclonal antibody (Act 1-7) followed by labelling with Cy3 conjugated goat anti-mouse IgG (Materials and Methods, 5.4.). Confocal images of immunolabelled cells exhibit that GFP-DLIM1 is enriched at the phagocytic cup formed due to attachment of yeast cells to the *Dictyostelium* cell surface and GFP-DLIM1 fluorescence coincides with the actin staining (Figure 17).

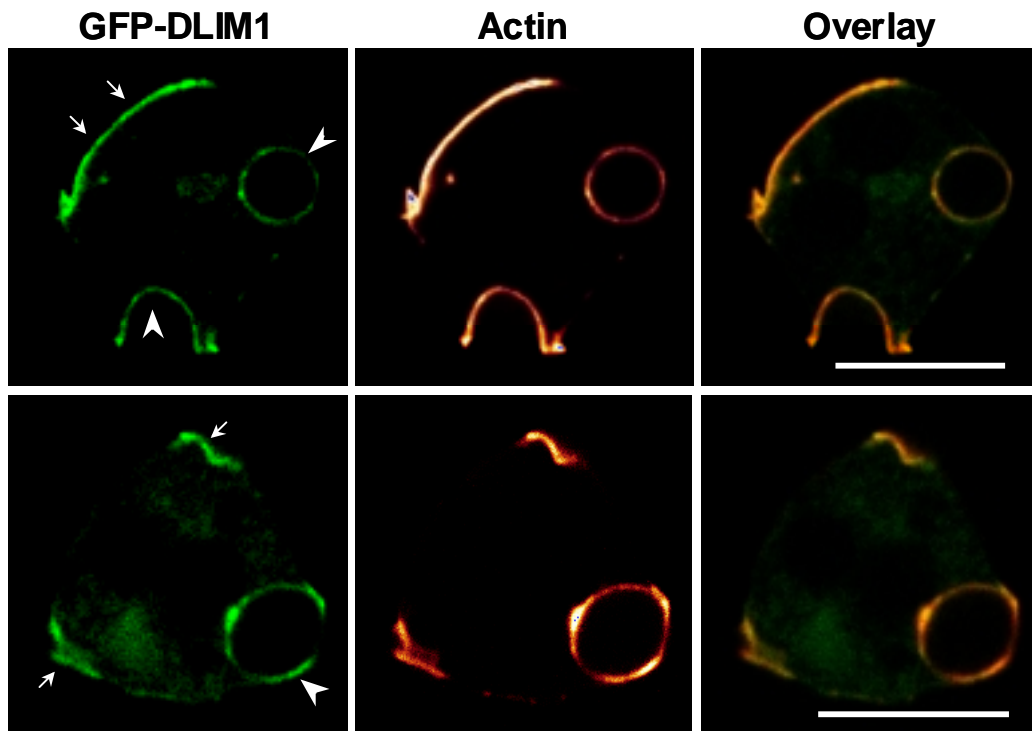


Figure 17. Distribution of GFP-DLIM1 in GFP-DLIM1 expressing cells fixed during the process of phagocytosis. GFP-DLIM1 expressing cells were incubated for 10 min with heat-killed yeast cells and were labelled after methanol-fixation with anti-actin monoclonal antibody (Act 1-7). Confocal images exhibit that GFP-DLIM1 is enriched at the phagocytic cup during uptake of the yeast particle. The fluorescence pattern of the GFP-DLIM1 fusion protein at the phagocytic cups as well as the cell-cortex coincides with actin staining, which can be appreciated in the overlay images. The arrowheads in GFP-DLIM1 panels mark the position of the yeast cell being phagocytosed and arrows represent the cortical fluorescence. Bars, 10 μm .

2.1.4. Localization of GFP-DLIM1 during exocytosis

Dictyostelium cells take up all their nutrients by endocytosis. Both particle- and fluid-containing vesicles are transiently surrounded by an actin coat. The actin coat is eventually shed by the vesicles as they transit through the cell leading to acidification and digestion of vesicle contents. The actin reassembles on the vesicles as they return to the cell cortex for exocytosis of the indigestible remnants (Rauchenberger *et al.*, 1997). Dynamics of GFP-DLIM1 distribution during exocytosis was investigated essentially according to that in case of phagocytosis (Materials and Methods, 6.3.), except that the GFP-DLIM1 expressing cells were incubated with TRITC-labelled yeast cells on a glass coverslip for about 1 h before obtaining confocal images.

A GFP-DLIM1 expressing cell in which exocytosis was monitored over several minutes is shown in Figure 18. The first frame (0 s) shows a GFP-DLIM1 expressing *Dictyostelium* cell with two already phagocytosed yeast particles (shown with and without asterisk) and a yeast particle that is in contact with the cell (marked with an arrowhead). At 5 min 18 s, one of the phagocytosed yeast (marked with an asterisk) comes in close proximity to the cell cortex and the phagocytic vacuole associates with the cell cortex, which leads to the appearance of GFP-DLIM1 fluorescence on one edge of the membrane surrounding the yeast particle (5 min 24 s). The GFP-DLIM1 fluorescence begins to appear on the other edge of the membrane surrounding the yeast particle (5 min 30 s) and starts diminishing from the site where it has initially appeared (5 min 36 s to 5 min 42 s). The GFP-DLIM1 protein continues to move on the membrane surrounding the yeast particle (5 min 48 s to 6 min 12 s). The fusion protein disappears completely from the membrane surrounding the yeast particle from 6 min 30 s to 6 min 48 s, and at this stage fluorescence begins to appear on the region of the cell membrane that is in contact with the extracellular yeast particle (marked with an arrowhead). This may imply that the cell has stopped exocytosis and has started phagocytosing another yeast, but this was only a transient phase as at 7 min 06 s the cell reverses the process and starts exocytosis again which is marked by the reappearance of the GFP-DLIM1 fluorescence on the membrane surrounding the already phagocytosed yeast. The fluorescence increases at 7 min 12 s, thereafter starts diminishing (7 min 18 s to 7 min 24 s) till it disappears again (7 min 30 s). From 7 min 06 s to 7 min 24 s, almost one-third of the yeast has protruded out of the cell. At 7 min 30 s, the cell again starts phagocytosing as seen by the reappearance of fluorescence on the phagocytic cup (marked with an arrowhead). The GFP-DLIM1 fluorescence disappears from the phagocytic cup and reappears on the membrane at the site of exocytosis (7 min 48 s) and persists there till 9 min. Simultaneously, from 7 min 48 s to 9 min, the cell is trying to throw out the yeast particle with almost half of the yeast particle still inside the cell (7 min 48 s) and approximately two-third of the yeast particle protruding out of the cell (9 min). From 9 min 18 s to 10 min 24 s, the exocytosed yeast is still in contact with the cell and at 12 min 54 s the contact between the cell and the yeast is lost. The series of images shown in Figure 18 suggest that DLIM1 plays a role in exocytosis by possibly facilitating association of the late vacuole with the cell cortex.

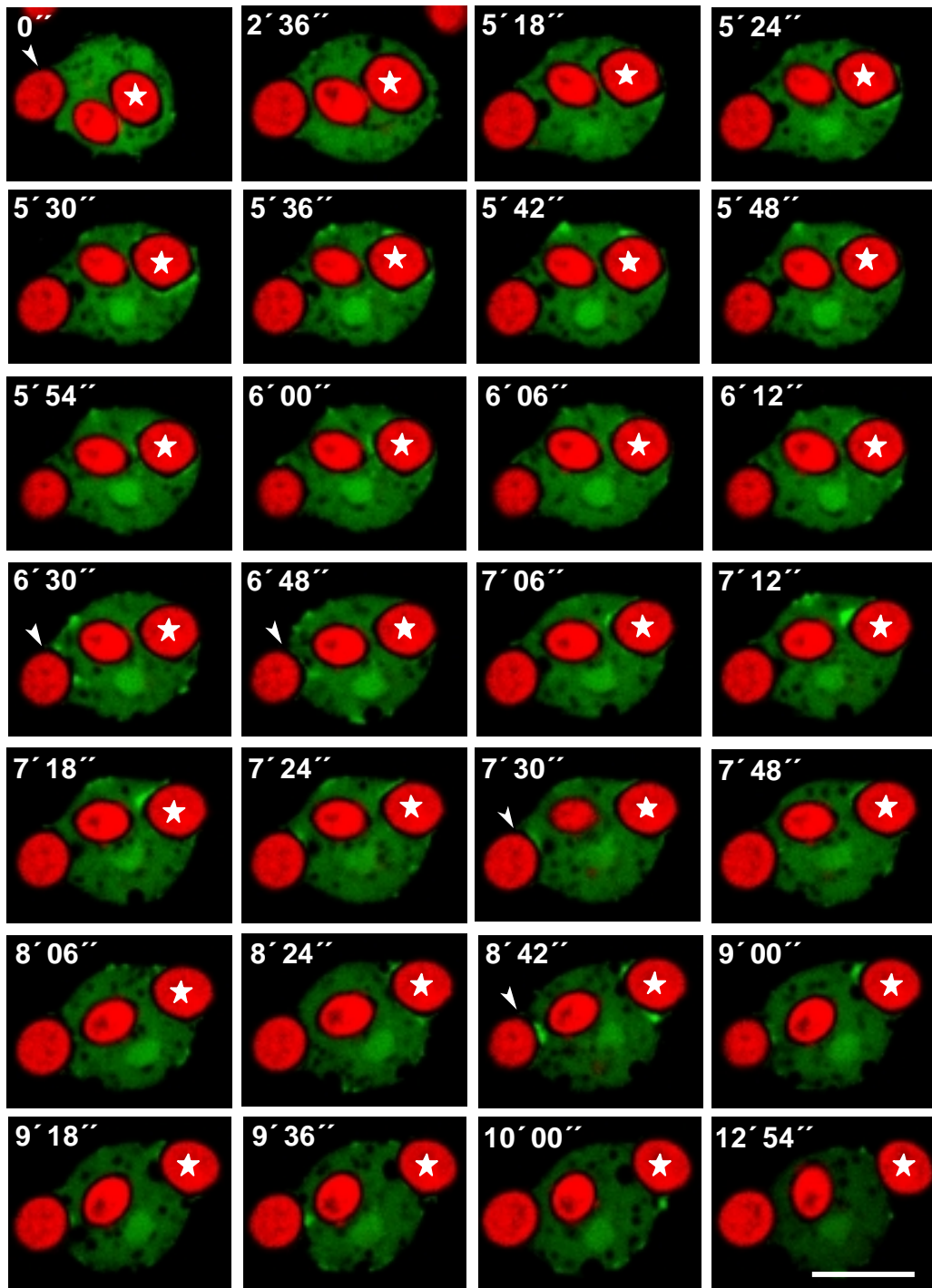


Figure 18. Dynamics of GFP-DLIM1 redistribution during exocytosis. GFP-DLIM1 cells were incubated with TRITC-labelled, heat-killed yeast cells for about 1 h. Confocal sections were obtained at the times indicated. Asterisk marks the yeast cell of interest and arrowhead marks the yeast that the GFP-DLIM1 expressing cell is trying to phagocytose. Note the accumulation of GFP-DLIM1 around the exocytotic vacuole as the cell prepares for exocytosis of the yeast cell. Bar, 10 μ m.

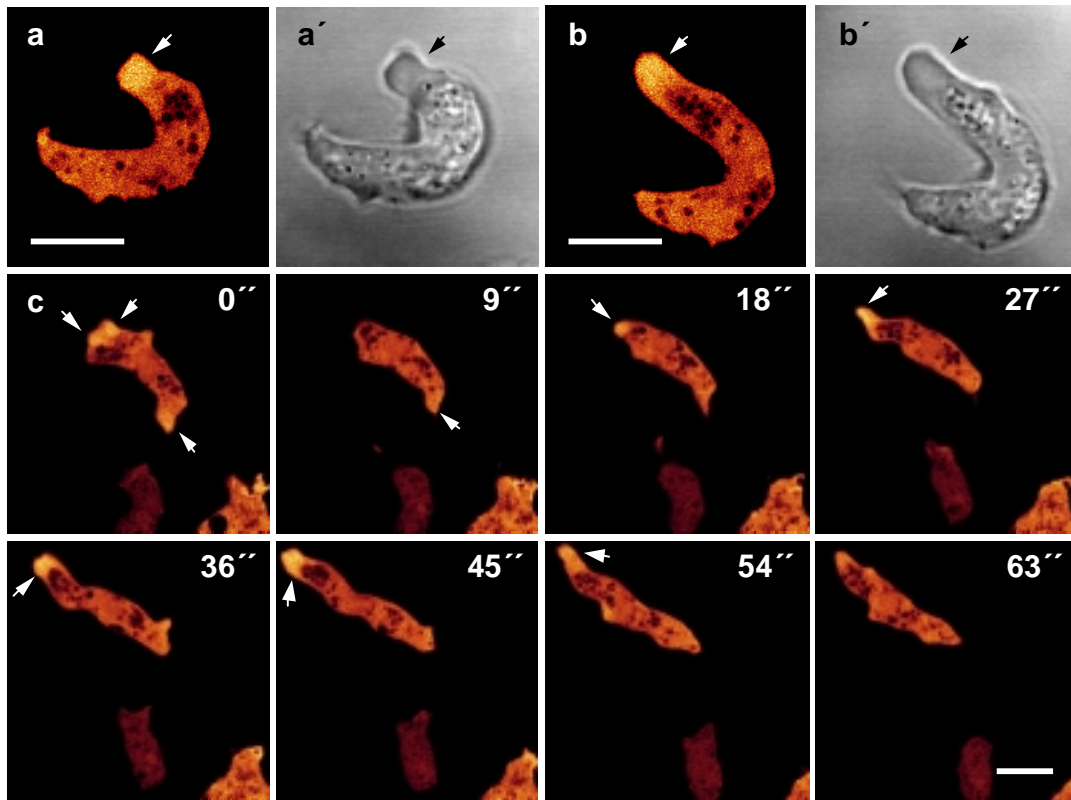


Figure 19. Dynamics of GFP-DLIM1 during cell-motility. GFP-DLIM1 cells were starved for 6 h in phosphate buffer in order to make them aggregation-competent. Aggregation-competent cells, in general, acquire an elongated shape with a well-defined front and tail. Fluorescence images of an aggregation-competent cell are shown in a and b and their respective phase-contrast images in a' and b'. Time series of an aggregation-competent GFP-DLIM1 expressing cell, which is rapidly extending pseudopods, is shown in c. Confocal images were taken at the times indicated. GFP-DLIM1 is found to accumulate to high levels in the pseudopods (indicated by arrows in all images). Bars, 10 μ m.

2.1.5. Localization of GFP-DLIM1 in motile cells

On starvation, *Dictyostelium* enters a developmental program and during early development cells become aggregation-competent having the ability to sense and respond to a cAMP gradient. The aggregation-competent cells attain a typical elongated shape with a well defined tail and front. These cells are highly motile in nature and move by extension of pseudopods in the direction of the chemoattractant. Extensive remodelling of the actin network accompanies the extension of pseudopods. Dynamics of GFP-DLIM1 during motility was investigated in aggregation-competent cells after 6 h of starvation. (Materials and Methods, 6.4.).

Figures 19a,b show the fluorescence images of an aggregation-competent GFP-DLIM1 expressing cell that is extending a pseudopod. The presence and location of the pseudopod, which is devoid of cytoplasm, can be easily distinguished in their respective phase-contrast images (Figures 19a',b'). GFP-DLIM1 was found to accumulate to high levels in the pseudopods. Indeed the entire pseudopod is filled with the GFP-DLIM1 fluorescence. Figure 19c shows the time series of redistribution of GFP-DLIM1 fluorescence in an aggregation-competent GFP-DLIM1 cell that is rapidly extending pseudopods. Images at different time points show that GFP-DLIM1 preferentially assembles in a newly formed pseudopod of the motile cell, where it remains when the mass of the cell moved in the direction of the leading pseudopod and/or until the pseudopod retracts.

2.2. N- and C-terminal DLIM1 deletion studies

LIM domains function as protein-binding interfaces and, in this capacity, are thought to influence subcellular protein localization and regulate protein function (Schmeichel and Beckerle, 1994). Since the DLIM1 protein is comprised primarily of two LIM domains, we were interested in the possibility that the site on DLIM1 that is responsible for its colocalization with actin and its involvement in the dynamic processes (pinocytosis, phagocytosis, exocytosis and motility) might be contained within a single LIM domain. To address this, N- and C-terminal DLIM1 deletion constructs were generated via a PCR-based approach (Materials and Methods, 3.19.6.).

The N- and C-terminal LIM domains of DLIM1 are referred to in the text as NLIM and CLIM, respectively and the intervening region between the two LIM domains that is rich in proline amino acid residues is referred to as P-rich sequence. The NLIM, P-rich sequence and CLIM regions of DLIM1 are depicted in Figure 20. Oligonucleotide primers were generated (depicted in Figure 20) to amplify DLIM1 cDNA sequences corresponding to a) the NLIM (a.a. 1-58); b) the NLIM and P-rich sequence (a.a. 1-111), which we refer to as NLIM-P; c) the CLIM (a.a. 110-182) and d) the CLIM and P-rich sequence (a.a. 57-182), which we refer to as CLIM-P. The primers were designed such that each amplified fragment was supplemented with an in-frame stop codon as well as flanking suitable restriction sites to facilitate subcloning (Materials and Methods, 1.9.). The resulting amplified DNA

fragments were cloned at the C-terminus of GFP in the pDEXRH expression vector under control of the actin-15 promoter and subsequently, the *Dictyostelium* cells were transformed by these constructs (Materials and Methods, 3.19.6.). Mutants expressing these GFP-fusion proteins were selected for their resistance to G418 and were used for localization studies *in vivo*. These fusion proteins are referred to in the text as GFP-NLIM, GFP-NLIM-P, GFP-CLIM and GFP-CLIM-P (Figure 20).

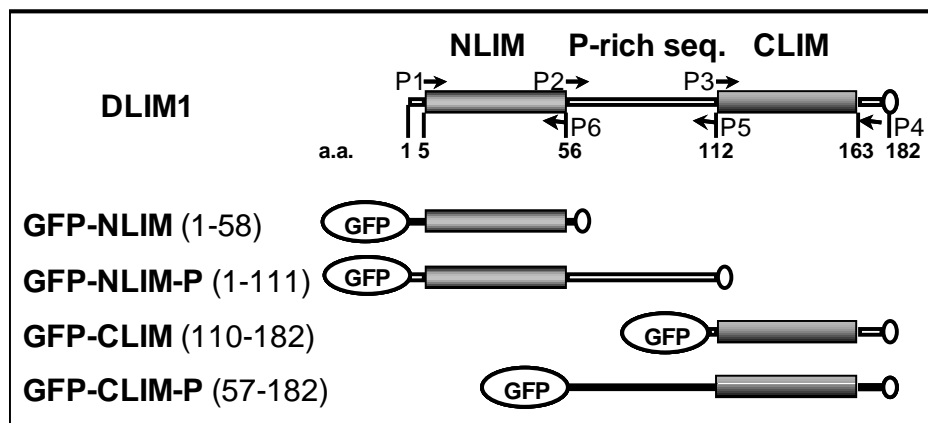


Figure 20. Schematic representation of terminally deleted DLIM1 proteins used for localization studies. Domain organization of DLIM1 is shown. NLIM and CLIM represent the N- and C-terminal LIM domain, respectively. P-rich seq. represents the intervening region between the two LIM domains that is rich in proline residues. The position and orientation of oligonucleotide primers used for amplification, NLIM 5' (P1), CLIM-P 5' (P2), CLIM 5' (P3), CLIM 3' (P4), NLIM-P 3' (P5), NLIM 3' (P6), are indicated by arrows. The primers were designed such that each amplified fragment was supplemented with an in-frame stop codon (represented by an oval-box at the 3'-end of each fragment). The amplified DNA fragments were cloned at the C-terminus of GFP in a pDEXRH expression vector under control of the actin-15 promoter. Figures in the brackets represent amino acid residues that were amplified and cloned. *Dictyostelium* cells were transformed by these constructs and the mutants obtained were analyzed under a confocal microscope.

Cells expressing these GFP-fusion proteins were grown axenically and prepared for imaging under a confocal laser scan microscope as described for GFP-DLIM1 expressing cells (Materials and Methods, 6.1.). The average intensity of the GFP fluorescence in our transformants expressing these GFP-fusion proteins was good with an exception of cells expressing GFP-NLIM. Only occasionally could we record cells displaying intense GFP-NLIM fluorescence. We could not improve the intensity of the GFP-NLIM fluorescence

even after a second transformation attempt to select for higher copy numbers of the integrated expression vectors. The immunoblot shown in Figure 21 proves that GFP-NLIM is not present in amounts as high as seen for GFP-NLIM-P, GFP-CLIM, GFP-CLIM-P and GFP-DLIM1.

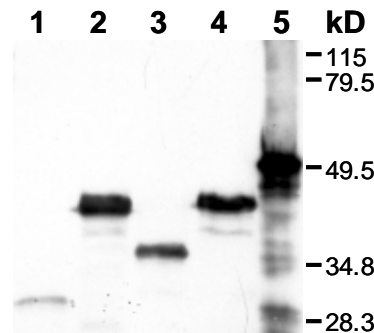


Figure 21. Immunoblot showing the expression levels of different GFP-fusion proteins in *Dictyostelium*. Whole cell homogenate of *Dictyostelium* cells expressing GFP-NLIM (lane 1), GFP-NLIM-P (lane 2), GFP-CLIM (lane 3), GFP-CLIM-P (lane 4) and GFP-DLIM1 (lane 5) fusion proteins was resolved on a 12% SDS-polyacrylamide gel, blotted onto a nitrocellulose membrane and immunolabelled with anti-GFP monoclonal antibody (K3-184-2). Equal amount of total cellular proteins (equivalent to 2×10^5 cells) was loaded in each lane. The immunoblots were processed after incubation with an appropriate HRP-conjugated secondary antibody by ECL-detection system for visualization of the specific immunolabelled bands.

Confocal studies performed with the cells expressing these GFP-fusion proteins (GFP-NLIM, GFP-NLIM-P, GFP-CLIM and GFP-CLIM-P) revealed that all the four GFP-fusion proteins exhibit a fluorescence pattern that is identical to the parent GFP-DLIM1 fusion protein with a preferential localization of each of the four GFP-fusion proteins at the cell-cortex, leading edges of the motile cells, and transient association with the macropinosomes (selected images are shown in Figure 22). Figure 22a shows a highly pixelated image of an aggregation-competent GFP-NLIM expressing *Dictyostelium* cell, which is due to the low average levels of GFP-NLIM in these cells. GFP-NLIM fluorescence can be detected in the pseudopod of the motile cell in addition to cytoplasmic distribution, like in the case of GFP-DLIM1 (Figure 19). GFP-NLIM-P fluorescence can be seen around the pinocytic vesicles (Figure 22b), which is essentially similar to that of the GFP-DLIM1 (Figure 14). Likewise,

cortical enrichment of GFP-CLIM and GFP-CLIM-P (Figure 22c,d) is also identical to that of the parent GFP-DLIM1 fusion protein (Figure 10b).

To investigate the distribution of GFP-NLIM, GFP-NLIM-P, GFP-CLIM and GFP-CLIM-P fusion proteins during the process of phagocytosis and to correlate it with the organization of the actin, cells expressing these GFP-fusion proteins were incubated with heat-killed yeast cells on a glass coverslip and immunolabelled after methanol fixation with anti-actin monoclonal antibody (Act 1-7) exactly according to the method described for GFP-DLIM1 expressing cells (Materials and Methods, 5.4.).

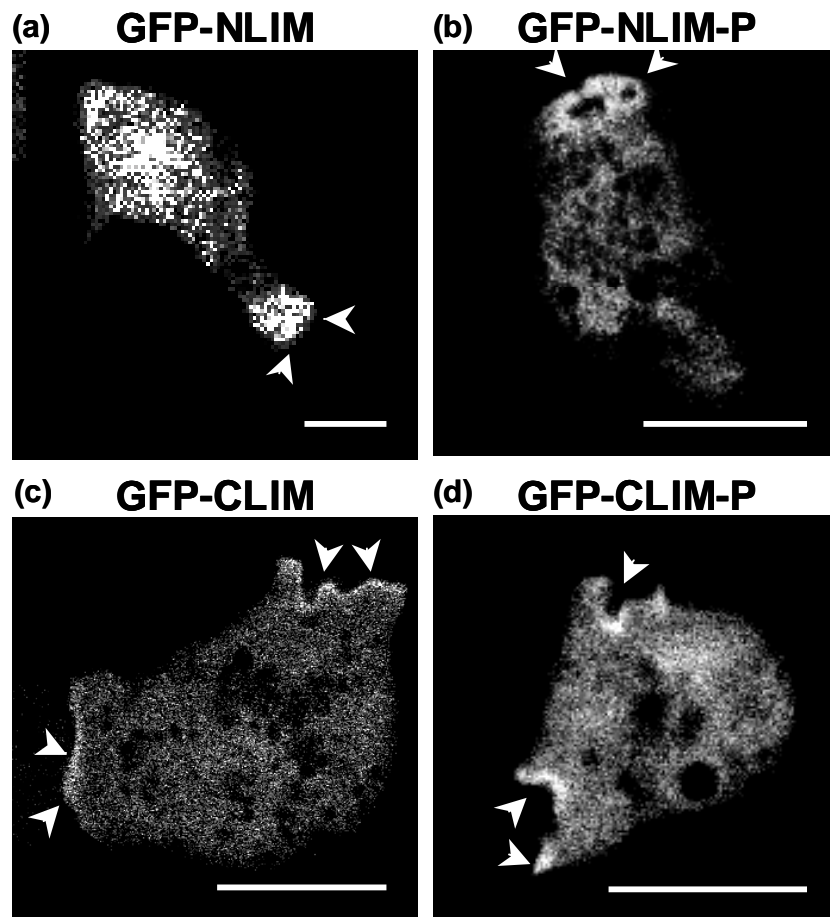


Figure 22. Subcellular localization of GFP-NLIM, GFP-NLIM-P, GFP-CLIM and GFP-CLIM-P. (a) GFP-NLIM accumulates in the pseudopod (marked by arrowheads) of an aggregation-competent cell. (b) GFP-NLIM-P fluorescence is visible on the coat that surrounds the pinocytic vesicle (marked by arrowheads). (c and d) Enrichment of GFP-CLIM (c) and GFP-CLIM-P (d) on the cell-cortex (marked by arrowheads) is visible. Bars, 10 μ m.

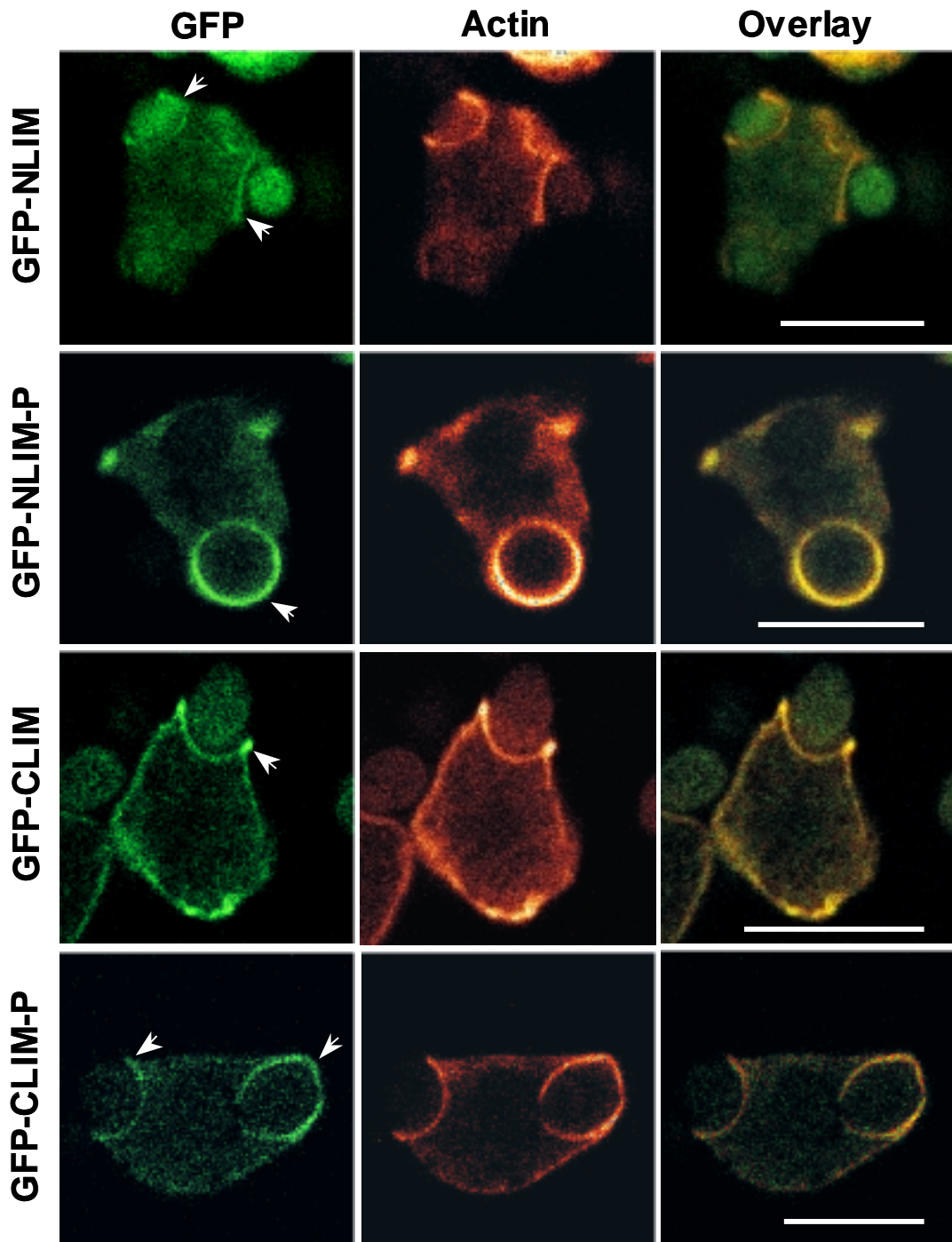


Figure 23. Distribution of GFP-NLIM, GFP-NLIM-P, GFP-CLIM and GFP-CLIM-P during phagocytosis. Cells expressing these terminally deleted DLIM1 proteins fused to GFP exhibit a fluorescence pattern that is identical to that of the parent GFP-DLIM1 fusion protein. All the truncated GFP-fusion proteins accumulate at the phagocytic cup (indicated by arrows) during uptake of the yeast cell and the fluorescence pattern of these truncated GFP-fusion proteins coincides with actin staining, as observed in overlay images. Bars, 10 μm .

Confocal images of immunolabelled cells exhibit that all the four GFP-fused DLIM1 deletion products are enriched at the phagocytic cups formed due to attachment of yeast cells to the *Dictyostelium* cell surface (Figure 23). Moreover, the fluorescence of all the four GFP-fusion proteins coincided with the actin staining. This as well as the above mentioned results suggest that either LIM domain of DLIM1 is sufficient for its colocalization with actin and its involvement in the dynamic processes.

3. Generation of DLIM1 specific monoclonal antibodies

We were interested in generating DLIM1 specific monoclonal antibodies, which will enable us not only to conduct immunolocalization studies in wild-type *Dictyostelium* cells but also to identify the binding partners of DLIM1. To achieve this, DLIM1 was expressed as either a histidine-tagged protein or a glutathione S-transferase (GST)-fusion protein in *E. coli*.

3.1. Expression and purification of DLIM1 as a histidine-tagged protein

Expression of DLIM1 as a N-terminal hexa-histidine fusion protein in *E. coli* was achieved by subcloning the DLIM1 cDNA sequence in-frame at the multiple cloning site of the pQE30 expression vector obtained from Qiagen (Materials and Methods, 3.19.7.). The expression was found to be maximal after 5 h of induction with 2 mM IPTG at 37°C. The expressed histidine-tagged DLIM1 migrated on SDS-polyacrylamide gels with a molecular weight of 30 kD (Figure 24a,b), which is significantly higher than the expected molecular weight (20 kD). We have confirmed employing mass spectroscopy that the protein migrating at 30 kD is indeed the histidine-tagged DLIM1 protein. The reason for this difference in the observed and the expected molecular weights is not known. The histidine-tagged DLIM1 protein was soluble only in denaturing 8 M urea-containing buffer and reducing the urea concentration by dialysis lead to precipitation of the histidine-tagged DLIM1 protein. The 8 M urea-soluble bacterial extract was, therefore, subjected to a Ni-NTA-agarose affinity column (Materials and Methods, 4.5.), which lead to the partial-purification of the histidine-tagged DLIM1 protein (Figure 24a,b).

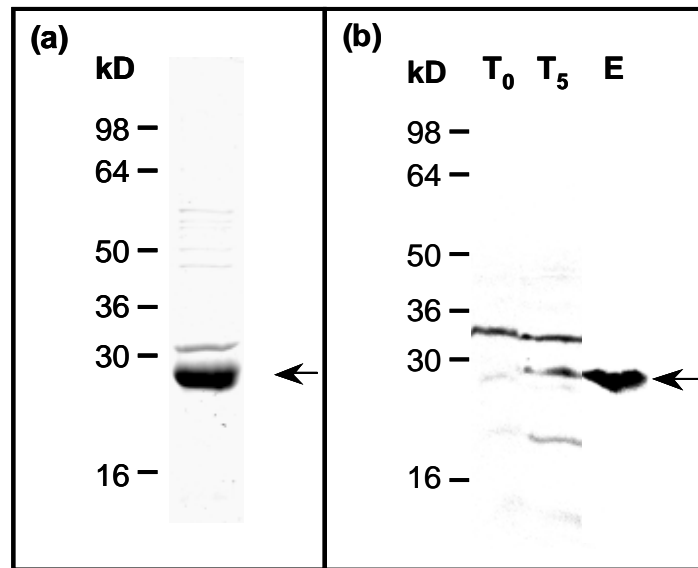


Figure 24. Purification of histidine-tagged DLIM1 protein from *E. coli*. (a) A Coomassie stained 12% SDS-polyacrylamide gel showing the partially-purified histidine-tagged DLIM1 protein. (b) Immunoblot labelled with anti-histidine antibody (Qiagen). A 12% SDS polyacrylamide gel was loaded with uninduced- (T₀), induced- (T₅) *E. coli* homogenate, and the partially-purified histidine-tagged DLIM1 protein (E) eluted from the Ni-NTA agarose column (Qiagen).

3.1.1. Generation of monoclonal antibodies using histidine-tagged DLIM1 as an antigen

The partially-purified histidine-tagged DLIM1 was resolved on SDS-polyacrylamide gel and the gel-slice containing the histidine-tagged DLIM1 protein was cut out and homogenised in PBS (Materials and Methods, 5.1.1.). Two BALB/c mice were immunized intra-peritoneally with this protein suspension and DLIM1 specific monoclonal antibodies were generated as described in Materials and Methods (5.1.). The hybridoma supernatants of the clones obtained were screened for DLIM1 specific antibody production by stripe tests (Materials and Methods, 5.1.4.2.) using whole cell homogenate of *E. coli* cells expressing histidine-tagged DLIM1, *Dictyostelium* wild-type AX2 whole cell homogenate and whole cell homogenate of *Dictyostelium* cells expressing GFP-DLIM1 fusion protein. Fourteen putative positive clones obtained were subsequently subcloned to get single-cell clones. Unfortunately, we could not get any DLIM1 specific monoclonal as none of the hybridoma supernatants from the monoclonal obtained was able to recognise the endogenous DLIM1

protein as well as the GFP-DLIM1 fusion protein in *Dictyostelium* homogenates. Moreover, all the monoclones secreted antibodies that were highly non-specific and cross-reacted with other *E. coli* and *Dictyostelium* proteins in immunoblot analyses as well as in immunofluorescence tests performed with wild-type *Dictyostelium* cells and GFP-DLIM1 expressing *Dictyostelium* cells. One of the reasons for not getting a DLIM1 specific antibody secreting monoclonal could be the fact that we have used a gel-eluted histidine-tagged DLIM1 fusion protein as an antigen for immunizing the mice. We, therefore, decided to express DLIM1 as a GST-fusion protein in *E. coli* and use the purified GST-DLIM1 fusion protein as an antigen for immunizing the mice.

3.2. Expression and purification of DLIM1 as a GST-fusion protein

For the expression of DLIM1 as a GST-fusion protein in *E. coli*, the full length DLIM1 cDNA was subcloned into the prokaryotic expression vector pGEX-2T (glutathione-S-transferase gene fusion system, Pharmacia) in-frame at the C-terminus of GST (Materials and Methods, 3.19.8.). The GST-DLIM1 fusion protein was expressed in *E. coli* strain XLI blue at different temperature conditions (30°C and 37°C) with varying concentrations of IPTG (0.1 mM, 0.5 mM and 1.0 mM) (Materials and Methods, 4.6.). Maximum yield was obtained after 3 h of induction with 1.0 mM IPTG at 37°C. The GST-DLIM1 fusion protein migrated on a SDS-polyacrylamide gel with a molecular weight of 47 kD (Figure 25a,b).

For purification of GST-DLIM1, bacterial cells were lysed after induction and the fusion protein was purified from the supernatant by affinity chromatography using glutathione-agarose beads (Materials and Methods, 4.6.). Figure 25a shows a Coomassie-stained gel exhibiting different fractions of GST-DLIM1 protein eluted after binding to glutathione-agarose beads. The presence of the GST-DLIM1 protein in the elute fractions was confirmed by immunoblotting (Figure 25b) using goat anti-GST antibody (Pharmacia). The purified fusion protein was dialysed against 10 mM ammonium-bi-carbonate to remove the salts present in the release buffer that had been used for elution of protein from the beads. After dialysis, the protein was lyophilised overnight, stored at -20°C and resuspended in an appropriate buffer before use.



Figure 25. Expression and purification of GST-DLIM1 fusion protein. (a) A Coomassie-stained 12% SDS-polyacrylamide gel. The gel was loaded with molecular weight marker (M), uninduced- (T_0) and induced- (T_3) *E. coli* homogenate, elute fractions (numbered 1 to 5) containing GST-DLIM1 fusion protein, supernatant left after binding of GST-DLIM1 fusion protein to the glutathione-agarose beads (S) and beads left after elution of the fusion protein (B). An arrow on the right indicates GST-DLIM1 fusion protein and a vertical bar on the right side indicates the degradation products of GST-DLIM1 fusion protein as confirmed by the immunoblot analysis. Apparent molecular weights (in kD) of standards are given on the left. (b) Immunoblot confirms the elution of GST-DLIM1 fusion protein. 12% SDS-polyacrylamide gel was loaded with uninduced- (T_0) and induced- (T_3) *E. coli* homogenate and elute fraction number 1 (E1). The blot was labeled with anti-GST antibody (Pharmacia). An arrow on the right indicates the GST-DLIM1 fusion protein and a vertical bar on the right indicates degradation products of the GST-DLIM1 fusion protein.

3.2.1. Generation of monoclonal antibodies using GST-DLIM1 fusion protein as an antigen

DLIM1 specific monoclonal antibodies were generated as described in Materials and Methods (5.1.). The primary screening of the hybridoma supernatant for DLIM1 specific antibody production was performed by indirect ELISA, using purified GST-DLIM1 fusion protein as an antigen (Materials and Methods, 5.1.4.1.). The hybridoma supernatants that appeared positive by ELISA screening were further analysed by stripe tests (Materials and Methods, 5.1.4.2.) using whole cell homogenate of *E. coli* cells expressing GST and GST-DLIM1 protein, to avoid the false positive clones that are commonly observed by ELISA.

We obtained only a single clone secreting DLIM1 specific antibodies (K5-253), whereas several clones we tested secreted antibodies that were specific to GST protein. The DLIM1

specific K5-253 clone was selected for cloning in order to establish a single hybridoma cell line. Seventeen independent single cell clones of the mother clone K5-253 were established and their supernatant was analysed by immunoblotting using homogenate of GFP-DLIM1 expressing *Dictyostelium* cells. Out of all the subclones screened, 4 subclones were selected (K5-253-3, K5-253-7, K5-253-8 and K5-253-15) based on their ability to recognise the GFP-DLIM1 fusion protein in *Dictyostelium* homogenate. The immunoblot shown in Figure 26 demonstrates the ability of the hybridoma supernatant of two of the subclones (K5-253-3 and K5-253-15) to recognise the GFP-DLIM1 fusion protein in the total cell homogenate (equivalent to 2×10^5 cells/lane) of axenically growing GFP-DLIM1 expressing *Dictyostelium* cells. However, none of the four subclones was able to recognise the endogenous DLIM1 protein in *Dictyostelium* homogenate (equivalent to 2×10^5 to 1×10^6 cells/lane) obtained from vegetatively growing AX2 cells as well as from AX2 cells that had been starved for 3 h or 6 h (Figure not shown). The four selected subclones were expanded to generate large quantities of monoclonal antibody. Expansion of the subclones, however, resulted in lack of antibody production by these subclones.

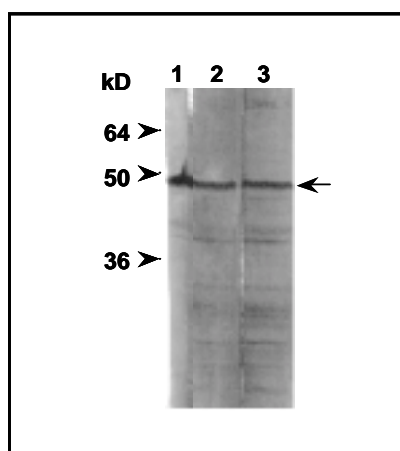


Figure 26. Immunoblot demonstrating the generation of DLIM1 specific monoclonal antibody. Total cellular proteins of GFP-DLIM1 expressing cells were extracted in 2x SDS sample buffer. The extracted proteins were resolved (equivalent to 2×10^5 cells/lane) on a 12% SDS-polyacrylamide gel, blotted onto a nitrocellulose membrane and immunolabelled with anti-GFP monoclonal antibody, K3-184-2 (lane 1); hybridoma supernatant of K5-253-3 (lane 2) and K5-253-15 (lane 3). Arrow on the right indicates GFP-DLIM1 fusion protein. The immunoblots were processed after incubation with an appropriate alkaline phosphatase-conjugated secondary antibody by BCIP/NBT colour development substrate reaction system for visualization of the specific immunolabelled bands.

In our immunolocalization studies in wild-type AX2 cells and GFP-DLIM1 expressing *Dictyostelium* cells, none of the hybridoma supernatants tested (K5-253-3, K5-253-7, K5-253-8 and K5-253-15) could recognise the endogenous DLIM1 protein in wild-type *Dictyostelium* cells. Moreover, none of the hybridoma supernatants was able to recognise the GFP-DLIM1 fusion protein in GFP-DLIM1 expressing cells, thus hampering further investigation.

4. *In vitro* binding of DLIM1 to F-actin

In our subcellular localization studies we have demonstrated that DLIM1 colocalizes with actin. We were, therefore, interested in investigating the binding capability of DLIM1 to actin *in vitro*. The F-actin binding activity of DLIM1 was analysed using actin sedimentation assays (Materials and Methods, 4.10.) in which purified GST-DLIM1 and G-actin were mixed and the actin polymerised by addition of 2 mM MgCl₂ in imidazole buffer (pH 7.0). The GST-DLIM1 fusion protein was observed to partially co-sediment with filaments of α -actin (purified from rabbit skeletal muscle; Figure 27) as well as *Dictyostelium discoideum* actin (Figure 28) even in the presence of high salt concentration (100 mM KCl). At 100 mM KCl concentration, actin binding efficiency of several actin-binding proteins has been observed to be drastically reduced, for example, α -actinin, comitin and Ddplastin (Witke, 1991; Jung *et al.*, 1996; Prassler *et al.*, 1997). Controls for GST-DLIM1 alone showed that GST-DLIM1 remained almost completely in the supernatant in the absence of actin (Figures 27, 28). The GST protein itself did not sediment with filaments of rabbit α -actin (Figure 27), thus suggesting a role for DLIM1 to bind F-actin. Interestingly, only the full length GST-DLIM1 fusion protein was able to cosediment with F-actin, whereas the degradation products of GST-DLIM1 remained almost completely in the supernatant; thus demonstrating the specificity of the full length GST-DLIM1 fusion protein to bind to actin.

Since Ca²⁺ is known to inhibit the binding of actin crosslinking proteins like 30 kD actin bundling protein, α -actinin and Ddplastin (Fechheimer and Taylor, 1984; Noegel *et al.*, 1987; Prassler *et al.*, 1997), we next investigated the binding efficiency of GST-DLIM1 to actin filaments in the presence or absence of Ca²⁺. The binding of GST-DLIM1 to actin

proved to be unaffected by the presence of 0.2 mM Ca^{2+} (Figure 28). We also note that *Dictyostelium* actin exhibits a lower degree of polymerisation as compared to rabbit α -actin (compare actin bands in supernatant and pellet fractions in Figures 27 and 28), a fact observed by other workers in the field as well.

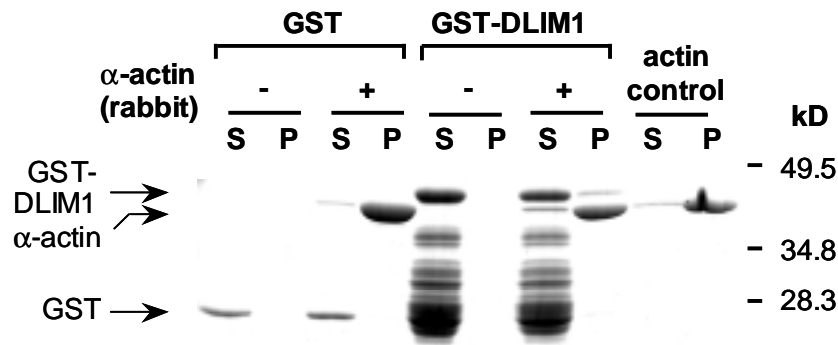


Figure 27. Cosedimentation assay of GST-DLIM1 with rabbit skeletal muscle actin (α -actin). GST protein or GST-DLIM1 fusion protein was incubated with G-actin (5 μM) in polymerisation buffer containing 2 mM MgCl_2 , 100 mM KCl and 1 mM EGTA for 30 min at room temperature. Pellets (P) and supernatants (S) were separated by high-speed centrifugation, and the proteins in these fractions were analysed by SDS-PAGE in 12% gels and staining with Coomassie blue. Controls for GST and GST-DLIM1 alone were performed without the addition of G-actin in the reaction mixture. The presence (+) or absence (-) of G-actin in the reaction mixture is indicated on the top of each lane. In the actin control, G-actin was polymerised in the absence of GST or GST-DLIM1.

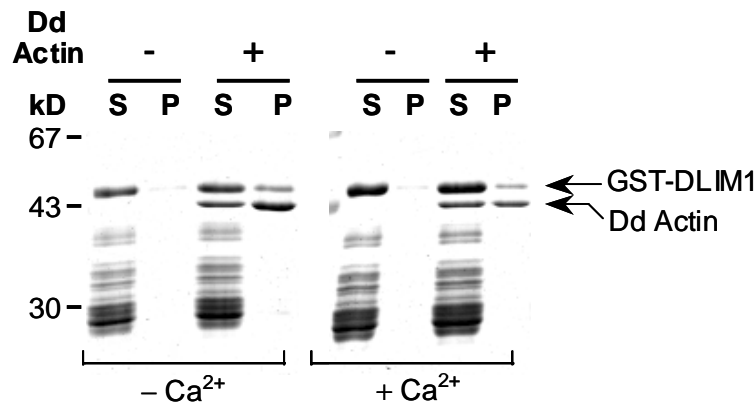


Figure 28. Cosedimentation assay of GST-DLIM1 with *D. discoideum* actin in the presence or absence of Ca^{2+} . G-actin (5 μM) from *D. discoideum* was incubated with GST-DLIM1 in polymerisation buffer containing 2 mM MgCl_2 , 100 mM KCl and either 1 mM EGTA (- Ca^{2+}) or 0.2 mM CaCl_2 (+ Ca^{2+}). Pellets (P) and supernatants (S) were separated by high-speed centrifugation, and the proteins in these fractions were analysed by SDS-PAGE in 12% gels and staining with Coomassie blue. Controls for GST-DLIM1 alone were performed without the addition of G-actin in the reaction mixture. The presence (+) or absence (-) of G-actin in the reaction mixture is indicated on the top of each lane.

Since members of the CRP family are capable of directly interacting with α -actinin (Pomies *et al.*, 1997), binding of GST-DLIM1 to actin was assayed in the presence of α -actinin (Figure 29). We speculated that if GST-DLIM1 has the ability to interact with α -actinin, the simultaneous presence of the GST-DLIM1 fusion protein and α -actinin in the polymerising mixture might either result in the formation of a multi-protein complex between GST-DLIM1, α -actinin and actin, which might lead to increased levels of the trapped GST-DLIM1 fusion protein that co-sediments with the F-actin; or the interaction between GST-DLIM1 and α -actinin might interfere in the actin-binding activity of GST-DLIM1 leading to reduced levels of the co-sedimented GST-DLIM1. GST-DLIM1 was observed to co-sediment with F-actin to the same levels as observed in control actin-binding assays performed in the absence of α -actinin. This suggests that α -actinin does not influence the actin-binding efficiency of GST-DLIM1. We can, however, not rule out any direct interaction between DLIM1 and α -actinin under these test conditions.

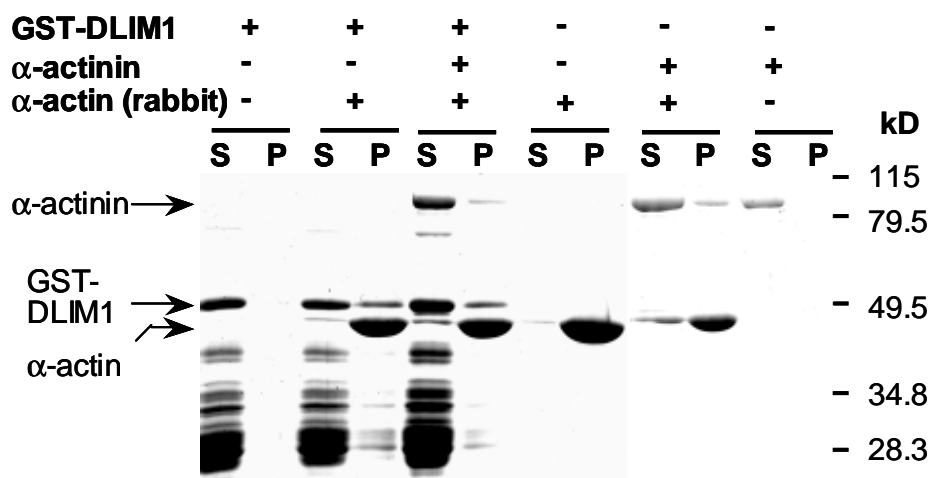


Figure 29. Cosedimentation assay of GST-DLIM1 with rabbit skeletal muscle actin (α -actin) in the presence or absence of α -actinin. G-actin (5 μ M) from rabbit skeletal muscle was incubated with GST-DLIM1 in polymerisation buffer containing 2 mM $MgCl_2$, 100 mM KCl and 1 mM EGTA in the presence or absence of α -actinin. Pellets (P) and supernatants (S) were separated by high-speed centrifugation, and the proteins in these fractions were analysed by SDS-PAGE in 12% gels and staining with Coomassie blue. Controls for GST-DLIM1 alone, actin alone and α -actinin alone are shown. The presence (+) or absence (-) of individual proteins in the reaction mixture is indicated on the top of each lane.

5. Generation of DLIM1⁻ mutant cells

To gain more insight into the function of DLIM1 *in vivo*, DLIM1⁻ mutant cells were generated via homologous recombination. To this end, a DLIM1 gene replacement vector was constructed by inserting a 1.4 kb blasticidin resistance cassette within the DLIM1 coding region of the genomic DLIM1 fragment (Materials and Methods, 3.19.4.). *Dictyostelium* AX2 cells were transformed with the DLIM1 gene replacement vector. The transformants were selected for growth in the presence of 3.5 µg/ml of blasticidin S in AX2 medium and single cell colonies were obtained by plating the transformants onto SM plates overlaid with *Klebsiella*. For further analyses, 148 clones were screened for the absence of an intact copy of DLIM1 gene by PCR assay using lysed cells as template (Materials and Methods, 3.14.). The absence of a ~900 bp fragment in the amplified PCR product of 14 of the transformants indicated that the intact copy of the DLIM1 gene is not present in these transformants. The positive clones obtained after PCR assay were further confirmed by Southern and northern blot analyses.

5.1. Molecular biological analyses for screening of DLIM1⁻ mutant cells

5.1.1. Southern blot analysis

Genomic DNA was isolated from the AX2 cells and 14 of the PCR-positive transformants and digested with EcoRI+NdeI restriction enzymes, which do not have any internal restriction site in the blasticidin resistance cassette. Hybridisation analysis with ³²P labelled full length DLIM1 cDNA (Figure 30b) revealed that a gene replacement event has occurred in at least 9 of these transformants, as the insertion of the 1.4 kb blasticidin resistance cassette causes a shift of the 4.3 kb EcoRI+NdeI fragment to a 5.7 kb fragment.

5.1.2. Northern blot analysis

Northern blot analysis was performed to confirm the absence of DLIM1 transcripts in 4 of the transformants selected on the basis of the results of Southern blot analysis. Absence of

DLIM1 RNA indicates that the disruption of the DLIM1 gene has occurred in all the transformants (Figure 30c). One of these transformants (no. 102-23) was selected for further cell-biological and biochemical characterizations and is referred to as DLIM1⁻ mutant.

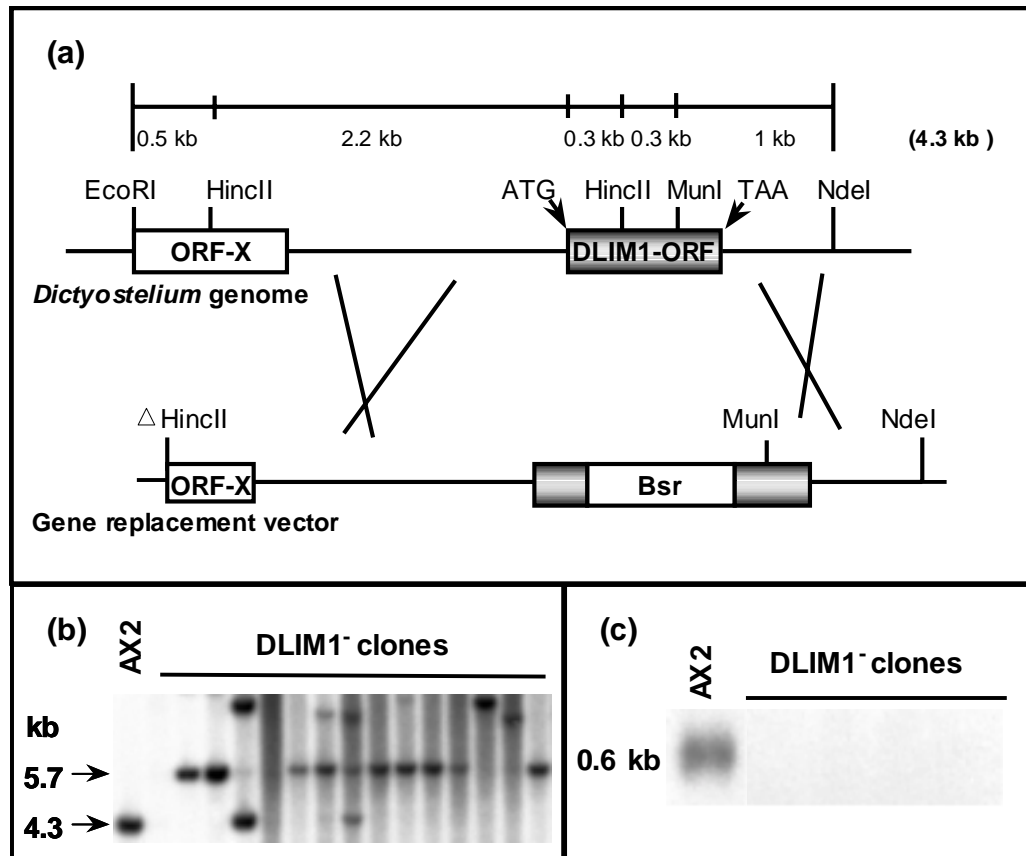


Figure 30. The generation of DLIM1⁻ mutants. (a) Disruption of the DLIM1 gene in wild-type AX2 cells by homologous recombination. To this end, a gene replacement vector was constructed by inserting a 1.4 kb blasticidin resistance (Bsr) cassette at the HincII site in the DLIM1 coding region. AX2 cells were transformed with this gene replacement vector and the transformants were screened by PCR, Southern and northern blot analyses. (b) Southern blot analysis of EcoRI+NdeI restricted genomic DNA of AX2 and mutant cells indicates that a gene replacement event has occurred, since insertion of the Bsr cassette causes the shift of a 4.3 kb band to a 5.7 kb band in the mutants. (c) Northern blot of total RNA (30 µg/lane) obtained from axenically growing AX2 cells and four of the transformants demonstrates that no message is present in the transformants. One of these transformants was selected for further cell-biological and biochemical characterizations and is referred to as DLIM1⁻ mutant. Both, Southern as well as northern blots were screened with ³²P labelled full length DLIM1 cDNA.

6. Characterization of DLIM1⁻ mutant

6.1. Determination of cell size

Qualitative examination of cultures of the DLIM1⁻ mutant cells grown in axenic medium suggested that the mutant cells were bigger in size as compared to the wild-type AX2 cells. For quantitative analysis, the size distribution of DLIM1⁻ mutant cells grown in shaking suspension was determined (Materials and Methods, 2.5.) and compared to that of the AX2 cells (Figure 31a,b). DLIM1⁻ mutant cells were found to be comparatively larger, with an average diameter of 13 μm as compared to the wild-type AX2 cells having an average diameter of 11 μm . The size histogram (Figure 31b) shows that 48% of AX2 cells are 10 μm in diameter, whereas only 27% of DLIM1⁻ cells have a diameter of 10 μm . Mutant cells exhibit a shift towards the bigger size range (12-16 μm). Only 17% of the total population of AX2 cells were 14 μm in diameter, while 34% of DLIM1⁻ cells exhibited a diameter of 14 μm . Moreover, only 0.8% of AX2 cells were 16 μm in diameter, whereas the population of cells with 16 μm diameter was 7% for DLIM1⁻ mutant cells.

6.2. Quantitation of nuclei

As mutant cells are larger in size in comparison to the wild-type AX2 cells, studies were performed to determine if the increase in mutant cell-size is due to a cytokinesis defect in DLIM1⁻ mutant cells. To this end, the number of nuclei/cell of DLIM1⁻ mutant cells were quantitated and compared with that of the AX2 cells employing immunofluorescence studies using the DNA binding dye DAPI (Materials and Methods, 5.3.). Observation of the DAPI labelled mutant cells under the fluorescence microscope revealed that the large-sized DLIM1⁻ mutant cells were multinucleated (Figure 32a,b). Quantitation of the number of nuclei/cell in the AX2 and mutant cells grown under shaking conditions revealed that more multinucleate cells are present in the cultures of DLIM1⁻ mutant than of the wild-type AX2 (Figure 32a'), suggesting that cytokinesis is not normal in DLIM1⁻ mutant cells.

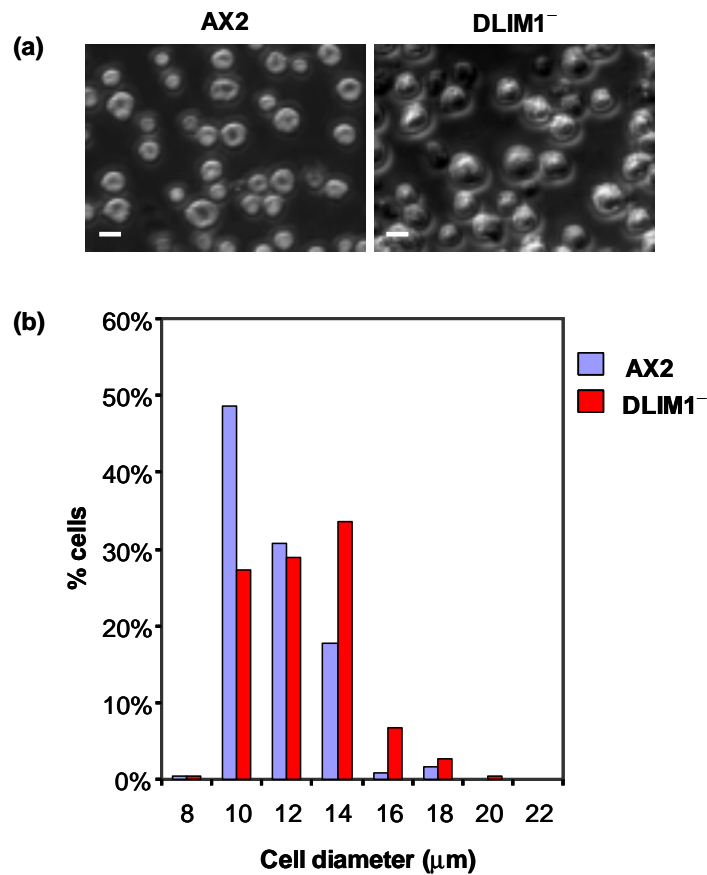


Figure 31. Size distribution of AX2 and DLIM1⁻ cells. (a) Phase contrast images of AX2 and DLIM1⁻ mutant cells showing completely rounded cells that were used for measuring diameters. (b) Size histograms of AX2 and DLIM1⁻ cells. Single cells were photographed and the diameters for 250-300 cells per strain determined from the prints. DLIM1⁻ cells are bigger than the wild-type AX2 cells. Bars, 10 μm.

Cytokinesis is believed to be facilitated by traction-mediated cytofission in cells attached to a substratum. This traction-mediated cytofission has been shown in Myosin II null cells, which are unable to form a cleavage furrow and to carry out appropriate cytokinesis (Knecht and Loomis, 1987; De Lozanne and Spudich, 1987; Fukui *et al.*, 1990). In order to examine whether division of DLIM1⁻ cells is also facilitated by traction-mediated cytofission, cells grown in suspension culture were transferred onto glass coverslips submerged in the same medium. The distribution of multinucleate cells was determined by DAPI staining after two days of continued growth on the glass surface (Figure 32b'). More binucleate and

multinucleate cells were observed in the cultures of DLIM1⁻ mutant cells than of the AX2 wild-type cells. These results are in accordance with that of the cultures grown in shaking suspension, indicating a mild cytokinesis defect in the DLIM1⁻ cells. The proportion of multinucleate wild-type AX2 cells as well as mutant cells decreases during growth on glass as compared to growth in shaking suspension, indicating attachment of cells to a surface during axenic growth favours cell division.

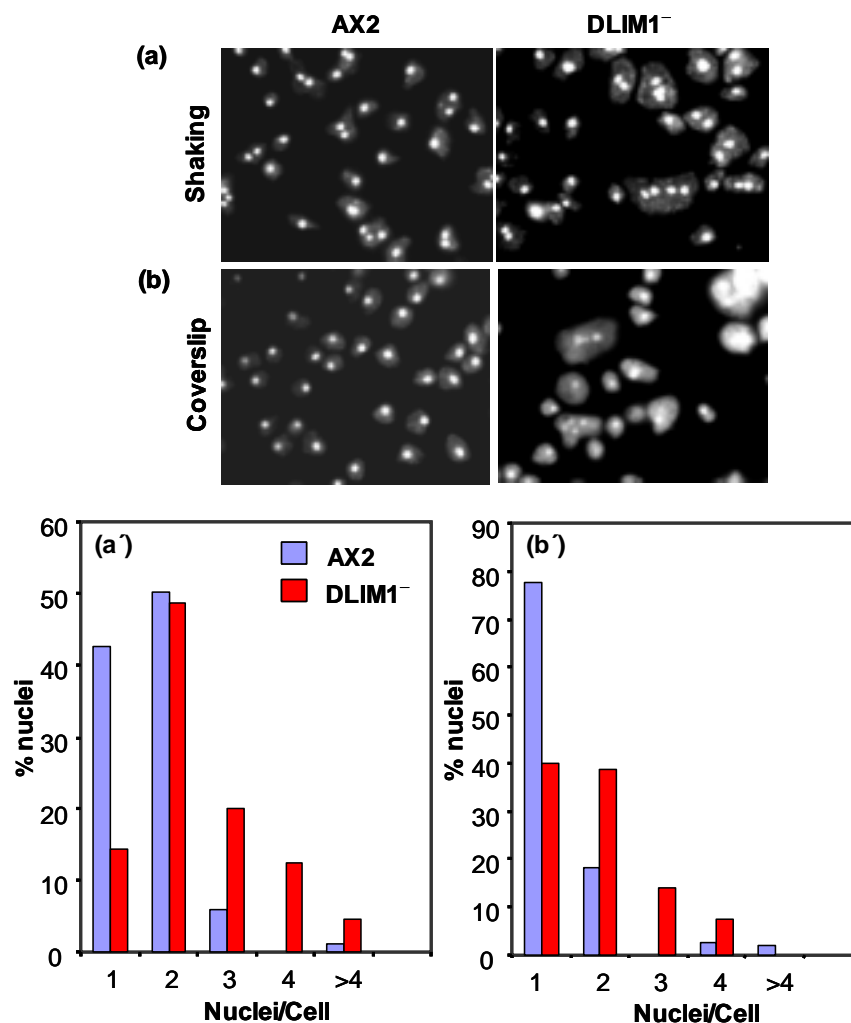


Figure 32. Quantitation of nuclei of AX2 and mutant cells. (a and b) Fluorescence images after DAPI staining of the nuclei of the AX2 and mutant cells grown either in shaking suspension (a), or on glass coverslips (b). (a' and b') Histograms illustrating quantitation of nuclei of the AX2 and mutant cells grown either in shaking suspension (a'), or on glass coverslips (b'). The cells shown are representatives of all the cells in the population. For all the strains, nuclei of 300-400 cells were counted. Wild-type AX2 cells are mainly mononucleated or binucleated, whereas many DLIM1⁻ cells also possess 4 and >4 nuclei.

6.3. Growth of mutant cells in axenic medium

Since cell growth is a result of interplay between a variety of cellular processes involving rearrangements of the actin cytoskeleton, growth rate of DLIM1⁻ mutant was determined and compared with that of wild-type AX2 cells. The growth patterns of AX2 and DLIM1⁻ cells were investigated at 160 rpm and 21°C with starting cell densities of 5×10^5 cells/ml and 1×10^5 cells/ml. Under both starting cell-density conditions, no significant difference was observed in the growth patterns of wild-type AX2- and derived mutant cells (Figure 33a,b). Wild-type AX2 cells attained maximum cell densities of 8.4×10^6 cells/ml and 1.1×10^7 cells/ml with a starting density of 1×10^5 cells/ml and 5×10^5 cells/ml, respectively, while DLIM1⁻ mutant cells attained maximum cell densities of 7.2×10^6 cells/ml and 1×10^7 cells/ml on starting the cultures with 1×10^5 cells/ml and 5×10^5 cells/ml, respectively. Wild-type AX2 cells and mutant cells grow with the same doubling time of 11 h and 13 h in the cultures started with 1×10^5 cells/ml and 5×10^5 cells/ml, respectively. This suggests that DLIM1 is not essential for the growth under optimal conditions.

6.4. Growth of mutant cells under stress conditions

Since *Dictyostelium discoideum* lives as a natural phagocyte in soil and feeds on yeast and bacteria, fluctuations in the environmental temperature, humidity and osmolarity pose physiological challenges to growth and survival of this free-living organism. It is, therefore, believed that certain proteins that are not essential under optimal laboratory conditions might play a role under stress conditions. For this reason, growth of DLIM1⁻ mutant cells was determined under conditions of temperature and osmotic stress and compared with that of the wild-type AX2 cells.

6.4.1. Growth under temperature stress

Wild-type AX2 cells and DLIM1⁻ mutant cells were grown under conditions of low and high temperature stresses. Cultures of AX2- and DLIM1⁻ mutant-cells grown at 15°C in axenic medium at 160 rpm with a starting density of 5×10^5 cells/ml, exhibited similar growth

patterns (Figure 34a). AX2 as well as DLIM1⁻ cells attained maximum cell densities of 3.0×10^6 cells/ml and exhibited a similar doubling time of 38 h. However, growth of DLIM1⁻ mutant cells was significantly impaired when the cultures were grown at 27°C in axenic medium at 160 rpm with a starting density of 5×10^5 cells/ml (Figure 34b). Under these conditions, AX2 cells reached cell density of 5.4×10^6 cells/ml with a doubling time of 13 h. The DLIM1⁻ cells were clearly impaired showing a prolonged doubling time of 19 h and reduced cell density at saturation. Moreover, DLIM1⁻ mutant cells became very small in size and showed rapid cell-lysis under high temperature condition.

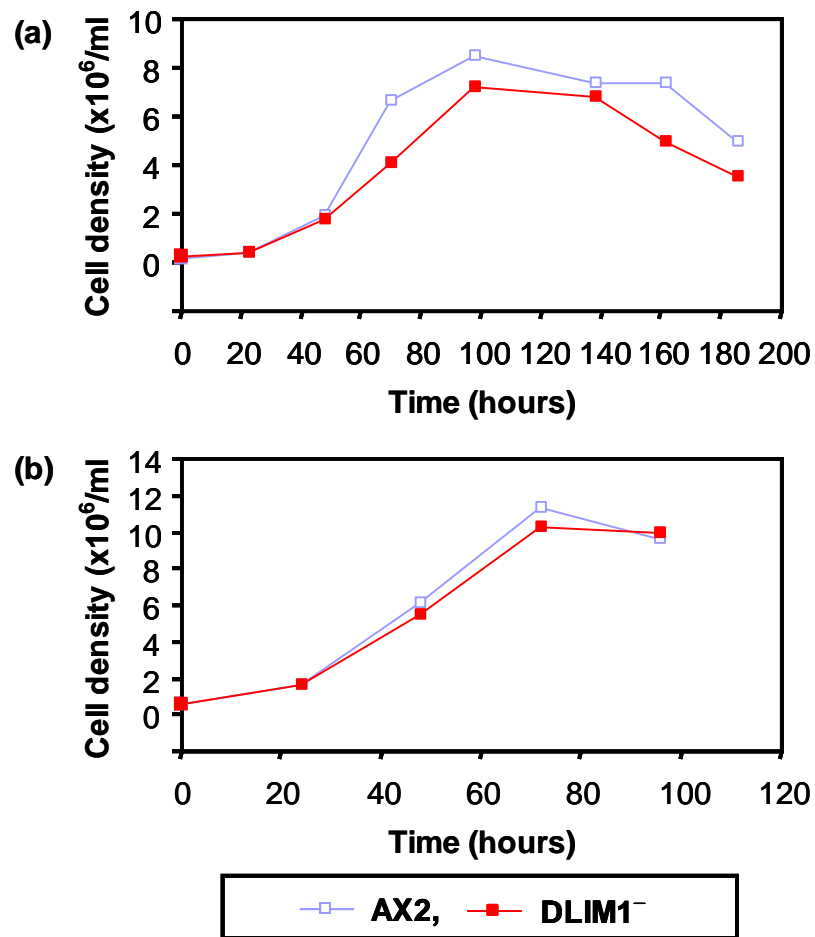


Figure 33. Growth of wild-type AX2 and mutant strains in axenic medium. (a and b) Cultures were inoculated with either 1×10^5 cells/ml (a), or 5×10^5 cells/ml (b), and grown at 21°C with shaking at 160 rpm. Cells were counted at indicated time points. Growth is not impaired in the DLIM1⁻ mutant. The data plotted here are from a single experiment, but similar results were obtained for three independent experiments with both the conditions.

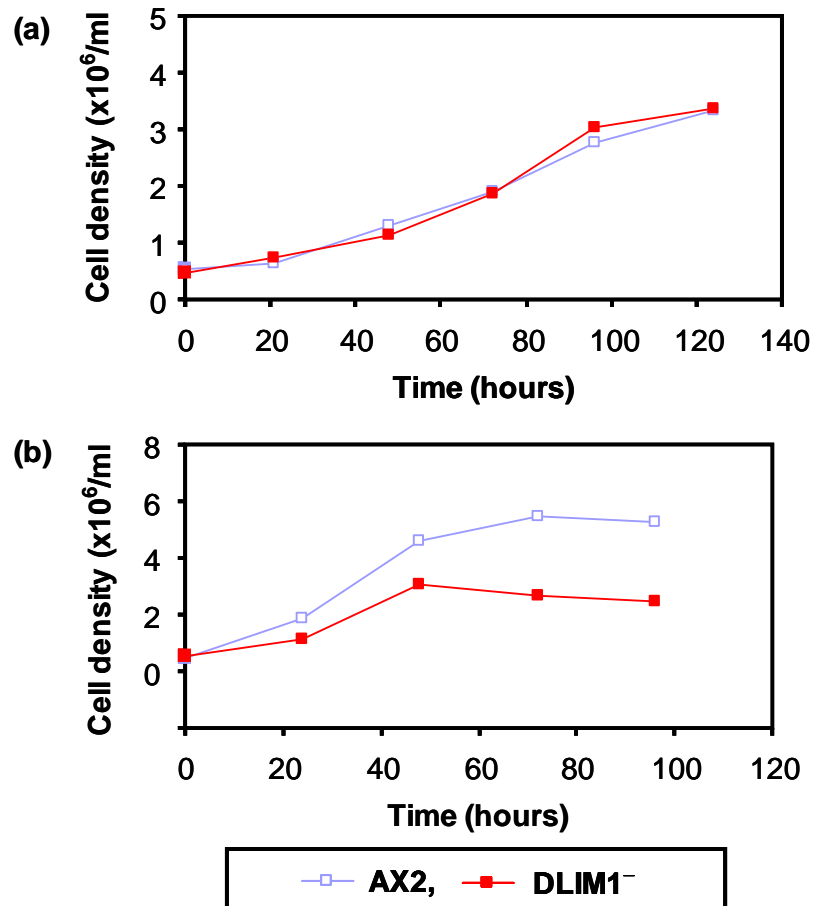


Figure 34. Growth of DLIM1⁻ mutant cells in comparison with AX2 under temperature stress conditions. (a and b) Cultures were inoculated with 5×10^5 cells/ml and grown with shaking at 160 rpm either at 15°C (a), or at 27°C (b). No differences in growth were observed when the cultures were grown at 15°C. However, growth of DLIM1⁻ mutant cells was significantly impaired when grown at 27°C. The curves shown are representative of three independent experiments.

6.4.2. Growth under osmotic stress

Dictyostelium discoideum amoebae have developed successful means to avoid the harmful consequences of rapidly changing osmotic conditions in the natural habitat. Synthesis of stress proteins and accumulation of compatible osmolytes facilitate repair and recovery of cells in response to exposure of cells to high osmolarities (Kwon and Handler, 1995). Eukaryotic cells, in addition to these processes, can quickly respond to changes in cell volume by rapid reorganization of their cytoskeleton. We, therefore, observed growth of the

DLIM1⁻ mutant cells in the presence of increased osmolarity. To achieve this, axenic medium was supplemented with either 30 mM NaCl or 115 mM sorbitol, and cultures were grown in axenic medium under optimal conditions (21°C and 160 rpm) with a starting density of 5×10^5 cells/ml.

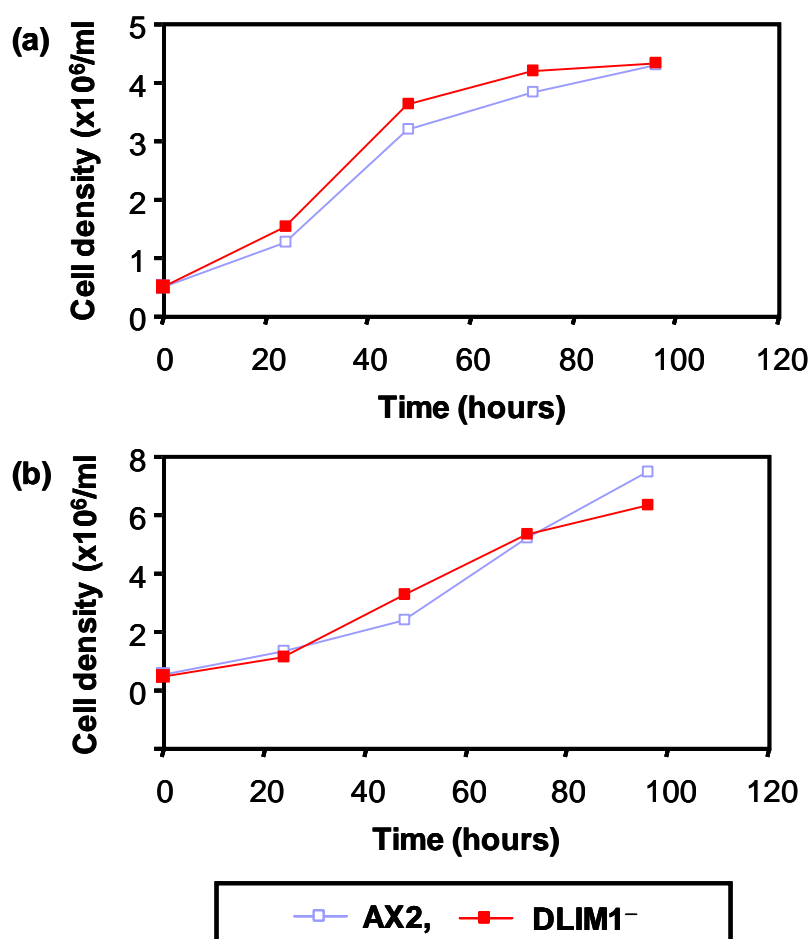


Figure 35. Growth of DLIM1⁻ mutant cells in comparison with AX2 under osmotic stress conditions. (a and b) Cultures were inoculated with 5×10^5 cells/ml and grown at 21°C with shaking at 160 rpm in axenic medium supplemented with either 30 mM NaCl (a), or 115 mM sorbitol (b). No significant differences in growth were observed under both the osmotic stress conditions. The curves shown are representative of three independent experiments.

In the presence of 30 mM NaCl, AX2 cells were able to grow to a density of 4.3×10^6 cells/ml at saturation with a doubling time of 18 h. Similar cell density at saturation and comparable doubling time was observed for DLIM1⁻ mutant cells (Figure 35a). In the presence of 115 mM sorbitol, AX2 cells grew with a doubling time of 20 h and reached a

maximum density of 7.4×10^6 cells/ml (Figure 35b). DLIM1⁻ mutant cells exhibited no significant difference in their growth pattern with only slightly reduced cell density at saturation (6.3×10^6 cells/ml) and comparable doubling times. These results suggest that the growth of the DLIM1⁻ mutant cells is not affected under conditions of increased osmolarity.

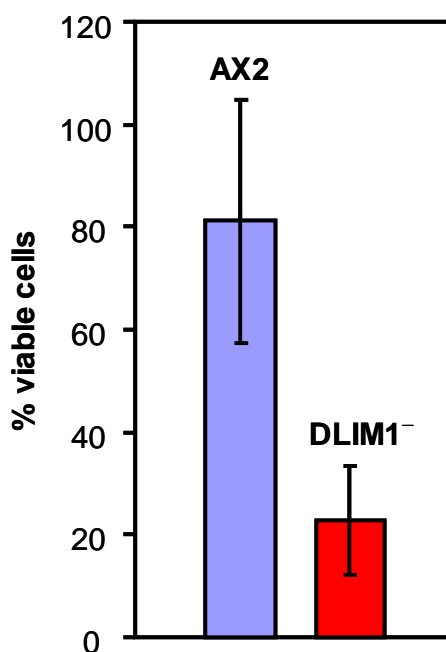


Figure 36. Response of AX2 and mutant cells to osmotic shock. Cells were shaken in Soerensen phosphate buffer in the presence of 0.4 M sorbitol for 2 h, diluted in low osmolarity solution and plated onto SM agar plates with *Klebsiella*. DLIM1⁻ mutant cells showed decreased viability, while wild-type AX2 cells were only slightly affected. The values plotted are the average of four independent experiments. In each set of experiment, each strain was plated onto four independent plates. Bars indicate standard deviation.

6.5. Response to osmotic shock

Since the role of a cytoskeletal protein in the cytoskeletal rearrangements elicited by adaptation to sustained altered osmolarity could differ from that of the acute osmotic shock, response of the DLIM1⁻ mutant cells to acute osmotic shock was analysed. To this end, a viability assay was performed by exposing the cells for 2 h to 0.4 M sorbitol and then diluted into a solution of low osmolarity (Materials and Methods, 2.6.). Histograms shown in Figure 36 reveal that survival of AX2 cells was much better than the DLIM1⁻ mutant cells as

osmotic shock led to marked reduction in the viability of DLIM1⁻ mutant cells. AX2 cells showed a high viability of $81 \pm 23.7\%$, whereas viability of DLIM1⁻ mutant cells after osmotic shock was only $22.8 \pm 10.6\%$. This indicates that the DLIM1⁻ mutant cells are less tolerant to osmotic shock, which might reflect a reduced strength of the cortical cytoskeleton in these mutant cells.

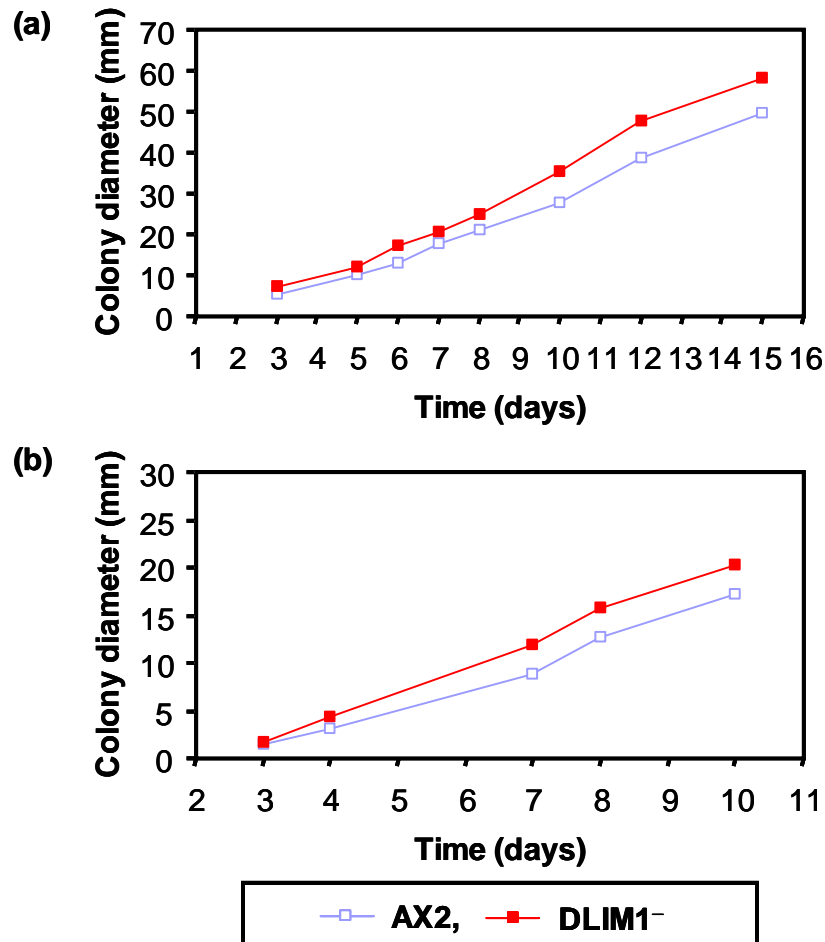


Figure 37. Growth on agar plates with bacteria as food source. (a) SM agar plates with *Klebsiella aerogenes* were inoculated with wild-type AX2 and mutant cells using a toothpick. (b) AX2 and mutant cells were plated onto *Klebsiella* overlaid SM plates by spreader dilution, so as to get clones arising from growth of single cells. Increase in colony diameter was recorded as a measure of growth rate. Under both the conditions, growth rate of DLIM1⁻ cells is slightly increased. The curves shown are representative of three independent experiments.

6.6. Growth on agar plates with bacteria as food source

The growth of AX2- and derived DLIM1⁻ mutant-cells was also observed on SM agar plates in the presence of *Klebsiella aerogenes* as their food source. The cells were either inoculated in the centre (Figure 37a), or plated by spreader dilution to get single cell colonies of *Dictyostelium* (Figure 37b) on SM agar plates overlaid with *Klebsiella aerogenes* (Materials and Methods, 2.1.2.). The increase in colony diameter was taken as a relative measure of the growth rate in both the conditions. Figure 37 shows that colonies of DLIM1⁻ cells grow slightly faster on *Klebsiella* lawns than those measured for AX2 cells.

6.7. Development of mutant cells

Upon starvation *Dictyostelium* cells undergo a developmental cycle in which single amoebae aggregate to form a multicellular fruiting body. This involves differentiation of *Dictyostelium* cells into spore-cells and stalk-cells and requires the sequential expression of developmentally regulated genes. We, therefore, decided to investigate the consequence of the absence of DLIM1 gene on the developmental process in the DLIM1⁻ mutant cells.

6.7.1. Development under submerged condition on plastic surface

To determine the role of DLIM1 during early stages of development, wild-type AX2 cells and DLIM1⁻ cells were placed in monolayer under starvation buffer on plastic petridishes (Materials and Methods, 2.2.3.) and the developmental stages were photographed at indicated time points. Figure 38 shows that wild-type AX2 cells form large aggregates by 13 h of development. However, DLIM1⁻ mutant cells still display streams of moving cells at this time point, which persist even after 16 h of development. Rather than coalescing to a single centre as in case of the AX2 cells, individual streams of DLIM1⁻ mutant cells often fractured along their length forming smaller aggregates (18 h to 24 h). Moreover, onset of development in DLIM1⁻ cells is delayed by 4-5 h (Figure 38).

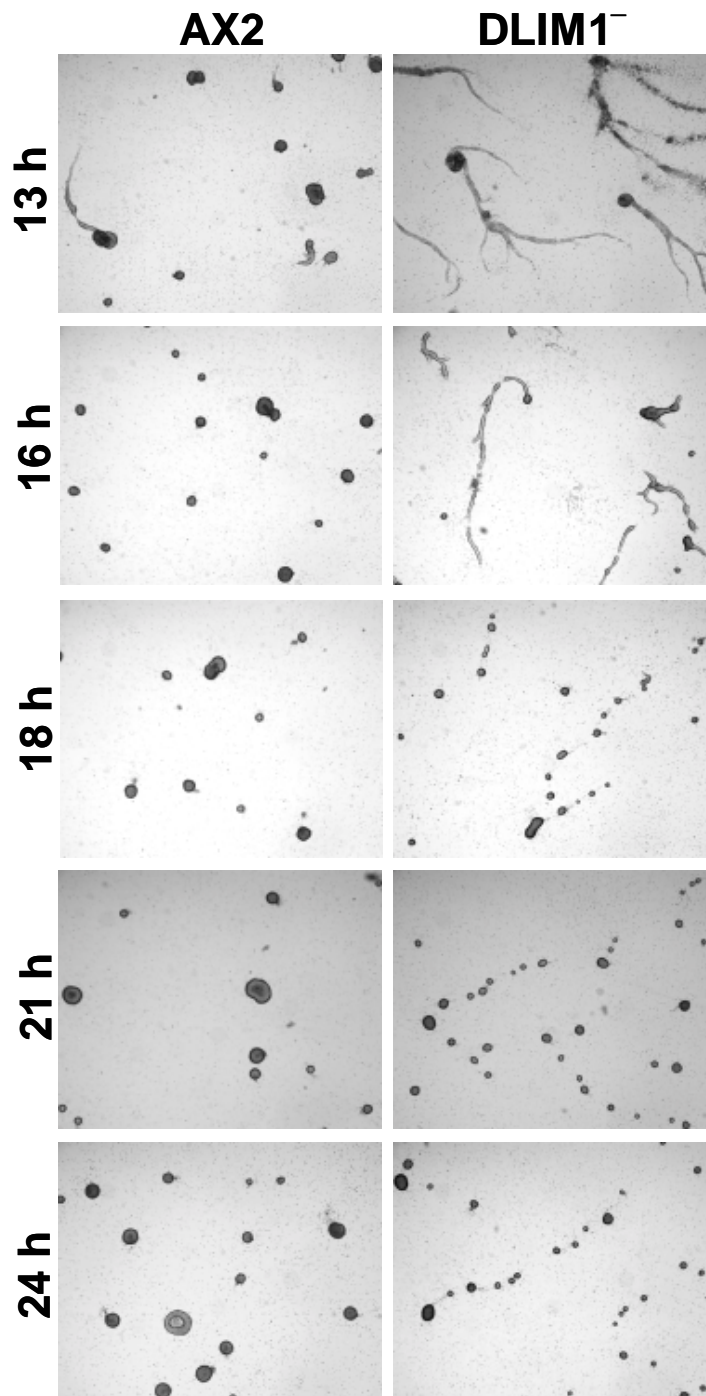
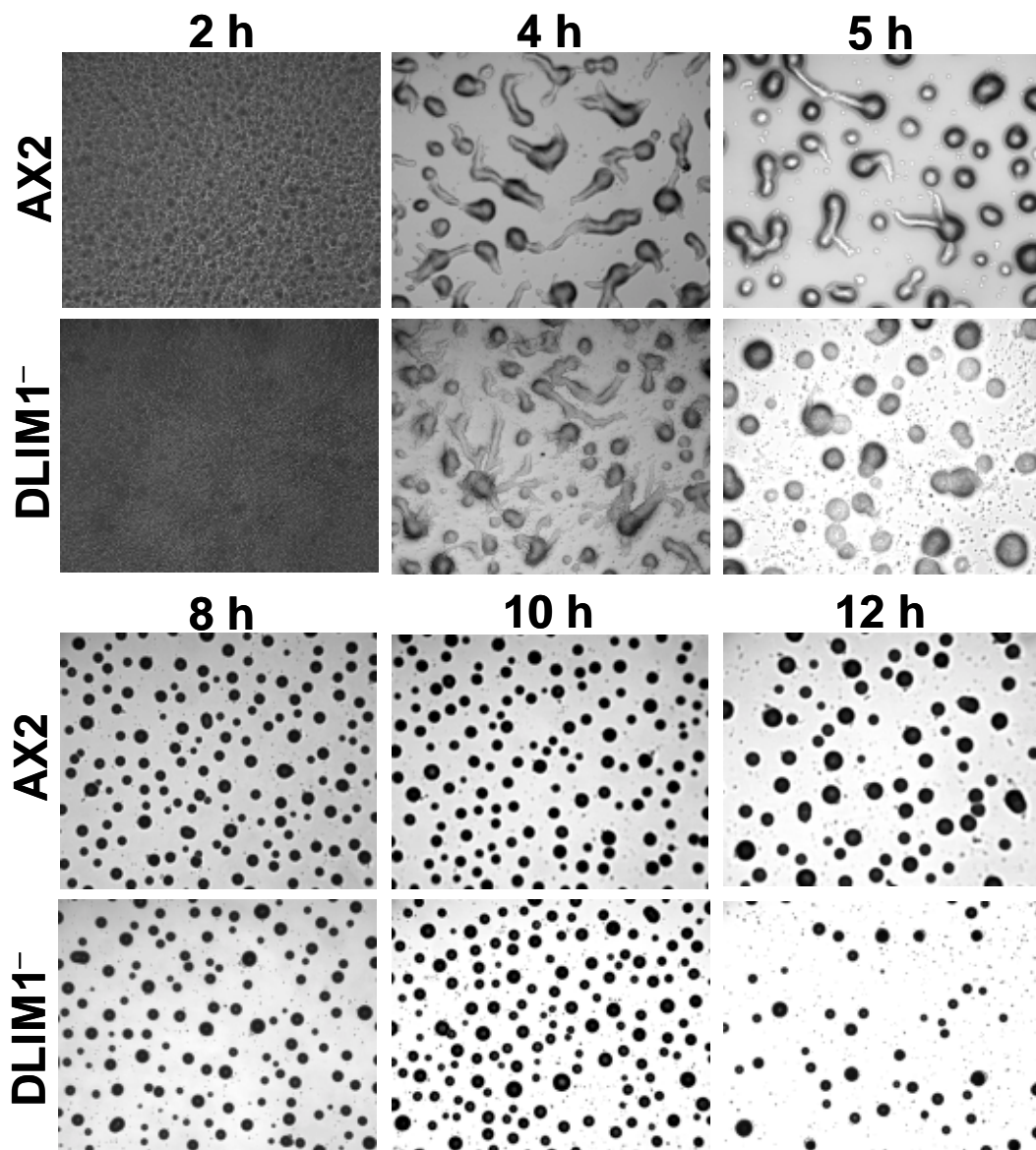


Figure 38. Development under submerged condition on plastic surface. The cultures were plated in monolayers submerged under starvation buffer in plastic petridishes. The cultures were incubated for development at 21°C and photographed after 13 h. Wild-type AX2 cells form large aggregates within 13 h, while mutant cells show a delay of 4-5 h and make smaller aggregates.

6.7.2. Development on agar plates

The cells can aggregate in starvation buffer under submerged conditions, while post-aggregation development and fruiting require a solid substratum and the commonly used substratum to study development is agar. Therefore, developmental pattern of DLIM1⁻ mutant cells was also assessed on an agar surface.



(Figure contd. on next page.....)

(.....figure contd. from previous page)

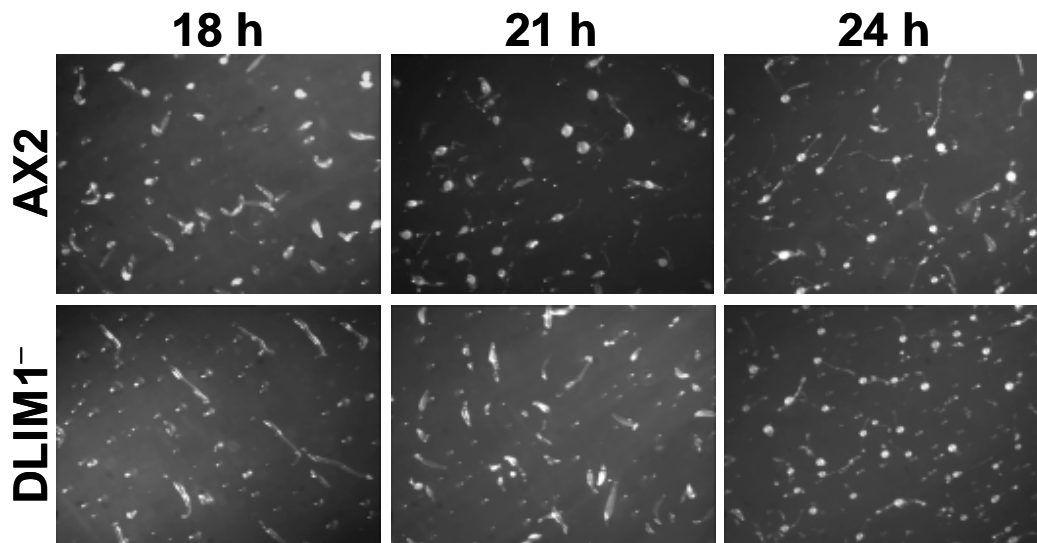


Figure 39. Development of wild-type AX2 and mutant cells on agar plates. Cells were plated on water-agar plates and allowed to undergo development at 21°C. The pictures were taken at indicated time points. No significant differences were observed during pre- as well as post-aggregative development and DLIM1⁻ mutant cells form morphologically similar fruiting bodies within 21-24 h.

Cells were allowed to develop on phosphate-buffered agar plates as well as on water-agar plates (Materials and Methods, 2.2.2.). Figure 39 shows developmental patterns of AX2 and DLIM1⁻ mutant cells on water-agar plates. The delay in onset of development in DLIM1⁻ cells, as seen when the DLIM1⁻ cells were developed under submerged conditions (Figure 38), was not observed during development on water agar plates. Both AX2 as well as DLIM1⁻ cells form large streams of elongated cells (4 h) that aggregate (5 h) to make mounds at approximately 8 h of development. No significant differences were observed during post-aggregative development and mutants pass through all the stages of development forming morphologically similar fruiting bodies within 21-24 h. Similar results were observed in case of cells developed on phosphate-buffered agar plates (Figure not shown). The different early developmental pattern observed on agar and under submerged condition on plastic surface could be due to either a defect in cAMP relay signalling or substrate dependent adhesion.

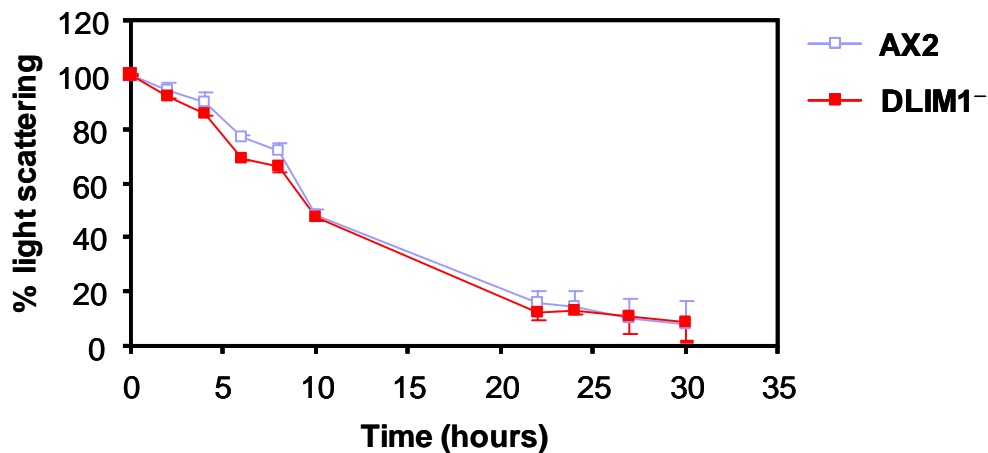


Figure 40. Time course of agglutination of AX2 and DLIM1⁻ mutant cells in shaking suspension. Cultures were resuspended in Soerensen phosphate buffer at the same total cell volume and assigned a value of 100%. At the indicated time points light scattering at 600 nm was measured in a spectrophotometer. Each point represents the mean of two independent experiments. Bars represent standard deviation.

6.8. Analysis of spore germination

The spores of *Dictyostelium discoideum* germinate in three well-defined stages: activation, swelling and emergence of amoebae from the swollen spores. The actin cytoskeleton has been observed to play a role in early steps of activation of germination. Therefore, efficiency of germination of DLIM1⁻ spores was assessed by a quantitative analysis. At the end of development on agar, spores were randomly collected with a loop and suspended in Soerensen phosphate buffer. Spores were then heat-activated at 45°C for 30 min and a defined number of heat-activated spores were plated on bacterial lawns. The number of colonies formed per plate was scored (Materials and Methods, 2.7.). No significant differences in the spore germination of DLIM1⁻ mutant cells and the wild-type cells were observed, with viability of spores being 56-63% for AX2 as well as the DLIM1⁻ mutant.

6.9. Cell-to-cell adhesion of mutant cells

Cell-adhesion assay was performed to determine if lack of DLIM1 affects the ability of the cells to aggregate, which might arise due to alteration in the cytoskeleton at contact sites. For

this, the time course of agglutination of the AX2 and mutant cells in shaking suspension was assessed by measuring the decrease in light scattering at 600 nm (Materials and Methods, 2.9.). Under these conditions, aggregates are formed that recapitulate many of the developmental events that occur on a solid surface (Takeuchi *et al.*, 1988). Figure 40 shows the scattering of light by AX2 and mutant cells in Soerensen phosphate buffer at indicated time points of development. Agglutination in DLIM1⁻ mutant cells is comparable to wild-type AX2 cells.

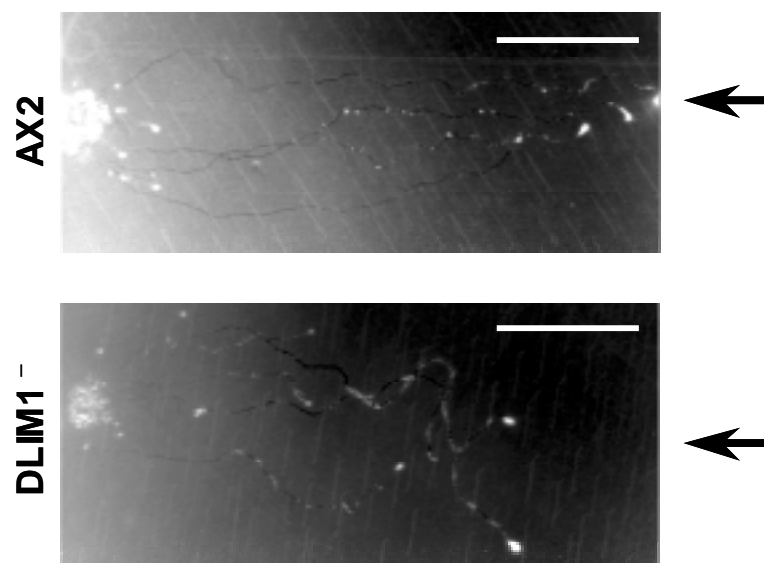


Figure 41. Phototaxis assay of wild-type AX2 and DLIM1⁻ mutant cells. The cells were inoculated onto water-agar plates and incubated for three days in the presence of unidirectional light source. The resultant slugs and slug-trails were transferred to the nitrocellulose filters, stained with amido black and photographed. The direction of light is indicated by arrows on the right. The results shown are representative of four independent experiments. Bar, 1 cm.

6.10. Qualitative phototaxis assay

Dictyostelium discoideum cells form motile slugs after aggregation. These slugs move towards the source of light leaving a slime sheath behind them. The ability of the slugs of the DLIM1⁻ mutant cells to perform phototactic response was analysed by a qualitative phototaxis assay (Materials and Methods, 2.8.). Figure 41 shows the migration paths of DLIM1⁻ mutant slugs in comparison to AX2 slugs in the presence of lateral light coming

through a slit of 3 mm. The wild-type AX2 slugs migrate directly towards the light source. Though the DLIM1⁻ slugs also migrate towards the light source, they show slight detours during their movement.

4. Discussion

1. DLIM1 is a group 2 LIM domain protein

We have isolated and characterized a LIM domain containing protein of *Dictyostelium discoideum*, which we refer to as DLIM1. Two more LIM domain containing proteins have been reported from *Dictyostelium*, DdLim (Prassler *et al.*, 1998) and LIM2 (Chien *et al.*, 2000). Both DdLim and LIM2 proteins are reported to be associated with the actin cytoskeleton playing a role in its rearrangement. Another cytoskeleton-associated LIM domain containing protein designated as DLIM2 has been identified from *Dictyostelium* and work on DLIM2 is in progress in our lab (Khurana, T., personal communication). Both DdLim and DLIM2 contain a single copy of LIM domain located at the N-terminus and have

been, therefore, classified under group 2 according to the classification proposed by Dawid *et al.* (1998). LIM2, which exhibits 5 copies of LIM domains at its C-terminus, has been classified as a group 3 LIM protein. DLIM1 is comprised primarily of two LIM domains that are separated by an intervening sequence of 55 amino acid residues. This and the organization of the LIM domains of DLIM1 classify DLIM1 as a group 2 LIM domain protein. Infact DLIM1 exhibits highest degree of homology to the LIM domain containing proteins belonging to group 2 (Figure 7), with the strongest overall sequence homology to members of the CRP family (29-31 % identity, 43-45% similarity). In contrast to the other group 2 family members, the LIM domains of DLIM1 are not followed by a glycine-rich region. DLIM1 is, however, not an only exception to this as DLIM1 shares this feature with a pollen specific LIM protein of *Helianthus annuus*, SF3 (Baltz *et al.*, 1992). Another structural feature of DLIM1 protein is the presence of a proline-rich region between the two LIM domains (Figure 6). The functional significance of this proline-rich region is not known. We speculate that this proline-rich region acts as a linker region that separates the LIM domains in DLIM1 and confers both lateral and rotational freedom on the LIM domains, thereby potentially enabling DLIM1 molecules within *Dictyostelium* cells to present a wide variety of orientations for recruitment of protein partners.

2. Subcellular localization of DLIM1

Members of the CRP family have been observed to play a regulatory or structural role in the actin cytoskeleton owing to their interaction with actin-binding proteins and their localization at focal contacts and stress fibres in mammalian cells. The presence of the LIM domains in these proteins allows them to function as a template or adapter capable of promoting specific protein-protein interactions at the cytoskeleton (Sadler *et al.*, 1992; Arber *et al.*, 1994; Brown *et al.*, 1998). The specificity of protein-protein interactions mediated by LIM domains has been demonstrated since all the three members of the CRP family are capable of directly interacting with zyxin and α -actinin (Sadler *et al.*, 1992; Schmeichel and Beckerle, 1994; Louis *et al.*, 1997; Pomies *et al.*, 1997). The *Dictyostelium* DdLim protein localizes in the cell cortex and has been suggested to act as an adapter protein at the cytoskeleton-membrane interface where it is involved in a receptor-mediated Rac-1 signalling pathway that leads to actin polymerisation in lamellipodia and ultimately cell

motility (Prassler *et al.*, 1998). Likewise, *Dictyostelium* LIM2 protein is also localized in the cell cortex and is required for cell motility and chemotaxis (Chien *et al.*, 2000). We were, therefore, interested in elucidating the subcellular localization of DLIM1 and the role it plays in *Dictyostelium*. We have investigated the intracellular localization of DLIM1 by expressing a green fluorescent protein (GFP)-fusion protein in *Dictyostelium* AX2 cells. This approach also allowed us to follow the dynamics of DLIM1 *in vivo*.

2.1. DLIM1 not only colocalizes with but also binds to actin

Confocal studies performed with the GFP-DLIM1 expressing cells indicate that DLIM1 is mainly enriched in areas of the cell cortex (Figure 10b). The cortical fluorescence of GFP-DLIM1 always coincided with the actin staining in immunolabelled cells (Figure 12). DdLim, too, has been observed to colocalize with the F-actin at the cytoskeleton (Prassler *et al.*, 1998). However, LIM2 is associated with the cell-cortex but it does not colocalize with the F-actin (Chien *et al.*, 2000). Occasional localization of DLIM1 in the nucleus was also observed, the functional significance of which is yet unclear. A putative nuclear targeting signal (KKYGPK) has been identified in the CRPs leading to their bimodal subcellular distribution, initially present exclusively in nuclei of early undifferentiated muscle cells and later accumulating to high levels in the cytoplasm (Arber *et al.*, 1994; Stronach *et al.*, 1996). We could, however, not identify a putative nuclear targeting signal in the DLIM1 sequence. GFP-DdLim fusion protein has also been observed to accumulate in the nucleus. DdLim also does not harbour a nuclear targeting signal in its sequence (Prassler *et al.*, 1998).

Colocalization of DLIM1 and actin in our localization studies encouraged us to assess the binding capability of DLIM1 to actin *in vitro*. We have demonstrated in actin-sedimentation assays using a GST-DLIM1 fusion protein that DLIM1 binds to filaments of rabbit skeletal muscle actin (α -actin) as well as *Dictyostelium discoideum* actin even in the presence of high salt (100 mM KCl) concentration (Figures 27, 28). To our knowledge this is the first report demonstrating an interaction between a protein that is comprised only of LIM domains and actin. Though an actin-binding LIM protein (abLIM) has been reported, the domain responsible for an interaction between abLIM and actin has been mapped to the dematin-like domain present at the C-terminus of the abLIM (Roof *et al.*, 1997). Ca^{2+} did not influence F-

actin binding by DLIM1 (Figure 28). Often actin cross-linkages are disrupted in response to signals that cause an increase in cytoplasmic Ca^{2+} and three of the actin crosslinking proteins from *Dictyostelium* cells, 30 kD F-actin bundling protein, α -actinin and Ddplastin, are known to be inhibited by Ca^{2+} (Fechheimer and Taylor, 1984; Noegel *et al.*, 1987; Prassler *et al.*, 1997). However, in these instances modules on the proteins have been identified that are responsible for Ca^{2+} -binding.

Since members of the CRP family are capable of directly interacting with α -actinin (Pomies *et al.*, 1997), we have tested an influence of the presence of α -actinin on the actin-binding efficiency of DLIM1 and did not observe any impact (Figure 29), though we do not rule out the possibility of an interaction between DLIM1 and α -actinin. A recent report demonstrated that the ability of CRP1 to interact with α -actinin depends on an 18-residue sequence (amino acid residues 62-79) occurring within the protein's N-terminal glycine-rich repeat that follows the N-terminal LIM domain (Harper *et al.*, 2000). This region has been observed to be both necessary and sufficient to support the association with α -actinin. Moreover, a site directed mutagenesis analysis of the CRP1's binding region revealed the critical importance of a single lysine residue (lysine 65 of CRP1) that is required for its partnership with α -actinin (Harper *et al.*, 2000). DLIM1, in contrast, exhibits a very low homology to CRPs within this region and exhibits the presence of only 4 glycine residues as against 7 glycine residues of CRP1 in the 18-residue sequence that follows the N-terminal LIM domain (Figure 7a). Moreover, DLIM1 has a leucine residue at the position that corresponds to the critical lysine residue of CRP1, thus favouring our observation.

2.2. DLIM1 is involved in the dynamic processes controlled by the actin cytoskeleton

Expression of GFP-DLIM1 fusion protein in *Dictyostelium* has permitted the visualization in living cells of DLIM1 dynamics, which closely match those of actin.

Dictyostelium cells take up fluid by macropinocytosis, which depends on the integrity of polymerised actin as demonstrated by treating the cells with cytochalasin A, an actin

depolymerising drug (Hacker *et al.*, 1997). Many actin-associated proteins are also involved in the process of macropinocytosis, but so far dynamic studies are available only for coronin, DAip1 and RacF1 (Hacker *et al.*, 1997; Konzok *et al.*, 1999; Rivero *et al.*, 1999a). A GFP-DLIM1 rich membrane invaginates and the edges of the protrusion fuse to form an endocytic vesicle enclosing the extracellular fluid and the GFP-DLIM1 protein coats this vesicle. Within less than 1 min after internalization, the GFP-DLIM1 dissociates from the coat surrounding the vesicle although the vesicle is still present, indicating the involvement of DLIM1 during early steps of pinocytosis (Figure 14). An identical protein-redistribution pattern has been observed for GFP-coronin, GFP-DAip1 and GFP-RacF1 as they associate with the coat surrounding the macropinosomes during early stages of pinocytosis and, like GFP-DLIM1, dissociate from the coat surrounding the vesicle within less than 1 min after internalisation of the vesicle (Hacker *et al.*, 1997; Konzok *et al.*, 1999; Rivero *et al.*, 1999a).

Particle uptake or phagocytosis is a very active process in *Dictyostelium* involving rearrangement of the actin cytoskeleton and like fluid-phase endocytosis depends on the integrity of polymerised actin (Maniak *et al.*, 1995; Hacker *et al.*, 1997). As the particle attaches to the membrane of *Dictyostelium* cells, phagocytosis is induced and a phagocytic cup is formed by the plasma membrane in association with the actin cortex. Immunolocalization studies, GFP-fusions and data from knockout mutants suggest that besides actin, various actin-associated proteins are also involved in distinct stages of phagocytosis (reviewed in Noegel and Schleicher, 2000). Coronin, an actin-associated protein accumulates at the phagocytic cups within 45 s after attachment of a particle and separates from the phagosome within 1 min after ingestion is completed (Maniak *et al.*, 1995). Besides coronin, myosin IB, myosin VII, ABP120/gelation factor, a 34 kD actin-bundling protein and *Dictyostelium* actin-interacting protein (DAip1) are some of the other known proteins that take part in phagocytosis and localize with actin at the phagocytic cup during early stages of phagocytosis (Fukui *et al.*, 1989; Cox *et al.*, 1996; Rivero *et al.*, 1996a; Konzok *et al.*, 1999; Titus, 1999). DLIM1 also seems to be involved in the early stages of phagocytosis, since GFP-DLIM1 fluorescence accumulates to high levels at the phagocytic cup surrounding the yeast particle, persists there as the cup progresses and complete uptake of the yeast occurs, and dissociates completely from the phagosome within 1 min of the yeast uptake (Figure 15). This pattern of redistribution strongly resembles that observed in GFP-coronin and

GFP-DAip1 expressing cells (Maniak *et al.*, 1995; Konzok *et al.*, 1999). Moreover, fluorescence of GFP-DLIM1 coincides with the actin staining during phagocytosis, indicating that DLIM1 might play a role in the rearrangement of the actin cytoskeleton during phagocytosis (Figure 17).

We have observed the reversibility of GFP-DLIM1 accumulation upon unsuccessful ingestion resulting in release of a yeast particle even after half of its body is covered by a phagocytic cup (Figure 16), suggesting that relocation of GFP-DLIM1 does not irreversibly influence the molecular events involved in phagocytosis. This observation is in agreement with a zipper-mechanism proposing a local and sequential regulation of phagocytosis, and argues against a trigger-mechanism initiating a phagocytosis process that would run until phagocytosis is completed (Swanson and Baer, 1995).

Besides taking part in phagocytosis and pinocytosis, DLIM1 is involved in exocytosis. We have observed GFP-DLIM1 fusion protein to preferentially accumulate on the membrane surrounding the yeast particle shortly before exocytosis of the yeast (Figure 18). We, therefore, conclude that DLIM1 transiently associates with the coat that surrounds particle-containing vesicles, dissociates from the coat upon internalisation of the vesicles, but reassembles on the vesicles as they return to the cell cortex for exocytosis. We speculate a similar pattern of DLIM1 redistribution during fluid-phase exocytosis as well. Our observation is in accordance with that reported for coronin and actin (Rauchenberger *et al.*, 1997). Coronin as well as the actin cytoskeletal coat that surrounds both particle- and fluid-containing vesicles in *Dictyostelium* are eventually shed by the vesicles as they transit through the cell. After dissociation of the cytoskeletal coat, acidification to pH 5 is followed by neutralization and reassembly of both actin as well coronin on the vesicles as they return to the cell cortex for exocytosis of the indigestible remnants (Rauchenberger *et al.*, 1997).

DLIM1 also seems to be involved in motility of the cells. Cell motility is an essential aspect of all the developmental stages of *Dictyostelium*, which involve signalling pathways and actin cytoskeleton. In these cells the localization of several cytoskeletal and signalling components during chemotaxis has been studied using GFP and immunohistochemical staining. It has been shown that actin, coronin, talin, cofilin and CAP transiently accumulate

at the leading edges of the motile *Dictyostelium* cells (Gerisch *et al.*, 1995; Kreitmeier *et al.*, 1995; Gottwald *et al.*, 1996; Aizawa *et al.*, 1997; Westphal *et al.*, 1997). Confocal studies performed with the vegetatively growing GFP-DLIM1 expressing cells revealed that the fusion-protein accumulates at the leading edge of the motile cells (Figure 11). Moreover in aggregation-competent GFP-DLIM1 expressing cells, which attain an elongated shape and rapidly extend pseudopods in the direction of the chemoattractant, the fusion-protein preferentially accumulates in the pseudopods of the migrating cells where it remains until the pseudopod is retracted and then it shifts to the newly formed pseudopod, thereby playing a role in cell motility (Figure 19). The cytoskeleton associated protein DdLim has also been observed to accumulate at the extreme membrane rims of newly formed protrusions in aggregation-competent cells and is involved in cell motility (Prassler *et al.*, 1998). Taken together, the localization of DLIM1 in dynamic parts of the cell cortex suggests a role in the formation and/or stability of actin filaments.

LIM domains have been demonstrated to act as a discrete protein-binding unit (Schmeichel and Beckerle, 1994). Since DLIM1 is comprised primarily of two LIM domains and either LIM domain of DLIM1 is sufficient for its involvement in the dynamic processes and its colocalization with actin as observed in our N- and C-terminal DLIM1 deletion studies, we presume that the LIM domains of DLIM1 interact with either actin or other cytoskeleton-associated proteins that are also involved in the dynamic processes. The association of LIM domains with specific protein partners is now known to have a critical role in the control of its subcellular distribution and activity (Brown *et al.*, 1996; Mao *et al.*, 1997). Moreover, because of the capacity of individual LIM domains to dock with unique protein partners, it has been proposed that proteins with multiple LIM domains might act as adapter molecules that facilitate the assembly of biologically active protein complexes within the cell (Beckerle, 1997; Dawid *et al.*, 1998). In light of this as well as our observations on association of DLIM1 with actin and involvement of its domains in the dynamic processes, we speculate that DLIM1 behaves as an adapter molecule with one of the LIM domains of DLIM1 specifically interacting with F-actin, while the other LIM domain may remain accessible to additional cytoskeleton-associated proteins. Domain mapping for actin-binding site on DLIM1 needs to be performed in order to support this hypothesis.

3. DLIM1⁻ mutant analyses

We have shown that DLIM1 is a single copy gene and its expression is developmentally regulated with DLIM1 transcripts being most abundant during growth and early development (Figures 8a,b), suggesting a possible role of the DLIM1 protein during cell growth and/or early development. To investigate the function of DLIM1 *in vivo* we have disrupted the DLIM1 gene of AX2 cells with blasticidin S resistance cassette via homologous recombination. The phenotypes of the DLIM1⁻ mutant cells are discussed below and a comparison of the phenotypes observed in DLIM1⁻ mutant cells and DLIM2⁻ mutant cells (Khurana, T., personal communication) is summarised in Table 1.

3.1. Increase in cell-size and impaired cytokinesis

DLIM1⁻ mutant cells are larger in size as compared to AX2 cells when grown in shaking suspension and these large-sized mutant cells were found to be multinucleated in comparison to most of the uni- and bi-nucleated wild-type AX2 cells (Figures 31; 32a,a'). This suggests that DLIM1⁻ mutant cells exhibit impaired cytokinesis. This phenotype of DLIM1⁻ mutant cells resembles that of the single mutant cells lacking myosin II, coronin, CAP and double mutant cells lacking α -actinin/gelation factor (De Lozanne and Spudich, 1987; Manstein *et al.*, 1989; Pollenz *et al.*, 1992; de Hostos *et al.*, 1993; Rivero *et al.*, 1996b; Noegel *et al.*, 1999). Lack of all of these cytoskeleton-associated proteins resulted in a cytokinesis defect leading to large multinucleated cells. We also note that the proportion of multinucleated DLIM1⁻ mutant cells decreases when the cells were shifted from suspension culture to a glass surface (Figure 32b'). This behaviour of mutant cells resembles that of myosin II deficient cells. A traction mediated rudimentary cytokinesis is observed in myosin II null cells when they are attached to substratum (Fukui *et al.*, 1990). Myosin II is located in the cleavage furrow, supporting its role in cytokinesis (Yumura *et al.*, 1984). However, we have never observed DLIM1 at the cleavage furrow in fluorescence studies performed with cells expressing the GFP-DLIM1 fusion protein (Results not shown).

3.2. Reduced growth under stress conditions and increased sensitivity to osmotic shock

Growth of the DLIM1⁻ mutant cells under optimal conditions in shaking suspension as well as on SM agar plates with bacterial food source is comparable to wild-type AX2 cells (Figures 33, 37). Infact colonies of DLIM1⁻ cells grow slightly faster on *Klebsiella* lawns than those measured for AX2 cells (Figure 37). This suggests that there is not a major impediment to phagocytosis and pinocytosis in the DLIM1⁻ mutant cells, which is in contrast to our localization studies performed with GFP-DLIM1 expressing cells that suggest a role for DLIM1 in these processes. However, the rate of growth in suspension culture and in the presence of bacteria as a food source are rather insensitive tests of pinocytosis and phagocytosis, respectively. Future studies on quantitation of the rates of pinocytosis and phagocytosis will be more conclusive.

Growth of DLIM1⁻ mutant cells under stress conditions (like low-/high-temperature or hyperosmotic conditions) that mimic the natural physiological challenges to growth and survival of this free-living organism suggested an additional role of the DLIM1 protein in the growth of the cells. Growth of the DLIM1⁻ mutant cells was significantly impaired at high temperature (27°C) with a significantly prolonged doubling time and reduced cell density at saturation (Figure 34b). DLIM1⁻ mutant cells exhibited rapid cell-lysis under high temperature conditions. This suggests that the cortical cytoskeleton of the DLIM1⁻ cells is not strong enough to resist the environmental stress conditions of higher temperature and that the DLIM1 protein may be required for maintaining the cell cortex under these conditions. Slow growth under conditions of reduced temperature and increased osmolarity has been observed in mutants lacking actin crosslinking proteins, a 34 kD actin-bundling protein and α -actinin, respectively (Rivero *et al.*, 1999b). We have, however, not observed any significant effect on the growth of DLIM1⁻ mutant cells under conditions of reduced temperature (15°C) and hyperosmotic stress (30 mM NaCl or 115 mM sorbitol) (Table 1). In contrast, slow growth of DLIM2⁻ cells under conditions of increased temperature (27°C) and increased osmolarity (115 mM sorbitol) has been observed (Khurana, T., personal communication; Table 1).

Since the role of a cytoskeletal protein in the cytoskeletal rearrangements elicited by adaptation to sustained altered osmolarity could differ from that of the acute osmotic stress, we tested the sensitivity of the mutant cells towards acute osmotic shock. Viability of DLIM1⁻ mutant cells is markedly reduced on exposure to osmotic shock (Figure 36, Table 1). The increased sensitivity in DLIM1⁻ cells to osmotic shock is also in agreement with a reduced strength of the cortical cytoskeleton. Severe defects in the osmoregulatory pathway resulting in premature cell-death under high osmotic stress has been demonstrated for cells that lack dokA, a member of a family of histidine kinase-like genes that play regulatory roles in eukaryotic cell function (Schuster *et al.*, 1996). There are increasing evidences indicating that the actin cytoskeleton plays an important role in the adaptation to situations of altered tonicity. In yeast a rapid disassembly and redistribution of the actin cytoskeleton occurs in response to an osmotic stress and genetic and morphological studies performed with osmosensitive mutants indicate that actin-binding proteins could be involved in actin redistribution during osmotic shock (Chowdhury *et al.*, 1992). *Dictyostelium* cells respond to hyperosmotic stress by shrinking spontaneously, followed by rearrangement of cytoskeletal proteins. The two main components of the cytoskeleton, actin and myosin II, are phosphorylated as a consequence of osmotic shock (Zischka *et al.*, 1999). Disassembly of myosin II filaments is an essential part of the hyperosmotic stress response in *Dictyostelium*, which allows the cell to adopt a spherical shape and provides the mechanical strength necessary to resist extensive shrinkage (Kuwayama *et al.*, 1996). The *Dictyostelium* cytoskeleton associated LIM protein, DdLim, decreases in amount in the cytoskeletal fraction isolated from osmotically shocked cells (Zischka *et al.*, 1999). Exposure of DLIM2⁻ cells to osmotic shock led to a marked reduction in the viability of DLIM2⁻ cells (Khurana, T., personal communication; Table 1). Our results as well as these reports point to an interplay of the various components of the actin cytoskeleton in response to osmotic stress.

3.3. Defect in early development

Dictyostelium cells undergo a developmental process on deprivation of nutrients. Upon starvation, cells start emitting cAMP pulses and aggregate into mounds. These mounds after a series of morphological changes give rise to fruiting bodies. The transformation of a monolayer of single cells into multicellular three dimensional aggregates occurs due to

cytoskeleton based chemotactic motility and intercellular adhesion (Gerisch, 1987; Bozzaro and Ponte, 1995; Parent and Devreotes, 1996).

Table 1. Summary of phenotypes observed in mutant strains

Investigated response	strain	
	DLIM1 ⁻	* DLIM2 ⁻
Cell size	large	large
Growth 21°C	wt	wt
Growth 15°C	wt	wt
Growth 27°C	impaired; ↓ density	impaired; ↓ density
Growth on bacteria	slightly fast	slightly slow
Growth in NaCl	wt	slow; ↑ doubling time
Growth in sorbitol	wt	wt
Osmotic shock	highly sensitive	highly sensitive
Development on plastic	defect in early development; small aggregates	defect in early development; small aggregates
Development on agar	wt	defect in early development; small aggregates
Phototaxis of slugs	wt; slight detours	wt; slight detours
Spore viability	wt	wt

wt, similar to wild-type AX2 cells; ↓, reduced; ↑, increased
 *Data for DLIM2⁻ mutant cells was obtained from Khurana, T., personal communication

When the developmental pattern of mutant cells was examined on water-agar plates or phosphate-buffered agar plates, DLIM1⁻ mutant cells completed the developmental cycle and passed through all stages of development without macroscopically evident disorders (Figure 39). Interestingly, the DLIM1⁻ mutant cells exhibited a 4-5 h delay in initiation of development when placed under a layer of starvation buffer on a plastic surface (Figure 38). Moreover, under this comparatively stringent plating conditions, individual streams of DLIM1⁻ cells did not coalesce to a single centre, as in case of the AX2 cells, and often fractured along their length forming smaller aggregates of variable size. DLIM2⁻ mutant cells, however, exhibit a 4-5 h delay in the formation of aggregates on agar plates as well as

under submerged conditions on a plastic surface (Khurana, T., personal communication; Table 1). This difference in early development pattern observed for DLIM1⁻ cells on agar and under submerged condition on plastic surface can be attributed to either a defect in cAMP relay signalling or substrate dependent adhesion. We note that the cAMP signals, which the cells emit upon starvation and leads to the aggregation of cells, are more diffused when the cells are placed under a layer of starvation buffer as compared to when the cells are plated on agar plates. We, therefore, speculate that DLIM1⁻ mutant cells exhibit a defect in cAMP relay signalling, a defect that becomes more obvious when the cells are starved under liquid medium. A similar phenotype has also been observed for cells that lack Darlin, a protein that binds to small GTPases in *Dictyostelium*. Darlin⁻ cells complete all stages of development on agar plates, however, when starved under liquid medium the mutant cells were unable to form aggregation centres and streams (Vithalani *et al.*, 1998).

4. DLIM1: an overview

Our results suggest that DLIM1 is involved in the regulation of the actin cytoskeleton and plays a role in phagocytosis, pinocytosis, exocytosis, cytokinesis and cell motility. DLIM1 also contributes to the maintenance of the strength of the actin cytoskeleton as is evident by the inability of the mutant cells to grow under conditions of high temperature as well as the increased sensitivity of the mutant cells to osmotic shock. The accumulation of DLIM1 in the pseudopods of the motile cells and the phagocytic cups suggests that DLIM1 converts signals originating from different processes on the cell surface into activities of the cytoskeleton. Since chemotactic responses to cAMP are mediated through heterotrimeric G proteins (Devreotes, 1994) and DLIM1 assembles at the leading edge and pseudopod of a cell, it is tempting to assume that DLIM1 is located in a signalling pathway downstream of the heterotrimeric G proteins. The defect exhibited by the DLIM1⁻ mutant cells when starved under liquid medium on plastic surface is in accord with this notion. To integrate incoming signals and to transmit them downstream to regulatory proteins of the actin cytoskeleton, a protein must form complexes with a number of other proteins. The LIM domains of DLIM1 predispose DLIM1 to act as an adapter molecule facilitating multiple protein-protein interactions at the cytoskeleton. We have demonstrated that DLIM1 binds to

F-actin and either LIM domain of DLIM1 is sufficient for its colocalization with actin. We, therefore, speculate that one of the LIM domains of DLIM1 interacts specifically with F-actin, while the other LIM domain remains accessible to additional cytoskeleton-associated proteins.

5. Summary

In the present study, we report the characterization of DLIM1, a novel LIM domain containing protein from *Dictyostelium discoideum*. A LIM domain is a unique double zinc-finger sequence motif found in a diverse class of proteins including transcription factors, proto-oncogene products and cytoskeletal components. DLIM1 is comprised primarily of two LIM domains that conform exactly to the organization of LIM domains in mammalian CRPs. DLIM1 exists as a single-copy gene in *Dictyostelium* genome and its transcription is developmentally regulated. To investigate the role of DLIM1, we have used a green fluorescent protein (GFP)-tagged version of DLIM1 and studied the dynamics of subcellular redistribution using a confocal laser scanning microscope. GFP-DLIM1 accumulates in areas of the cell cortex where it colocalizes with filamentous-actin. In our study of the dynamic

processes, we observed that GFP-DLIM1 associates with dynamic regions of the cell cortex that are enriched in filamentous actin: phagocytic cups, macropinosomes, exocytic vesicles and pseudopods. Furthermore, we have demonstrated the ability of DLIM1 to bind to filamentous-actin *in vitro*. Subcellular localization studies performed with N- and C-terminal DLIM1 deletion constructs revealed that either LIM domain of DLIM1 is sufficient for its involvement in the dynamic processes and its colocalization with actin. Recent studies have established the ability of individual LIM domains to dock with unique protein partners, thus influencing its subcellular distribution and activity. Since DLIM1 is comprised primarily of two LIM domains, we speculate that DLIM1 might act as an adapter molecule with one of the LIM domains of DLIM1 specifically interacting with F-actin, while the other LIM domain may remain accessible to additional cytoskeleton-associated proteins.

To gain more insight into the function of DLIM1 *in vivo*, cells lacking DLIM1 (DLIM1⁻ mutant) were generated by means of homologous recombination. DLIM1⁻ mutant cells exhibit a cytokinesis defect and are multinucleated. Growth of DLIM1⁻ mutant cells under optimal conditions in shaking suspension as well as on agar plates with bacterial food source is normal, suggesting that there is not a major impediment to phagocytosis and pinocytosis in the DLIM1⁻ cells. The cortical strength of the DLIM1⁻ mutant cells is reduced as is evident by the inability of the mutant cells to grow under high temperature as well as the increased sensitivity of the mutant cells to osmotic shock. DLIM1⁻ cells exhibit normal developmental pattern on agar plates giving rise to normal looking fruiting bodies bearing viable spores. However, when starved under a layer of starvation buffer on a plastic surface, DLIM1⁻ cells exhibit a 4-5 h delay in the initiation of development possibly because of a defect in cAMP relay signalling.

Our results suggest that DLIM1 acts as an adapter molecule mediating interactions between actin filaments and cytoskeleton-associated proteins at the cortical cytoskeleton where it associates with dynamic structures that are formed during pinocytosis, phagocytosis, exocytosis and extension of pseudopods; is involved in a signalling pathway that may modulate the chemotactic response during early development; contributes towards the maintenance of the strength of the actin cytoskeleton; and plays a role in cytokinesis.

5. Zusammenfassung

LIM-Domänen sind Sequenzmotive aus zwei Zinkfingern. Sie kommen in vielen verschiedenen Proteinen wie Transkriptionsfaktoren, Protoonkogenen und Zytoskelettkomponenten vor. DLIM1, eine neues LIM-Domänen-Protein aus *Dictyostelium* besteht aus zwei LIM-Domänen, die hohe Ähnlichkeit zu den LIM-Domänen in den CRPs (Cytsein-Rich-Proteins) aus Säugern aufweisen.

Um die in vivo Rolle von DLIM1 zu analysieren, haben wir die Verteilung und das Verhalten von GFP-DLIM1 in lebenden Zellen analysiert. GFP-DLIM1 reichert sich im Zellkortex in Bereichen an, die F-Aktin enthalten und lagert sich bei Aufnahme von Partikeln (Phagozytose) und Flüssigkeit (Makropinozytose) an die entstehenden Phagosomen

bzw. Pinosomen an. GFP-DLIM1-Anlagerung findet auch bei Exozytose an das Exosom statt, und bei der Pseudopodienbildung reichert sich DLIM1 in Pseudopodien an. Domänenanalyse hat gezeigt, dass sich beide LIM-Domänen als GFP-Fusionsproteine wie das Vollängenkonstrukt verhalten. Für DLIM1 haben wir auch zeigen können, dass es nicht nur mit Aktin kolokalisiert, sondern mit F-Aktin direkt interagiert und unter relativ stringenten Bedingungen mit F-Aktin kosedimentiert.

Für LIM-Domänen wird postuliert, dass sie mit spezifischen Partnerproteinen interagieren und eine Adaptorfunktion besitzen. Diese Interaktionen bestimmen auch die subzelluläre Lokalisation. Da DLIM1 im Wesentlichen aus nur zwei LIM-Domänen besteht, könnte es mit einer seiner Domänen an Aktin binden, während die zweite LIM-Domäne Interaktionen zu weiteren Proteinen vermittelt, die möglicherweise ebenfalls Zytoskelett-assoziiert sind. Welche LIM-Domäne für welche Interaktion zuständig ist, muss noch geklärt werden.

Generierung und Analyse einer Minusmutante für DLIM1 haben Hinweise darauf ergeben, dass zelluläre Eigenschaften, die mit dem Zytoskelett in Verbindung gebracht werden, in der Mutante beeinträchtigt sind. So haben wir einen Defekt in der Zytokinese beobachtet, der zu einer Zunahme von mehrkernigen Zellen führt. Ausserdem sind die Mutanten sensitiver gegen erhöhte Wachstumstemperaturen und gegen osmotischen Schock. Beide Defizienzen können auf ein geschwächtes kortikales Aktinnetzwerk zurückgeführt werden. Inwieweit und ob eine verzögerte Entwicklung in Submerskultur durch einen Defekt im cAMP-Signalsystem bedingt ist, ist zu überprüfen.

Zusammenfassend kann die Rolle von DLIM1 so gesehen werden, dass es auf Grund seiner vorgeschlagenen Adaptorfunktion Interaktionen zwischen dem Aktinnetzwerk und weiteren Zytoskelett-assoziierten Proteinen ermöglicht und so an einer Vielzahl von Prozessen wie Pinozytose, Phagozytose, Exozytose, Pseudopodienbildung und möglicherweise Signaltransduktionsprozessen beteiligt ist.

Bibliography

Adachi, H., Hasebe, T., Yoshinaga, K., Ohta, T. and Sutoh, K. (1994) Isolation of Dictyostelium discoideum cytokinesis mutants by restriction enzyme-mediated integration of the blasticidin S resistance marker. *Biochem Biophys Res Commun*, **205**, 1808-14.

Aizawa, H., Fukui, Y. and Yahara, I. (1997) Live dynamics of Dictyostelium cofilin suggests a role in remodeling actin latticework into bundles. *J Cell Sci*, **110**, 2333-44.

Arber, S., Barbayannis, F.A., Hanser, H., Schneider, C., Stanyon, C.A., Bernard, O. and Caroni, P. (1998) Regulation of actin dynamics through phosphorylation of cofilin by LIM-kinase. *Nature*, **393**, 805-9.

Arber, S. and Caroni, P. (1996) Specificity of single LIM motifs in targeting and LIM/LIM interactions in situ. *Genes Dev*, **10**, 289-300.

Arber, S., Halder, G. and Caroni, P. (1994) Muscle LIM protein, a novel essential regulator of myogenesis, promotes myogenic differentiation. *Cell*, **79**, 221-31.

- Arber, S., Hunter, J.J., Ross, J., Jr., Hongo, M., Sansig, G., Borg, J., Perriard, J.C., Chien, K.R. and Caroni, P.** (1997) MLP-deficient mice exhibit a disruption of cardiac cytoarchitectural organization, dilated cardiomyopathy, and heart failure. *Cell*, **88**, 393-403.
- Bach, I.** (2000) The LIM domain: regulation by association. *Mech Dev*, **91**, 5-17.
- Baltz, R., Domon, C., Pillay, D.T. and Steinmetz, A.** (1992) Characterization of a pollen-specific cDNA from sunflower encoding a zinc finger protein. *Plant J*, **2**, 713-21.
- Barkalow, K., Witke, W., Kwiatkowski, D.J. and Hartwig, J.H.** (1996) Coordinated regulation of platelet actin filament barbed ends by gelsolin and capping protein. *J Cell Biol*, **134**, 389-99.
- Beckerle, M.C.** (1997) Zyxin: zinc fingers at sites of cell adhesion. *Bioessays*, **19**, 949-57.
- Bellis, S.L., Miller, J.T. and Turner, C.E.** (1995) Characterization of tyrosine phosphorylation of paxillin in vitro by focal adhesion kinase. *J Biol Chem*, **270**, 17437-41.
- Bonner, J. T.** (1947) Evidence for the formation of cell aggregates by chemotaxis in development of the slime mold Dictyostelium discoideum. *J Exp Zool*, **106**, 1-26.
- Bozzaro, S. and Ponte, E.** (1995) Cell adhesion in the life cycle of Dictyostelium. *Experientia*, **51**, 1175-88.
- Brown, M.C., Perrotta, J.A. and Turner, C.E.** (1996) Identification of LIM3 as the principal determinant of paxillin focal adhesion localization and characterization of a novel motif on paxillin directing vinculin and focal adhesion kinase binding. *J Cell Biol*, **135**, 1109-23.
- Brown, M.C., Perrotta, J.A. and Turner, C.E.** (1998) Serine and threonine phosphorylation of the paxillin LIM domains regulates paxillin focal adhesion localization and cell adhesion to fibronectin. *Mol Biol Cell*, **9**, 1803-16.
- Bullock, W.O., Fernandez, J.M. and Short, J.M.** (1987) XL1-blue: A high efficiency plasmid transforming recA Escherichia coli strain with beta-galactosidase selection. *BioTechniques*, **5**, 376-8.
- Chien, S., Chung, C.Y., Sukumaran, S., Osborne, N., Lee, S., Ellsworth, C., McNally, J.G. and Firtel, R.A.** (2000) The Dictyostelium LIM domain-containing protein LIM2 is essential for proper chemotaxis and morphogenesis. *Mol Biol Cell*, **11**, 1275-91.
- Chowdhury, S., Smith, K.W. and Gustin, M.C.** (1992) Osmotic stress and the yeast cytoskeleton: phenotype-specific suppression of an actin mutation. *J Cell Biol*, **118**, 561-71.
- Claviez, M., Pagh, K., Maruta, H., Baltes, W., Fisher, P. and Gerisch, G.** (1982) Electron microscopic mapping of monoclonal antibodies on the tail region of Dictyostelium myosin. *Embo J*, **1**, 1017-22.
- Cox, D., Wessels, D., Soll, D.R., Hartwig, J. and Condeelis, J.** (1996) Re-expression of ABP-120 rescues cytoskeletal, motility, and phagocytosis defects of ABP-120-Dictyostelium mutants. *Mol Biol Cell*, **7**, 803-23.
- Crawford, A.W. and Beckerle, M.C.** (1991) Purification and characterization of zyxin, an 82,000-dalton component of adherens junctions. *J Biol Chem*, **266**, 5847-53.

- Crawford, A.W., Pino, J.D. and Beckerle, M.C.** (1994) Biochemical and molecular characterization of the chicken cysteine-rich protein, a developmentally regulated LIM-domain protein that is associated with the actin cytoskeleton. *J Cell Biol*, **124**, 117-27.
- Csank, C., Taylor, F.M. and Martindale, D.W.** (1990) Nuclear pre-mRNA introns: analysis and comparison of intron sequences from *Tetrahymena thermophila* and other eukaryotes. *Nucleic Acids Res*, **18**, 5133-41.
- Dawid, I.B., Breen, J.J. and Toyama, R.** (1998) LIM domains: multiple roles as adapters and functional modifiers in protein interactions. *Trends Genet*, **14**, 156-62.
- Dawid, I.B., Toyama, R. and Taira, M.** (1995) LIM domain proteins. *C R Acad Sci III*, **318**, 295-306.
- de Hostos, E.L., Rehfuess, C., Bradtke, B., Waddell, D.R., Albrecht, R., Murphy, J. and Gerisch, G.** (1993) Dictyostelium mutants lacking the cytoskeletal protein coronin are defective in cytokinesis and cell motility. *J Cell Biol*, **120**, 163-73.
- De Lozanne, A. and Spudich, J.A.** (1987) Disruption of the Dictyostelium myosin heavy chain gene by homologous recombination. *Science*, **236**, 1086-91.
- Devereux, J., Haerberli, P. and Smithies, O.** (1984) A comprehensive set of sequence analysis programs for the VAX. *Nucleic Acids Res*, **12**, 387-95.
- Devreotes, P.N.** (1994) G protein-linked signaling pathways control the developmental program of Dictyostelium. *Neuron*, **12**, 235-41.
- Edwards, D.C. and Gill, G.N.** (1999) Structural features of LIM kinase that control effects on the actin cytoskeleton. *J Biol Chem*, **274**, 11352-61.
- Ennis, H.L. and Sussman, M.** (1975) Mutants of Dictyostelium discoideum defective in spore germination. *J Bacteriol*, **124**, 62-4.
- Faix, J., Gerisch, G. and Noegel, A.A.** (1992) Overexpression of the csA cell adhesion molecule under its own cAMP-regulated promoter impairs morphogenesis in Dictyostelium. *J Cell Sci*, **102**, 203-14.
- Fechheimer, M. and Taylor, D.L.** (1984) Isolation and characterization of a 30,000-dalton calcium-sensitive actin cross-linking protein from Dictyostelium discoideum. *J Biol Chem*, **259**, 4514-20.
- Feuerstein, R., Wang, X., Song, D., Cooke, N.E. and Liebhaber, S.A.** (1994) The LIM/double zinc-finger motif functions as a protein dimerization domain. *Proc Natl Acad Sci U S A*, **91**, 10655-9.
- Flick, M.J. and Konieczny, S.F.** (2000) The muscle regulatory and structural protein MLP is a cytoskeletal binding partner of betaI-spectrin. *J Cell Sci*, **113**, 1553-64.
- Freyd, G., Kim, S.K. and Horvitz, H.R.** (1990) Novel cysteine-rich motif and homeodomain in the product of the *Caenorhabditis elegans* cell lineage gene *lin-11*. *Nature*, **344**, 876-9.
- Fukui, Y., De Lozanne, A. and Spudich, J.A.** (1990) Structure and function of the cytoskeleton of a Dictyostelium myosin-defective mutant. *J Cell Biol*, **110**, 367-78.
- Fukui, Y., Lynch, T.J., Brzeska, H. and Korn, E.D.** (1989) Myosin I is located at the leading edges of locomoting Dictyostelium amoebae. *Nature*, **341**, 328-31.

- Gerisch, G.** (1987) Cyclic AMP and other signals controlling cell development and differentiation in Dictyostelium. *Annu Rev Biochem*, **56**, 853-79.
- Gerisch, G., Albrecht, R., Heizer, C., Hodgkinson, S. and Maniak, M.** (1995) Chemoattractant-controlled accumulation of coronin at the leading edge of Dictyostelium cells monitored using a green fluorescent protein-coronin fusion protein. *Curr Biol*, **5**, 1280-5.
- Gottwald, U., Brokamp, R., Karakesisoglou, I., Schleicher, M. and Noegel, A.A.** (1996) Identification of a cyclase-associated protein (CAP) homologue in Dictyostelium discoideum and characterization of its interaction with actin. *Mol Biol Cell*, **7**, 261-72.
- Hacker, U., Albrecht, R. and Maniak, M.** (1997) Fluid-phase uptake by macropinocytosis in Dictyostelium. *J Cell Sci*, **110**, 105-12.
- Hanahan, D.** (1983) Studies on transformation of Escherichia coli with plasmids. *J Mol Biol*, **166**, 557-80.
- Harper, B.D., Beckerle, M.C. and Pomies, P.** (2000) Fine mapping of the alpha-actinin binding site within cysteine-rich protein. *Biochem J*, **350**, 269-274.
- Holmes, D.S. and Quigley, M.** (1981) A rapid boiling method for the preparation of bacterial plasmids. *Anal Biochem*, **114**, 193-7.
- Jung, E., Fucini, P., Stewart, M., Noegel, A.A. and Schleicher, M.** (1996) Linking microfilaments to intracellular membranes: the actin-binding and vesicle-associated protein comitin exhibits a mannose-specific lectin activity. *Embo J*, **15**, 1238-46.
- Karlsson, O., Thor, S., Norberg, T., Ohlsson, H. and Edlund, T.** (1990) Insulin gene enhancer binding protein Isl-1 is a member of a novel class of proteins containing both a homeo- and a Cys-His domain. *Nature*, **344**, 879-82.
- Kimmel, A.R. and Firtel, R.A.** (1983) Sequence organization in Dictyostelium: unique structure at the 5'-ends of protein coding genes. *Nucleic Acids Res*, **11**, 541-52.
- Knecht, D.A. and Loomis, W.F.** (1987) Antisense RNA inactivation of myosin heavy chain gene expression in Dictyostelium discoideum. *Science*, **236**, 1081-6.
- Konrat, R., Krautler, B., Weiskirchen, R. and Bister, K.** (1998) Structure of cysteine- and glycine-rich protein CRP2. Backbone dynamics reveal motional freedom and independent spatial orientation of the LIM domains. *J Biol Chem*, **273**, 23233-40.
- Konrat, R., Weiskirchen, R., Krautler, B. and Bister, K.** (1997) Solution structure of the carboxyl-terminal LIM domain from quail cysteine-rich protein CRP2. *J Biol Chem*, **272**, 12001-7.
- Konzok, A., Weber, I., Simmeth, E., Hacker, U., Maniak, M. and Muller-Taubenberger, A.** (1999) DAip1, a Dictyostelium homologue of the yeast actin-interacting protein 1, is involved in endocytosis, cytokinesis, and motility. *J Cell Biol*, **146**, 453-64.
- Kosa, J.L., Michelsen, J.W., Louis, H.A., Olsen, J.I., Davis, D.R., Beckerle, M.C. and Winge, D.R.** (1994) Common metal ion coordination in LIM domain proteins. *Biochemistry*, **33**, 468-77.

- Kreitmeier, M., Gerisch, G., Heizer, C. and Muller-Taubenberger, A.** (1995) A talin homologue of Dictyostelium rapidly assembles at the leading edge of cells in response to chemoattractant. *J Cell Biol*, **129**, 179-88.
- Kuwayama, H., Ecke, M., Gerisch, G. and Van Haastert, P.J.** (1996) Protection against osmotic stress by cGMP-mediated myosin phosphorylation. *Science*, **271**, 207-9.
- Kwon, H.M. and Handler, J.S.** (1995) Cell volume regulated transporters of compatible osmolytes. *Curr Opin Cell Biol*, **7**, 465-71.
- Laemmli, U.K.** (1970) Cleavage of structural proteins during the assembly of the head of bacteriophage T4. *Nature*, **227**, 680-5.
- Lehrach, H., Diamond, D., Wozney, J.M. and Boedtker, H.** (1977) RNA molecular weight determinations by gel electrophoresis under denaturing conditions, a critical reexamination. *Biochemistry*, **16**, 4743-51.
- Louis, H.A., Pino, J.D., Schmeichel, K.L., Pomies, P. and Beckerle, M.C.** (1997) Comparison of three members of the cysteine-rich protein family reveals functional conservation and divergent patterns of gene expression. *J Biol Chem*, **272**, 27484-91.
- Lowry, O.H., Rosebrough, N.J., Farr, A.L. and Randall, R.J.** (1951) Protein measurement with the Folin phenol reagent. *J Biol Chem*, **193**, 265-75.
- Malchow, D., Nagele, B., Schwarz, H. and Gerisch, G.** (1972) Membrane-bound cyclic AMP phosphodiesterase in chemotactically responding cells of Dictyostelium discoideum. *Eur J Biochem*, **28**, 136-42.
- Maniak, M., Rauchenberger, R., Albrecht, R., Murphy, J. and Gerisch, G.** (1995) Coronin involved in phagocytosis: dynamics of particle-induced relocalization visualized by a green fluorescent protein Tag. *Cell*, **83**, 915-24.
- Manstein, D.J., Titus, M.A., De Lozanne, A. and Spudich, J.A.** (1989) Gene replacement in Dictyostelium: generation of myosin null mutants. *Embo J*, **8**, 923-32.
- Mao, S., Neale, G.A. and Goorha, R.M.** (1997) T-cell oncogene rhombotin-2 interacts with retinoblastoma-binding protein 2. *Oncogene*, **14**, 1531-9.
- Marsh, J.L., Erfle, M. and Wykes, E.J.** (1984) The pIC plasmid and phage vectors with versatile cloning sites for recombinant selection by insertional inactivation. *Gene*, **32**, 481-5.
- Michelsen, J.W., Sewell, A.K., Louis, H.A., Olsen, J.I., Davis, D.R., Winge, D.R. and Beckerle, M.C.** (1994) Mutational analysis of the metal sites in an LIM domain. *J Biol Chem*, **269**, 11108-13.
- Nellen, W., Datta, S., Reymond, C., Sivertsen, A., Mann, S., Crowley, T. and Firtel, R.A.** (1987) Molecular biology in Dictyostelium: tools and applications. *Methods Cell Biol*, **28**, 67-100.
- Nix, D.A. and Beckerle, M.C.** (1997) Nuclear-cytoplasmic shuttling of the focal contact protein, zyxin: a potential mechanism for communication between sites of cell adhesion and the nucleus. *J Cell Biol*, **138**, 1139-47.
- Noegel, A., Witke, W. and Schleicher, M.** (1987) Calcium-sensitive non-muscle alpha-actinin contains EF-hand structures and highly conserved regions. *FEBS Lett*, **221**, 391-6.

- Noegel, A.A., Rivero, F., Albrecht, R., Janssen, K.P., Kohler, J., Parent, C.A. and Schleicher, M.** (1999) Assessing the role of the ASP56/CAP homologue of Dictyostelium discoideum and the requirements for subcellular localization. *J Cell Sci*, **112**, 3195-203.
- Noegel, A.A. and Schleicher, M.** (2000) The actin cytoskeleton of Dictyostelium: a story told by mutants. *J Cell Sci*, **113**, 759-66.
- Okano, I., Hiraoka, J., Otera, H., Nunoue, K., Ohashi, K., Iwashita, S., Hirai, M. and Mizuno, K.** (1995) Identification and characterization of a novel family of serine/threonine kinases containing two N-terminal LIM motifs. *J Biol Chem*, **270**, 31321-30.
- Parent, C.A. and Devreotes, P.N.** (1996) Molecular genetics of signal transduction in Dictyostelium. *Annu Rev Biochem*, **65**, 411-40.
- Perez-Alvarado, G.C., Kosa, J.L., Louis, H.A., Beckerle, M.C., Winge, D.R. and Summers, M.F.** (1996) Structure of the cysteine-rich intestinal protein, CRIP. *J Mol Biol*, **257**, 153-74.
- Perez-Alvarado, G.C., Miles, C., Michelsen, J.W., Louis, H.A., Winge, D.R., Beckerle, M.C. and Summers, M.F.** (1994) Structure of the carboxy-terminal LIM domain from the cysteine rich protein CRP. *Nat Struct Biol*, **1**, 388-98.
- Pfaff, S.L., Mendelsohn, M., Stewart, C.L., Edlund, T. and Jessell, T.M.** (1996) Requirement for LIM homeobox gene Isl1 in motor neuron generation reveals a motor neuron-dependent step in interneuron differentiation. *Cell*, **84**, 309-20.
- Pollenz, R.S., Chen, T.L., Trivinos-Lagos, L. and Chisholm, R.L.** (1992) The Dictyostelium essential light chain is required for myosin function. *Cell*, **69**, 951-62.
- Pomies, P., Louis, H.A. and Beckerle, M.C.** (1997) CRP1, a LIM domain protein implicated in muscle differentiation, interacts with alpha-actinin. *J Cell Biol*, **139**, 157-68.
- Prassler, J., Murr, A., Stocker, S., Faix, J., Murphy, J. and Marriott, G.** (1998) DdLIM is a cytoskeleton-associated protein involved in the protrusion of lamellipodia in Dictyostelium. *Mol Biol Cell*, **9**, 545-59.
- Prassler, J., Stocker, S., Marriott, G., Heidecker, M., Kellermann, J. and Gerisch, G.** (1997) Interaction of a Dictyostelium member of the plastin/fimbrin family with actin filaments and actin-myosin complexes. *Mol Biol Cell*, **8**, 83-95.
- Raper, K. B.** (1935) Dictyostelium discoideum, a new species of slime mould from decaying forest leaves. *J Agr Res*, **50**, 135-147.
- Rauchenberger, R., Hacker, U., Murphy, J., Niewohner, J. and Maniak, M.** (1997) Coronin and vacuolin identify consecutive stages of a late, actin-coated endocytic compartment in Dictyostelium. *Curr Biol*, **7**, 215-8.
- Rivero, F., Albrecht, R., Dislich, H., Bracco, E., Graciotti, L., Bozzaro, S. and Noegel, A.A.** (1999a) RacF1, a novel member of the Rho protein family in Dictyostelium discoideum, associates transiently with cell contact areas, macropinosomes, and phagosomes. *Mol Biol Cell*, **10**, 1205-19.
- Rivero, F., Furukawa, R., Fechheimer, M. and Noegel, A.A.** (1999b) Three actin cross-linking proteins, the 34 kDa actin-bundling protein, alpha-actinin and gelation factor (ABP-120), have both unique and redundant roles in the growth and development of Dictyostelium. *J Cell Sci*, **112**, 2737-51.

- Rivero, F., Furukawa, R., Noegel, A.A. and Fehheimer, M.** (1996a) Dictyostelium discoideum cells lacking the 34,000-dalton actin-binding protein can grow, locomote, and develop, but exhibit defects in regulation of cell structure and movement: a case of partial redundancy. *J Cell Biol*, **135**, 965-80.
- Rivero, F., Koppel, B., Peracino, B., Bozzaro, S., Siegert, F., Weijer, C.J., Schleicher, M., Albrecht, R. and Noegel, A.A.** (1996b) The role of the cortical cytoskeleton: F-actin crosslinking proteins protect against osmotic stress, ensure cell size, cell shape and motility, and contribute to phagocytosis and development. *J Cell Sci*, **109**, 2679-91.
- Roof, D.J., Hayes, A., Adamian, M., Chishti, A.H. and Li, T.** (1997) Molecular characterization of abLIM, a novel actin-binding and double zinc finger protein. *J Cell Biol*, **138**, 575-88.
- Sadler, I., Crawford, A.W., Michelsen, J.W. and Beckerle, M.C.** (1992) Zyxin and cCRP: two interactive LIM domain proteins associated with the cytoskeleton. *J Cell Biol*, **119**, 1573-87.
- Sambrook, J., Fritsch, E.F. and Maniatis, T.** (1989) *Molecular Cloning. A Laboratory Manual*. 2nd ed. Cold Spring Harbor Laboratory Press, Cold Spring Harbor, New York.
- Sanchez-Garcia, I. and Rabbitts, T.H.** (1994) The LIM domain: a new structural motif found in zinc-finger-like proteins. *Trends Genet*, **10**, 315-20.
- Schaller, M.D. and Parsons, J.T.** (1995) pp125FAK-dependent tyrosine phosphorylation of paxillin creates a high-affinity binding site for Crk. *Mol Cell Biol*, **15**, 2635-45.
- Schmeichel, K.L. and Beckerle, M.C.** (1994) The LIM domain is a modular protein-binding interface. *Cell*, **79**, 211-9.
- Schmeichel, K.L. and Beckerle, M.C.** (1998) LIM domains of cysteine-rich protein 1 (CRP1) are essential for its zyxin-binding function. *Biochem J*, **331**, 885-92.
- Schuster, S.C., Noegel, A.A., Oehme, F., Gerisch, G. and Simon, M.I.** (1996) The hybrid histidine kinase DokA is part of the osmotic response system of Dictyostelium. *Embo J*, **15**, 3880-9.
- Shaulsky, G., Fuller, D. and Loomis, W.F.** (1998) A cAMP-phosphodiesterase controls PKA-dependent differentiation. *Development*, **125**, 691-9.
- Simpson, P.A., Spudich, J.A. and Parham, P.** (1984) Monoclonal antibodies prepared against Dictyostelium actin: characterization and interactions with actin. *J Cell Biol*, **99**, 287-95.
- Smolich, B., Vo, M., Buckley, S., Plowman, G. and Papkoff, J.** (1997) Cloning and biochemical characterization of LIMK-2, a protein kinase containing two LIM domains. *J Biochem (Tokyo)*, **121**, 382-8.
- Southern, E.M.** (1975) Detection of specific sequences among DNA fragments separated by gel electrophoresis. *J Mol Biol*, **98**, 503-17.
- Stanyon, C.A. and Bernard, O.** (1999) LIM-kinase1. *Int J Biochem Cell Biol*, **31**, 389-94.
- Stronach, B.E., Siegrist, S.E. and Beckerle, M.C.** (1996) Two muscle-specific LIM proteins in Drosophila. *J Cell Biol*, **134**, 1179-95.

- Studier, F.W. and Moffatt, B.A.** (1986) Use of bacteriophage T7 RNA polymerase to direct selective high-level expression of cloned genes. *J Mol Biol*, **189**, 113-30.
- Sussman, M.** (1951) The origin of cellular heterogeneity in the slime molds, Dictyosteliaceae. *J Exp Zool*, **118**, 407-17.
- Swanson, J.A. and Baer, S.C.** (1995) Phagocytosis by zippers and triggers. *Trends Cell Biol*, **5**, 89-93.
- Takeuchi, I., Kakutani, T. and Tasaka, M.** (1988) Cell behavior during formation of prestalk/prespore pattern in submerged agglomerates of Dictyostelium discoideum. *Dev Genet*, **9**, 607-14.
- Titus, M.A.** (1999) A class VII unconventional myosin is required for phagocytosis. *Curr Biol*, **9**, 1297-303.
- Towbin, H., Staehelin, T. and Gordon, J.** (1979) Electrophoretic transfer of proteins from polyacrylamide gels to nitrocellulose sheets: procedure and some applications. *Proc Natl Acad Sci U S A*, **76**, 4350-4.
- Turner, C.E. and Miller, J.T.** (1994) Primary sequence of paxillin contains putative SH2 and SH3 domain binding motifs and multiple LIM domains: identification of a vinculin and pp125Fak-binding region. *J Cell Sci*, **107**, 1583-91.
- Vithalani, K.K., Parent, C.A., Thorn, E.M., Penn, M., Larochele, D.A., Devreotes, P.N. and De Lozanne, A.** (1998) Identification of darlin, a Dictyostelium protein with Armadillo-like repeats that binds to small GTPases and is important for the proper aggregation of developing cells. *Mol Biol Cell*, **9**, 3095-106.
- Wallraff, E. and Wallraff, H.G.** (1997) Migration and bidirectional phototaxis in Dictyostelium discoideum slugs lacking the actin cross-linking 120 kDa gelation factor. *J Exp Biol*, **200**, 3213-20.
- Wang, J.S., Coburn, J.P., Tauber, A.I. and Zaner, K.S.** (1997) Role of gelsolin in actin depolymerization of adherent human neutrophils. *Mol Biol Cell*, **8**, 121-8.
- Way, J.C. and Chalfie, M.** (1988) mec-3, a homeobox-containing gene that specifies differentiation of the touch receptor neurons in *C. elegans*. *Cell*, **54**, 5-16.
- Wertman, K.F., Wyman, A.R. and Botstein, D.** (1986) Host/vector interactions which affect the viability of recombinant phage lambda clones. *Gene*, **49**, 253-62.
- Westphal, M., Jungbluth, A., Heidecker, M., Muhlbauer, B., Heizer, C., Schwartz, J.M., Marriott, G. and Gerisch, G.** (1997) Microfilament dynamics during cell movement and chemotaxis monitored using a GFP-actin fusion protein. *Curr Biol*, **7**, 176-83.
- Williams, K.L. and Newell, P.C.** (1976) A genetic study of aggregation in the cellular slime mould Dictyostelium discoideum using complementation analysis. *Genetics*, **82**, 287-307.
- Witke, W.** (1991) Dictyostelium α -actinin: Struktur und Funktion. PhD thesis (in German), Ludwig-Maximilians-Universität München.
- Yang, N., Higuchi, O., Ohashi, K., Nagata, K., Wada, A., Kangawa, K., Nishida, E. and Mizuno, K.** (1998) Cofilin phosphorylation by LIM-kinase 1 and its role in Rac-mediated actin reorganization. *Nature*, **393**, 809-12.

Yao, X., Perez-Alvarado, G.C., Louis, H.A., Pomies, P., Hatt, C., Summers, M.F. and Beckerle, M.C. (1999) Solution structure of the chicken cysteine-rich protein, CRP1, a double-LIM protein implicated in muscle differentiation. *Biochemistry*, **38**, 5701-13.

Young, R.A. and Davis, R.W. (1983) Yeast RNA polymerase II genes: isolation with antibody probes. *Science*, **222**, 778-82.

Yumura, S., Mori, H. and Fukui, Y. (1984) Localization of actin and myosin for the study of ameboid movement in Dictyostelium using improved immunofluorescence. *J Cell Biol*, **99**, 894-9.

Zischka, H., Oehme, F., Pintsch, T., Ott, A., Keller, H., Kellermann, J. and Schuster, S.C. (1999) Rearrangement of cortex proteins constitutes an osmoprotective mechanism in Dictyostelium. *Embo J*, **18**, 4241-9.

Erklärung

Ich versichere, daß ich die von mir vorgelegte Dissertation selbständig angefertigt, die benutzten Quellen und Hilfsmittel vollständig angegeben und die Stellen der Arbeit - einschließlich Tabellen, Karten und Abbildungen -, die anderen Werke im Wortlaut oder dem Sinn nach entnommen sind, in jedem Einzelfall als Entlehnung kenntlich gemacht habe; daß diese Dissertation noch keiner anderen Fakultät oder Universität zur Prüfung vorgelegen hat; daß sie - abgesehen von unten angegebenen beantragten Teilpublikationen - noch nicht veröffentlicht ist, sowie, daß ich eine Veröffentlichung vor Abschluß des Promotionsverfahrens nicht vornehmen werde. Die Bestimmungen dieser Promotionsordnung sind mir bekannt. Die von mir vorgelegte Dissertation ist von Frau Prof. Dr. Maria Leptin betreut worden.

„Keine Teilpublikationen“

Köln, den 02.11.2000

Bharat Khurana

Curriculum Vitae

Name	Bharat Khurana
Date of birth	23.01.1972
Place of birth	New Delhi, India
Nationality	Indian
School education	
1977-1989	School education from 1 st to 12 th class
03.1987	10 th class examination, New Delhi, India
03.1989	12 th class examination, New Delhi, India
University Studies	
1989-1994	Bachelor of Veterinary Sciences & Animal Husbandry College of Veterinary Sciences, CCS Haryana Agricultural University, Haryana, India
1994-1997	Master of Veterinary Sciences Major subject: Veterinary Microbiology Advisor: Dr. R. Pandey, National Professor (ICAR), Department of Veterinary Microbiology, COVS, CCS Haryana Agricultural University, Haryana, India Title of the Master's thesis: 'Prevalence and preliminary characterization of group-A and non-group-A rotaviruses from asymptomatic neonatal bovine calves'
Doctoral study	
06.1997-01.2001	Advisors: Prof. Dr. Maria Leptin, Institute of Genetics Prof. Dr. Angelika A. Noegel, Institute of Biochemistry I, Medical Faculty, University of Cologne, Cologne, Germany Title of the Ph.D. thesis: 'Characterization of DLIM1, a novel cytoskeleton-associated LIM domain containing protein of <i>Dictyostelium discoideum</i> ' A student of the Graduate College 'Genetics of Cellular Systems', Institute of Genetics, University of Cologne, Cologne, Germany

Lebenslauf

Name	Bharat Khurana
Geburtsdatum	23.01.1972
Geburtsort	Neu Delhi, Indien
Staatsangehörigkeit	indisch
Schulausbildung	
1977-1989	Schulausbildung 1. bis 12. Klasse
03.1987	Abschlußprüfung 10. Klasse, Neu Delhi, Indien
03.1989	Abschlußprüfung 12. Klasse, Neu Delhi, Indien Zulassungsprüfung zum Universitätsstudium
Studium	
1989-1994	Studium der Veterinärmedizin (<i>Bachelor of Veterinary Sciences & Animal Husbandry</i>), CCS Haryana Agricultural University, Haryana, Indien
1994-1997	Diplomstudium der Veterinärwissenschaft, Veterinäre Mikrobiologie (<i>Master of Veterinary Sciences, Veterinary Microbiology</i>), CCS Haryana Agricultural University, Haryana, Indien Titel der Diplomarbeit: ‘Prevalence and preliminary characterization of group-A and non-group-A rotaviruses from asymptomatic neonatal bovine calves’
Promotionsstudium	
06.1997-01.2001	Betreuerin: Frau Prof. Dr. Maria Leptin, Institut für Genetik Frau Prof. Angelika A. Noegel, Institut für Biochemie I, Medizinische Fakultät der Universität zu Köln Thema: ‘Characterization of DLIM1, a novel cytoskeleton-associated LIM domain containing protein of <i>Dictyostelium discoideum</i> ’ Student im Graduierten-Kolleg ‘Genetik zellulärer Systeme’, Institut für Genetik, der Universität zu Köln